ELECTRICAL CONDUCTIVITY OF NICKEL NANOSTRAND POLYMER COMPOSITES

by

Nathan D. Hansen

A dissertation submitted to the faculty of
The University of Utah
in partial fulfillment of the requirements for the degree of

Doctor of Philosophy

Department of Mechanical Engineering

The University of Utah

August 2012

The University of Utah Graduate School

STATEMENT OF DISSERTATION APPROVAL

The dissertation of **Nathan D. Hansen**

has been approved by the following supervisory committee members:

Daniel O. Adams	, Chair	**4/26/12** Date Approved
David T. Fullwood	, Member	**4/26/12** Date Approved
Kenneth L. DeVries	, Member	**4/26/12** Date Approved
Debra Mascaro	, Member	**4/26/12** Date Approved
Kenneth L. Monson	, Member	**4/26/12** Date Approved

and by **Timothy A. Ameel**, Chair of the Department of **Mechanical Engineering**

and by Charles A. Wight, Dean of The Graduate School.

ABSTRACT

The electrical conductivity properties of nickel nanostrands in polymer composite systems are investigated and characterized. Recently developed nickel nanostrands feature a three-dimensionally interconnecting and branching nanostructure that is shown to be highly effective at imparting electrical conductivity in polymer composites.

A systematic investigation of material behaviors is undertaken, with results that have been or will be published in a series of journal articles. The content of the studies that form these articles is given herein as the core content of this work. The first study investigates the basic electrical and mechanical properties of nanostrands in a single polymer system. Key results indicate a strong dependence of conductivity properties on processing conditions, volume fraction of conductor, and sample geometry. Mechanical properties are not significantly altered by the presence of nanostrands. The dispersed nanostrand structure is next investigated through the development of statistical topology tools that can quantify nanostrand dispersions and correlate them to the electrical resistivity of composite films. Quantification of the dispersed nanostructure is a significant improvement over common literature approaches. The next step tests full percolation characterization across multiple polymer systems, and indicates a strong dependence on electrical resistivity between polymer types. Polymer constituent properties are found to be poor predictors of nanostrand composites conductivities, though further testing of addition metrics is expected to bring improved correlation. The

concluding investigation seeks electrical conductivity percolation models for nanostrand composites. Existing models show only moderate accuracy, and a newly developed combined percolation tunneling approached is suggested for improved fit to measured conductivity.

TABLE OF CONTENTS

LIST OF TABLES

LIST OF FIGURES

SYMBOLS AND ABBREVIATIONS

β	Betti number (dimensionless)
CVD	Chemical Vapor Deposition
γ	Surface energy (Energy per unit area)
NS	Nanostrand
NiNS	Nickel Nanostrands
Ω	ohm (unit of resistance)
φ	volume fraction
ρ	Electrical Resistivity (ohm-cm)
S	Siemens (unit of conductance)
σ	Electrical Conductivity (S/cm)
SEM	Scanning Electron Microscope
X	magnification unit

ACKNOWLEDGMENTS

The work published herein encompasses developments in the daunting task of characterization of new materials. I gratefully acknowledge the support of many entities and individuals who have been involved in this effort:

I gratefully and sincerely acknowledge Conductive Composites Company for materials, testing and fabrication support, and partial funding. This support has truly been a critical component in enabling this dissertation effort.

The professional advisement and insight of Dr. Daniel O. Adams of the University of Utah have been invaluable during the process of defining and accomplishing this work. Special thanks are also extended to Dr. David Fullwood of Brigham Young University, as well as all coauthors and doctoral committee members.

I personally extend thanks, gratitude, and love to many friends and family members. I fully recognize the sacrifices that my family has made to support me throughout my education. The support and love of George and Cyndy Hansen have been an essential part in this work. The unwavering support and love of Lyndie Hansen has been the most valuable element in accomplishing this effort, for which I am eternally grateful. I dedicate this work to my wife and children in honor of the many long days and late nights away from home that were paid as a price for this achievement.

1 INTRODUCTION

Polymer and fiber reinforced composites play an increasingly important role in commercial, defense, and private sectors. While polymeric systems are well suited for replacing metallic structures with respect to mechanical and processing properties, the electrical properties of polymeric systems are orders of magnitude apart from metals. This transition to polymeric systems occurs concurrently with an increase in utilization of and reliance on digital technologies which are highly sensitive to electromagnetic shielding.

Traditional metal structures naturally present an electrically conductive and shielding material, as isotropic metals have free valence electrons to facilitate electrical conduction. Polymer matrix composites are naturally not as well suited, consisting of insulating or moderately conducting fibers in an insulating matrix. Thus, the challenge is to find methods of engineering electrical conductivity and shielding properties into polymers and polymer composite systems while preserving fundamental advantages (mechanical, manufacturing, density, cost, etc.).

Traditional solutions for conductivity in polymers and polymer matrix composites have included metal filled polymers, intrinsically conductive polymers, and meshes, foils, and wires for laminate structures. The rapidly growing field of nanotechnology has presented new materials that can increase polymer composite conductivity. Traditional conductive additives (such as milled powders, coated spheres, platelets, etc.) have aspect ratios on the order of 1 to 10, while newer nanomaterials (such as carbon nanofibers)

have aspect ratios in the thousands. This aspect ratio advantage, combined with nanoscale geometries, means that less conductive material is required in terms of both volume percent and weight percent to achieve high conductivity levels [1-4].

The overriding objective of this work is to seek understanding of the electrical properties of metal filled polymers using nickel nanostrands. Previously, the majority of studies on nanostrand systems have dealt with characterization through empirical results. A main deliverable of this work is to investigate structure property relationships within nanostrand composites in order to develop a better predictive capability for electrical conduction behaviors. This is accomplished through examining screening metrics and predictive variables for characterizing the polymer dependent, but processing method and volume fraction independent, electrical conduction of nanostrand composites. Another main goal of this study is to correlate host polymer physical characteristics to nanocomposite bulk electrical resistivity properties. This approach includes both classical percolation characterization and dynamic percolation characterization, along with several physical property tests on polymer constituents. A concluding step of this work is to identify suitable materials models for predicting and analyzing electrical percolation behaviors in nanostrand polymer composites.

1.1 Brief Background: Understanding Metal Filled Polymers

The electrical properties of metal filled polymer systems can be modeled using percolation theory [5-8]. Classical percolation theory considers a connected network of conductive links in a nonconductive matrix across an infinite sample. In a nanostrand composite, this network structure is created by dispersed nanostrands connecting

throughout the polymer. When a sufficient volume of nanostrands are present to create an electrically conductive path, an abrupt change in conductivity is observed, referred to as the critical percolation threshold. The resistivity of the composite decreases dramatically above the percolation threshold, eventually approaching a stabilized conductivity level at the percolation limit. This limit presents a limiting value for well-dispersed conductive networks. For loadings beyond the percolation limit, a decrease in electrical and mechanical properties is often observed, indicating that the polymer host is no longer capable of facilitating additional increases in filler. A typical curve representing these behaviors is shown in Figure 1.1.

1.2 Nanostrands: Metal Polymer Nanocomposites

Nickel nanostrands (abbreviated as NiNS or NS) [9] are a relatively new material. They are a submicron diameter, high aspect ratio nanostructure. Nanostrands feature an intrinsic three-dimensionally interconnected structure that creates loops and demonstrates a branched nature, as shown in Figure 1.2.

Nanostrands are manufactured as a continuously interconnected “cake” of nickel, which can be reduced to a nanostructured, high porosity, three-dimensional nickel powder. The cake is subjected to a shear process that “tears” the nanostrand volume into a nanostructured powder. These discretized nanostrand structures are the key to the observed performance of nanostrand polymer composites. Nanostrand structures at various volume fractions are visible in the micrographs in Figure 1.3.

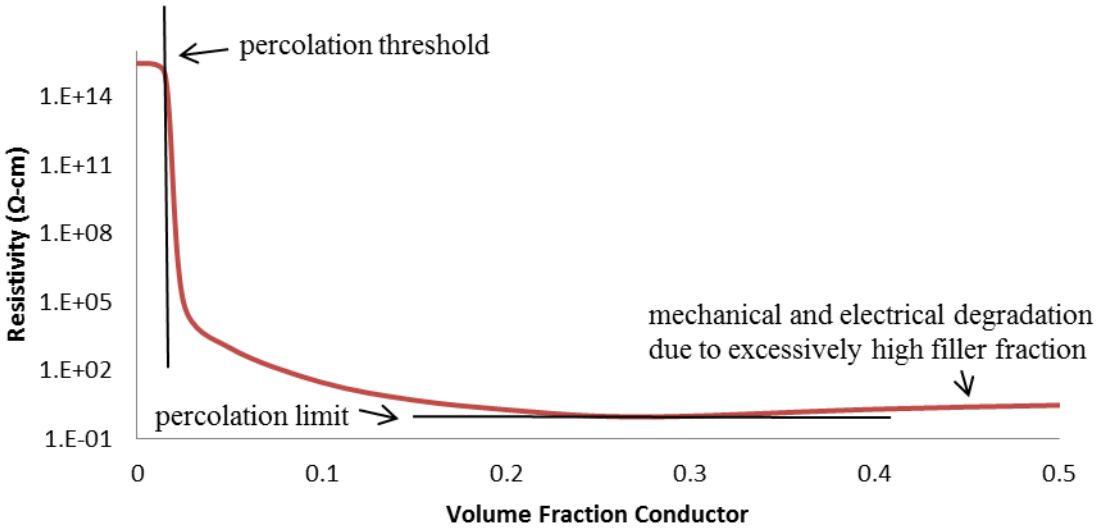

Figure 1.1: General electrical percolation behavior of conductors in polymer systems.

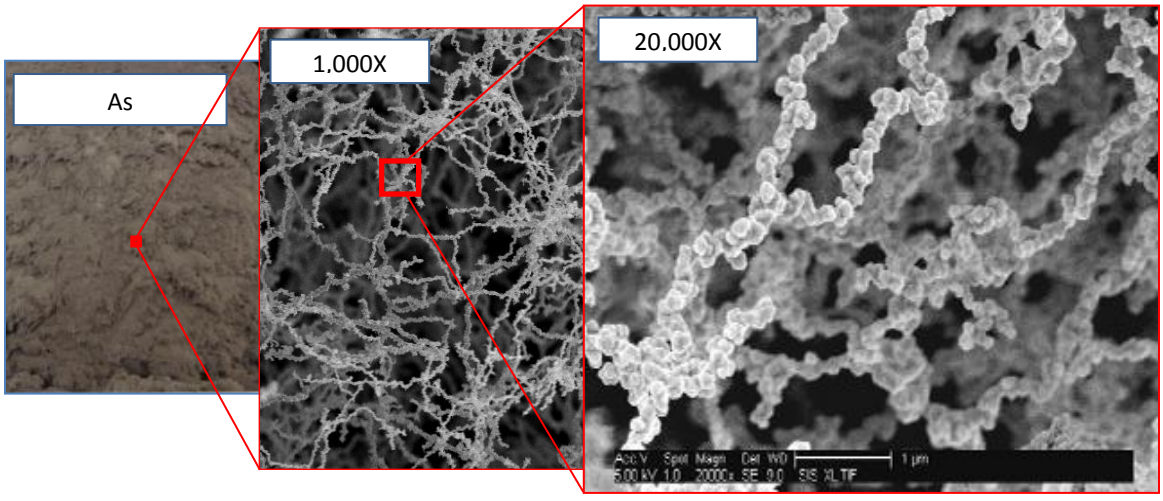

Figure 1.2: Nickel nanostrands, as manufactured, magnification from 1X to 20,000X.

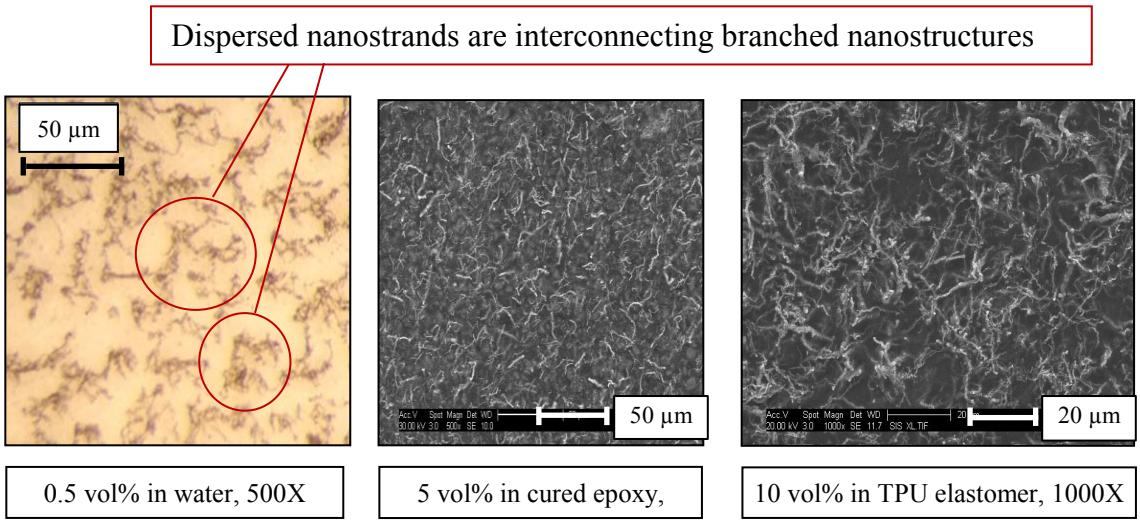

Figure 1.3: Nickel nanostrands dispersed in water at 0.5 volume percent (50 µm scale bar), cured epoxy at 5 volume percent (50 µm scale bar), and TPU elastomer at 10 volume percent (20 µm scale bar).

The looped and branched nature of the nanostrand structure allows for three-dimensional interconnects, thus facilitating percolation at low volume fractions. The branches on each strand help create further radial interconnects, providing additional three-dimensional connection opportunities. For example, two parallel nanostrands do not need to be oriented to intersect along their major axis, as they can connect with radial branches. This branched nature can also offer benefits in applications requiring field effect properties as the branches can serve as a multiplicity of antennas and transmitters.

The nanostrand structure can be viewed as a "skeleton" rather than a full "body" (as with more solidly structured additive particles). The void space of the nanostrand structure is filled with the host substrate, facilitating better continuity of host material properties while still providing conductive interconnections. Nanostrand mixtures percolate to higher conductivity levels than have been demonstrated with carbon

nanomaterials [3, 10-12]. Nanostrand polymer film conductivities regularly measure at or over 100 S/cm across multiple polymers, and as high as 1400 S/cm at the percolation limit, which is significantly higher than the maximum conductivity of 100 S/cm reported for treated carbon nanotubes in a 2009 review by Bauhofer et al. [13]. The Bauhofer study considers carbon nanotube conductivity results that span 147 experimental results, and most authors in the Bauhofer study reported maximum conductivities between 10^{-6} and 10^{2} S/cm in electrical conductivity. Typical results for nanostrands span 10^{-3} to 10^{3} S/cm. A comparative percolation curve for nickel nanostrands and carbon nanofibers is shown in Figure 1.4.

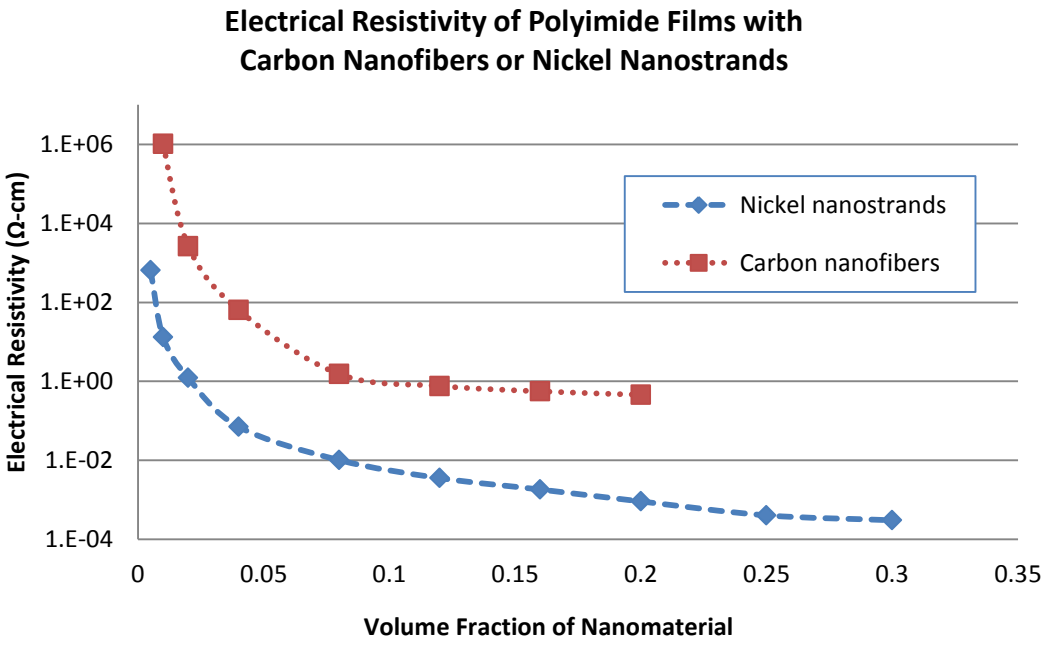

Figure 1.4: Percolative behaviors and resistivity of nickel nanostrands and carbon nanofibers in polyimide. Nanostrands percolate to resistivities that are several orders of magnitude lower than those of carbon nanomaterials, at equal volume fractions.

Nickel benefits from a metallic bonding structure, high electrical conductivity, and ferromagnetic properties. The raw material cost of nickel is relatively low and corrosion resistance is considered to be good.

Nanostrand materials are formed as a crystalline chain structure, and are therefore sensitive to processing methods which can break down the structure and reduce the aspect ratio and interconnects of the structure. Care must be taken when producing nanostrand mixtures to not overmix the system and break down the strands [4, 9].

Nanostrand polymer composites have been able to achieve conductivities in excess of 5000 Siemens/cm, and have been demonstrated in applications including electrostatic discharge [14], electromagnetic shielding [15-17], conductive adhesives [18, 19], caulks and gaskets [20], paints [21, 22], and lightning strike protection [15, 22-26]. Previous studies have indicated that the resultant conduction of a nanostrand composite can depend on multiple factors. For example, an early study [27] indicates that the resistivity of nanostrand composites is a function of the type of polymer used as the matrix material. This work extends that early effort through a systematic characterization of nanostrands across multiple polymer systems, including modeling efforts.

1.3 Processing Conditions, Electrical Resistivity, and Mechanical Properties

Initial discovery work [28] for nanostrands focuses on the basic conductivity performance of nanostrand polymer composites in terms of volume fraction and processing conditions. Basic electrical and mechanical behaviors are considered by testing the electrical resistivity and lap shear strength of nickel nanostrands in an epoxy

adhesive (Henkel® Hysol® EA 9396™). Independent parameters include volume fraction of nanostrands, sample thickness, and dispersion methods. Control variables include epoxy type, dispersion practices, and characterization methods.

In brief summary, the electrical resistivity of nanostrand polymer composites in epoxy is observed to be 10^{-2} to 10^{2} ohm-cm, depending on volume fraction, sample geometry, and dispersion method. Of particular note, the electrical resistivity of the nanostrand filled polymer system is not invariant with geometry; i.e., the electrical resistance of a sample does not rely linearly on sample dimensions and bulk electrical material properties. Conduction in these systems relies on percolated pathways, which introduces considerations that are nonlinear with changes in sample geometry. These considerations are factors such as the number of conductor insulator junctions, the distance between junctions, and characteristics of the dispersed conductive network. The mechanical strength of the composite system is not statistically different from the strength of the unfilled system at the volume loading and test methods considered (up to 7.5 volume percent in lap shear).

1.4 Quantifying and Correlating *In Situ* Nanostructures

To better understand conduction in nanostrand polymer composites, the structure of the conductive network must be observed, characterized, and quantified. Despite recent advances in the use of nanomaterials, few tools have been developed to quantify the *in situ* dispersion of nanoconductors within a polymer. It is common to see the dispersion of nanomaterials discussed in the literature in terms of “good” or “poor”, rather than in a quantified manner. Several authors have reported results for quantifying the dispersion of

carbon nanomaterials in composite systems (for example [29-31]), but no previous work has approached quantifying and correlating the unique structure of nickel nanostrands in polymer composites. A technique for analyzing and quantifying the dispersed nanostrand structure can be used to correlate the conductivity of composites systems and provide insight when dispersed in polymers. Understanding the *in situ* structure gives valuable insight to the mechanisms of conduction seen between samples. The ability to quantify the actual nanostructure is an essential element to developing more universal models that predict the conductivity of nanostrand composites (or of any conductive filled system).

In brief summary, the *in situ* dispersed nanostrand structure is quantified and correlated through the development of statistical topology analysis tools. The tools that are developed can also be used to quantify the dispersion of conductors, providing a significant improvement over the qualitative or altogether absent statements that are often found in the literature regarding dispersions. The quantification method uses digital microscopy and standard software packages, such as Matlab® and Photoshop®. A correlation relationship is found between the nanostrand homology dispersion characteristics and nanostrand polymer composite resistivity properties. The effects of processing conditions can be monitored and correlated to sample properties. This quantification and correlation method can be used as a sampling/screening tool during processing steps.

1.5 Percolation in Multiple Polymer Systems and Characterization of Constituents

The resistivity of nanostrand polymer composites is next investigated across multiple polymer systems. Full percolation curves for nanostrand polymer systems are also developed. As seen in Figure 1.5, prior percolation data for nanostrands focuses only on the percolation limit, and data at the percolation threshold is needed to fully understand conduction behaviors.

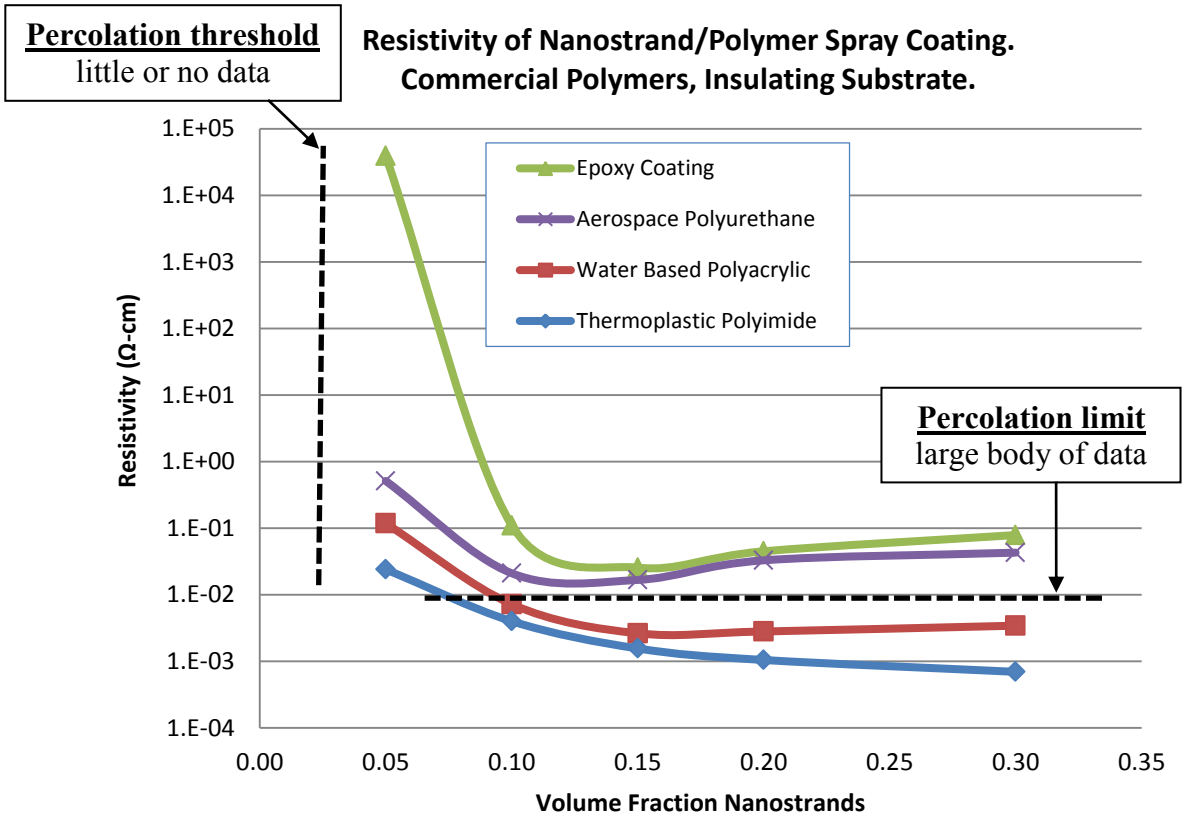

Figure 1.5: Regions of interest for further investigation into conduction mechanisms of nanostrand polymer composites.

The chosen polymers are all commercially available “off the shelf” systems, and include solvated thermoplastic polyimide, water based acrylic/urethane, aerospace grade polyurethane, industrial epoxy, silicone, aliphatic urethane, polyimide, solvated thermoplastic polyurethane, and polyvinylpyrrolidone. Percolation test samples consist of thin films on electrically insulating substrates. The control variables in this test are dispersion practices, nanostrand quality, fabrication and cure practices, and film thickness.

Each polymer system is tested for lyophilicity properties of the fluid (uncured or solvated) phase to a nickel surface, and also for hydrophobicity to the cured/set polymer surface. Cured polymer systems are also tested for voltage breakdown strength and electrical resistivity. These lyophilicity and hydrophobicity tests are used to investigate the effect of constituent materials surface energy interactions in dispersed nanostrand polymer conductivity properties. Nanostrand polymer samples are also tested for resistivity properties and mass during cure. All tests are correlated to the electrical conductivity of the cured nanocomposite films.

In brief summary, a strong dependence is seen in electrical resistivity as a function of polymer type. All of the polymers are insulating in their unfilled state, and their transition to conductor is expected under percolation theory. However, variances of several orders of magnitude in electrical resistivity are seen across polymer types at each volume fraction of nanostrands. For example, 3 volume percent of nanostrands is past the percolation limit for most polymer systems. However, epoxy and silicone do not exhibit percolated conductivity until 5 volume percent. All systems are at their percolation limits

within 15 volume percent of nanostrands, yet the resultant electrical conductivity at this loading differs by nearly two orders of magnitude. The physical and energy properties of the constituent materials are found to be poor predictors for conductivity properties.

1.6 Modeling Electrical Percolation in Nanostrand Polymer Composites

There has been very little previous investigation for conductivity models within nanostrand polymer composites. Previous efforts have found correlation to structure metrics [32] and quantum tunneling phenomena [33, 34]. These models do not fully account for DC conduction behaviors that are seen in nanostrand composites.

A review is made of modeling approaches to electrical conductivity in conductor insulator binary systems, particularly for metal filled polymers. This review identifies several promising approaches for modeling conductivity of nanostrands in polymer systems. These approaches are tested against measured electrical percolation curves.

In brief summary, suitable approaches from the literature are identified that approximate percolation conductivity behaviors for nanostrand polymer systems. The models are compared to empirical percolation data across multiple polymers. A new approach that combines a generalized effective media approach with tunneling percolation theory provides the most accurate model to available data.

2 INVESTIGATION OF ELECTRICALLY CONDUCTIVE STRUCTURAL ADHESIVES USING NICKEL NANOSTRANDS

Nathan Hansen [a], Daniel O. Adams [a], K.L. DeVries [a], Adam Goff [b], and George Hansen [c]

[a] Department of Mechanical Engineering, University of Utah
50 S Central Campus Dr. Rm 2110 – MEB
Salt Lake City, UT 84112, USA

[b] Luna Innovations
706 Forest Street, Suite A
Charlottesville, VA 22903, USA

[c] Conductive Composites Company
357 W 910 S
Heber City, UT 84032, USA

Published in The Journal of Adhesion Science and Technology [35].

2.1 Abstract

Several conductive nanomaterials are investigated for structural electrically conductive adhesive applications, including carbon nanofibers and nickel nanostrands. The suitability of nanostrands as a conductive filler is reviewed. Adhesive formulations based on Hysol 9396 epoxy are tested for electrical and structural properties. Several formulations are found to be capable of providing enhanced adhesive strength while affording excellent electrical conductivity. The development of full strength structural conductive adhesives can enable a wide range of applications where the strength of current commercially available electrically conductive adhesive systems is a limiting factor. Superior conductivity results are obtained by the nickel nanomaterials, with milliohm gap resistance and resistivity on the order of 10^{-2} ohm-cm possible at loading of 5 volume percent. Initial results indicate that these systems present good survivability in thermal cycling conditions.

2.2 Introduction

Electrically conductive adhesives have a long history as metal filled polymer systems [1]. Candidate materials have included silver, copper, nickel, and even organic materials such as carbon. The particular success of any filler, both technically and commercially, depends on various technical, practical, and economic considerations. Where conduction mechanisms across an adhesive bond are concerned, a primary performance metric is the ability of the filler to provide percolated conduction across the bond gap at a minimum

filler volume fraction. Recent advances in nanotechnology have provided a new class of potential conductive fillers [2].

In this study, a nanostructured metal filler is considered for electrically conductive epoxy adhesives. Nickel nanostrands have been the subject of recent investigation for a wide range of electromagnetic composites applications (for example, [2-8]). Nickel nanostrands (frequently abbreviated as NiNS) consist of high aspect ratio, three-dimensionally interconnected branched and looped nanostructured aggregates of pure nickel (see Figure 2.1). Their geometry is particularly well suited to electrical conduction percolation mechanisms and electromagnetic shielding applications. The high aspect ratio of nanostrands lowers the volumetric percolation threshold for conduction, and also allows a greater number of effective conduction paths for a given volume fraction in polymer systems. This geometry also provides excellent conductivity at lower volume fractions than other nickel geometries [9, 10].

Nanostrands present intrinsic advantages that are well suited for conduction mechanism in Electrically Conductive Adhesives (ECAs). The conductivity of nickel is beneficial over carbon nanofillers, and the raw material cost of nickel is attractive relative to silver. The electrical properties of nanostrand filled adhesives have been observed to compare well with silver and carbon filled adhesives as reported in the literature [11-13]. There are potential advantages to the use of nickel on corrosion sensitive platforms. The ferromagnetic properties of nickel present the possibility of anisotropic conduction behavior [14]. The conduction mechanism of nanostrands is such that lower volume fractions are required than with other fillers, which leads to weight savings, cost savings,

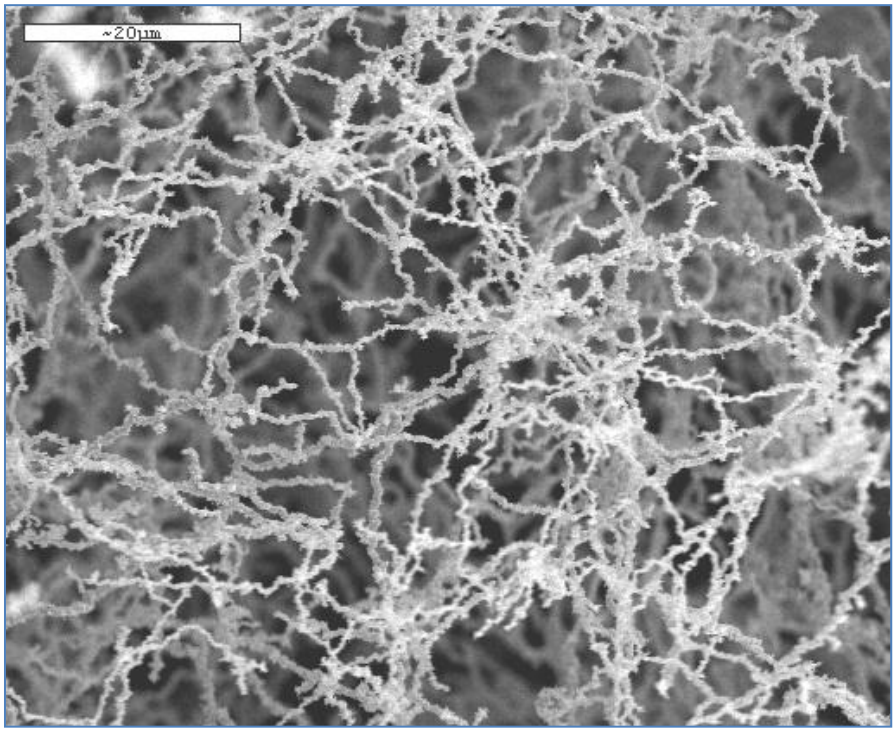

Figure 2.1: Nickel nanostrands, 20 µm scale bar.

and better mechanical properties. Nanostrands are easily dispersed in a wide range of polymeric systems by methods including centrifugal planetary mixers, doctor blade, and manual techniques. Dispersions have been made in polyimides, urethanes, acrylics, epoxies, silicones, thermoplastic polyurethane, isocyanates, and even water.

The purpose of this study was to identify salient metrics for creating a conductive structural ECA, and to identify a design envelope in terms of volume fraction and bond thickness for the conductivity of nickel nanostrands in Hysol EA 9396 epoxy adhesive. An additional intent of this study was to develop structural adhesives that show retention of lap shear strength relative to the unfilled adhesive system. All volume fractions used are below 6.5 volume percent. Improved conductivity is available at higher volume

fractions of nanostrands or with alternate dispersion methods. While the results are particular to this system, the test methodology and principles observed can be extended to other polymeric systems.

2.3 Experimental

2.3.1 Preparation of Nanostrand Adhesive Systems

In this test, nanostrands were dispersed in a two part resin system. Dispersion and mixing of nanomaterials was conducted in catalyzed resin. Nanostrands may also be dispersed in resin components separately, and then combined and catalyzed at a later time [15].

Nickel nanostrands are a continuous lattice of interconnected nickel chains, and are degraded excessively by high shear dispersion methods or sonication. Thus, low shear methods are most appropriate for achieving optimum electrical results. At the low volume fraction (1% to 6.5%) of conductor used in this study, there was found to be great latitude in dispersion requirements, as manually prepared samples exhibited similar performance to samples dispersed using an centrifugal planetary mixer. Due to their intrinsically three-dimensional structure, nanostrands are well suited for generating isotropic conductivity when dispersed in polymers. Nanostrands are manufactured as a continuously interconnected body of individual strands. Dispersion into polymeric systems requires a size reduction step in order to use the continuous nanomaterials as a discrete powder. Even in a powder format, the nanostrands retain an interconnected

nature. When properly dispersed, nanostrands are in the form of three-dimensional nanostructured aggregates, as illustrated in Figure 2.2.

Figure 2.3 shows an SEM micrograph cross section of 5 volume percent (28 weight percent) nickel nanostrands dispersed in epoxy adhesive. This is representative of a typical loading in an ECA that will have milliohm resistance across a 0.25 mm bond gap. By comparison, silver filled ECAs are typically 58-78 percent silver by weight, which corresponds to 14-29 percent by volume.

2.3.2 Electrical Testing – Bond Gap Resistance and Volume Resistivity

The properties tested in this study for the electrical performance of nanostrand adhesives were resistance between bonded surfaces (ohms) and bulk resistivity of the conductive adhesive (ohm-cm). The independent variables were bond thickness (gap distance) and volume fraction of nanostrands. Bond thickness was varied from 0.13 mm to 1.07 mm, and volume percentage of nanostrands was varied from 1 to 6.5 percent. Bond area was held constant at 1.267 cm^2. Additional samples using an alternate dispersion technique and very thick bonds (up to 2.59 mm) were investigated at 5 volume percent.

Bond gap resistance test specimens were fabricated by curing nanostrand adhesive between 6061 aluminum plates with a satin #4 brushed finish. All bonded surfaces were cleaned with laboratory grade alcohol immediately prior to bonding. Dielectric spacers were used to control bond thickness, with 12.7 mm diameter holes punched in the spacer for each test specimen. Replicate samples with a controlled dispersion method, bond area, volume, and thickness were made for each formulation. Test strips of five specimens

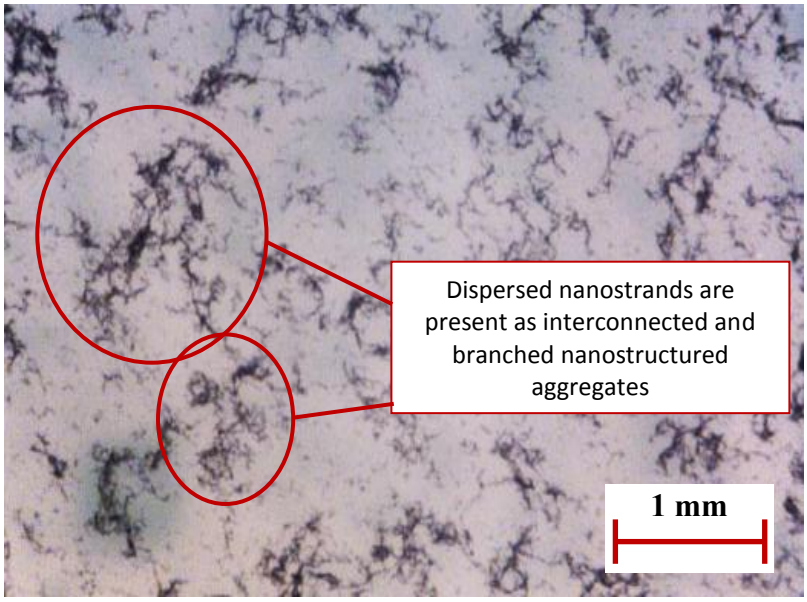

Figure 2.2: Low volume fraction conductor sample (~1 vol%) showing dispersion of nanostrand structures in water.

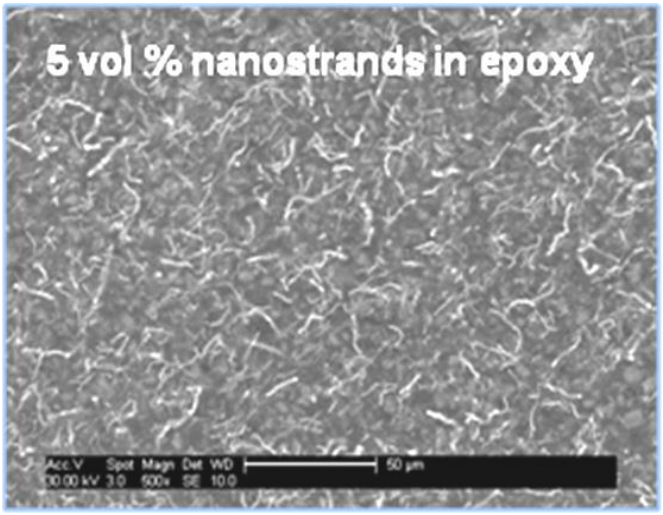

Figure 2.3: Five volume percent (28 wt%) nickel nanostrands dispersed in epoxy. This SEM cross section shows uniformity of dispersion and a large number of three-dimensional conduction paths.

were fabricated for each bond thickness and volume fraction of nanostrands. The DC electrical resistance across each specimen was measured using a Kelvin probe method and a four point milliohmmeter (Extech model 380560). All readings were taken at ambient conditions. Images from this testing process are shown in Figure 2.4. Five readings for each sample group were averaged and inspected for statistical deviation. Bulk resistivity calculations were made using these samples (see ASTM D 2739 [16]).

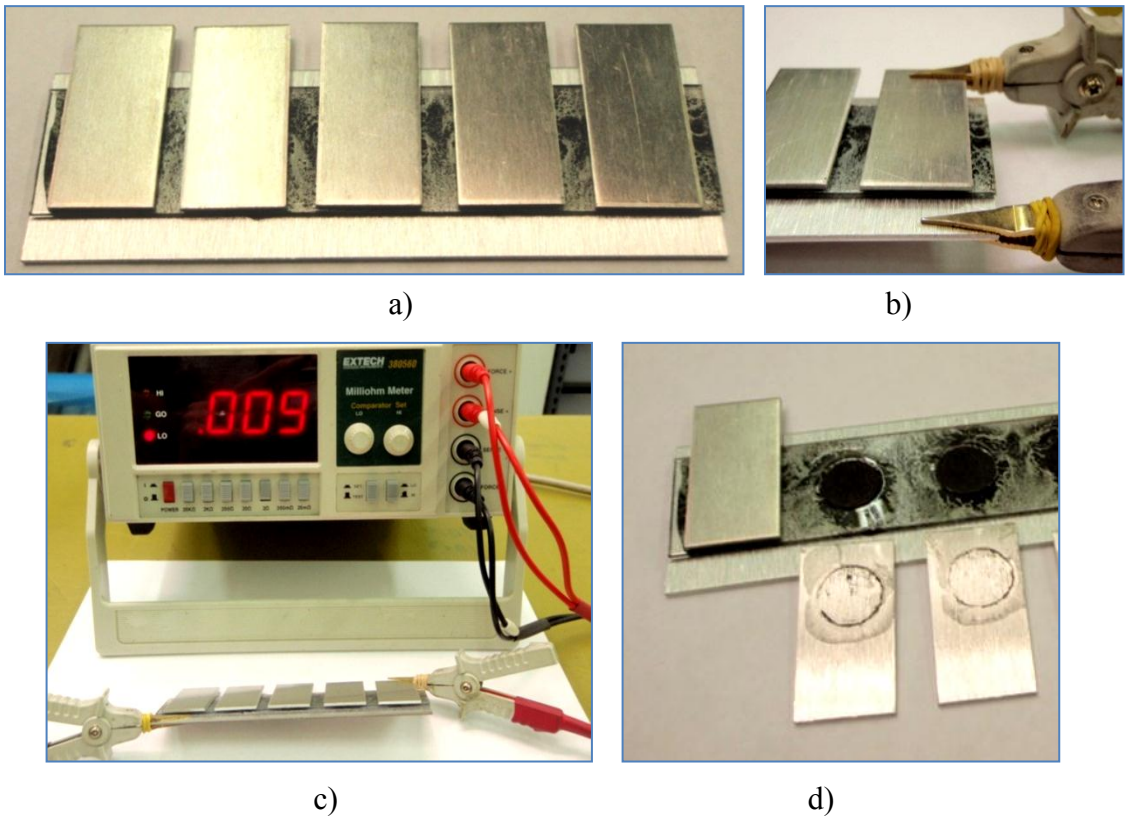

Figure 2.4: Test samples for measuring bond gap resistance and resistivity of conductive adhesive samples: a) Test strip, b) Kelvin probe resistance reading contact method (large backplate serves as common ground), c) global view of specimen under test, d) sample showing discs filled with nanostrand adhesive.

2.3.3 Lap Shear Strength

The primary purpose of this study was to develop ECA systems that retained the structural strength of the host adhesive while presenting low electrical resistance. The primary test method for structural properties used in this study was lap shear according to ASTM D1002 [17]. Both aluminum and carbon fiber composite adherends were tested. Aluminum adherends were found to be necessary for matching the adhesive manufacturer's published strength properties. Carbon fiber adherend test data are presented for comparative aerospace purposes.

2.3.4 Thermal Effects

Thermal effects were investigated to study the mechanical integrity of nanostrand adhesive in extreme environments. Adhesive strength degradation by thermal cycling was tested by cycling bonded lap shear samples 25 times from -57 °C to +100 °C, with specimens of unmodified adhesive and nanostrand adhesive. Cycled specimens were compared to uncycled specimens using ASTM D1002. Quasi-isotropic carbon fiber composite plates of M55J fibers and RS3 resin were used for adherends.

2.4 Results and Discussion

2.4.1 Electrical Results

The results presented herein represent a general design envelope for the electrical properties of nanostrands in 9396 epoxy adhesive. Figure 2.5 presents the bond gap resistance as a function of bond thickness for several nanostrand concentrations. The primary data series shown are for a standard dispersion method at typical bond

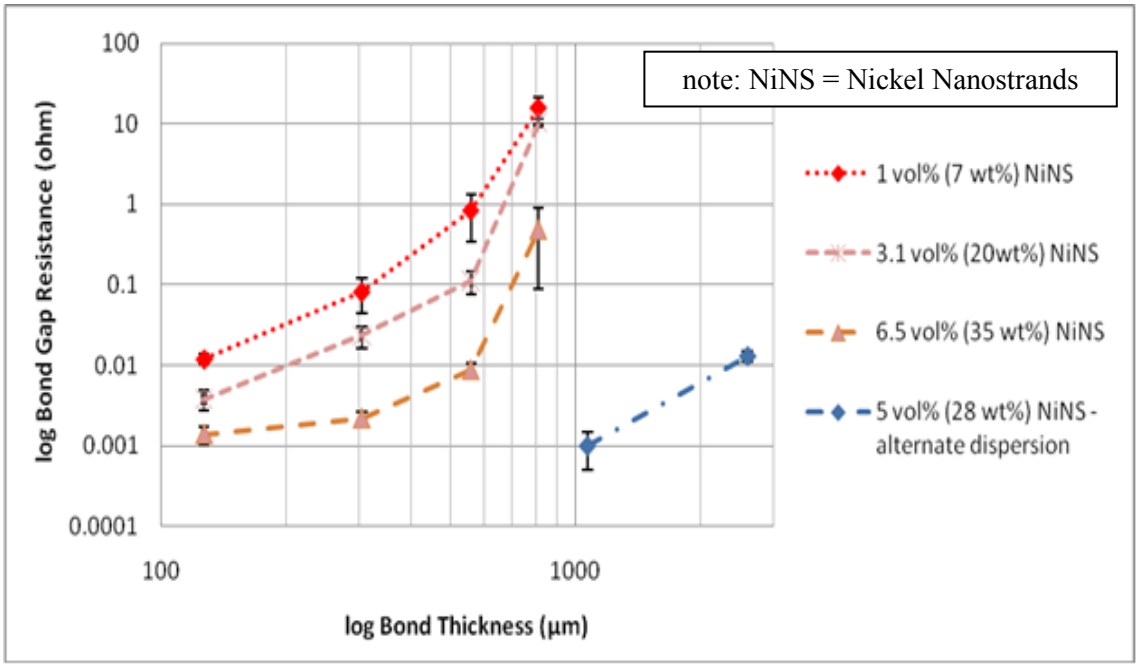

Figure 2.5: Electrical resistance across bond gap of nickel nanostrand filled Hysol 9396 epoxy joints (brushed #4 6061-T6 adherend, 12.7 mm diameter contact pad). Error bars represent plus or minus one standard deviation.

thicknesses. These electrical results correlate to the structural properties presented in Section 3.2. An alternate dispersion method produced an adhesive mixture that had a significantly higher viscosity, but also significantly lower resistance properties (as low as 0.012 ohm-cm at 5 volume percent nanostrands). Results using the alternate method have been regularly repeated in laboratory investigations with thick bonds, but have not yet been the subject of further development. The structural properties of adhesive mixtures using this alternate dispersion method are not yet well known. Resistance values below 100 milliohms are seen in all formulations for bond thicknesses at or below 305 µm. Milliohm resistance is seen at thinner bondlines, and subohm resistance is seen at bond thicknesses up to 762 µm.

Resistivity values are calculated by:

$$\rho = RAl^{-1} \quad [2.1]$$

where ρ is the bulk resistivity (ohm-cm), R is the resistance value (ohm) across a path of length l (cm) and contact area A (cm^2). Test results indicate that calculated bulk resistivity may range across 5 orders of magnitude, from 0.01 ohm-cm to over 100 ohm-cm, as seen in Figure 2.6.

The apparent increase in resistivity with bond thickness is likely due to an increasing number of particle to particle interconnects. While resistivity is intended to be an invariant material property, the nature of conduction in metal filled polymer systems, or any composite system, includes both microscale (such as quantum tunneling) and macroscale (distribution, contact resistance between particles) parameters. The diameter of a single nanostrand is 50 – 500 nm, however, the mean diameter of a nanostrand nanostructured cluster as distributed in a polymer (identified in Figure 2.2) is from approximately 100 μm up to a millimeter. This nanostructured aggregate is what forms a percolated pathway between bonded surfaces. Thin bond lines (a "shorter path") allow this pathway to be formed with minimal (if any) junctions between nanostrand clusters. However, as the bondline increases in thickness (a "longer path"), the percolation pathway will include an increasing number of junctions between nanostrand bodies. These parameters contribute nonlinearly to increases in the electrical resistivity of the ECA. Accordingly, the calculated electrical resistivity of the material will vary with the geometry of the test sample. Figure 2.7 gives a graphical explanation of electrical

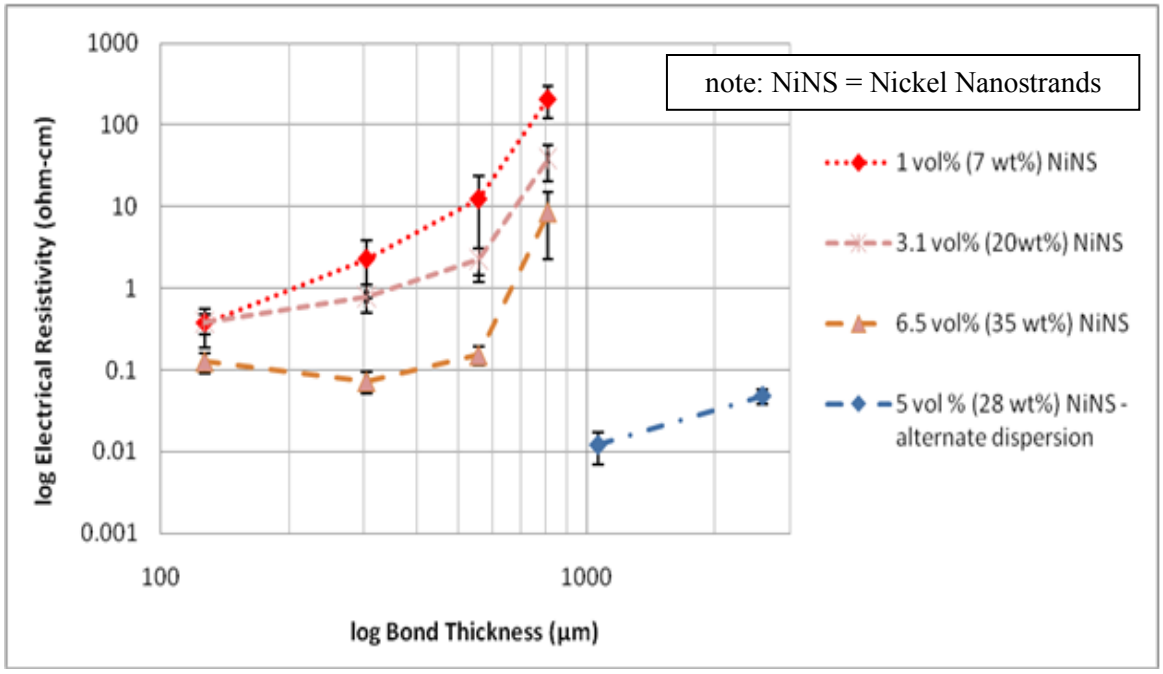

Figure 2.6: Electrical resistivity of nanostrands in Hysol 9396 adhesive disc samples (brushed #4 6061-T6 adherend, 12.7 mm diameter contact pad). These values are calculated from the same samples used for bond gap resistance tests in Figure 2.5. Error bars represent plus or minus one standard deviation.

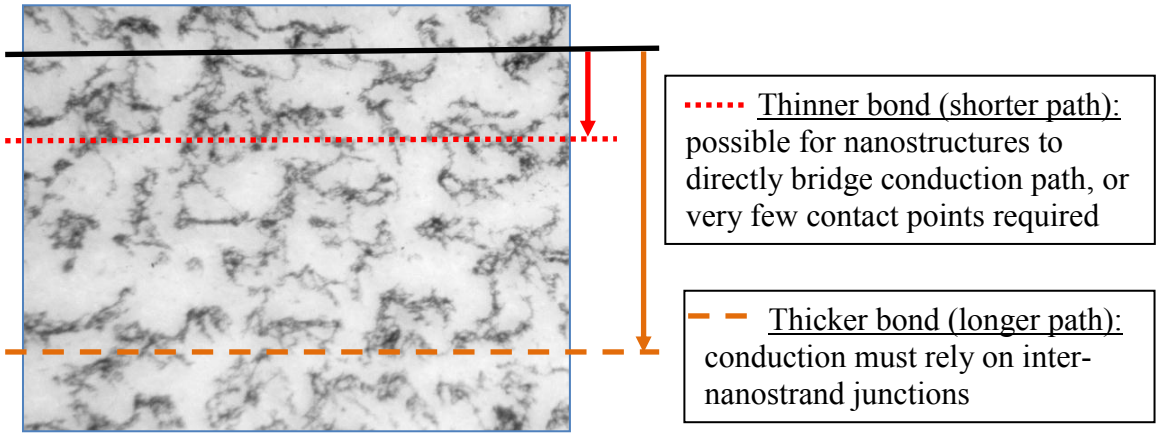

Figure 2.7: Schematic showing effect of bond thickness on conduction mechanisms between bonded surfaces (side view). Thin bond lines may be bridged directly by nanostructured aggregates, while thicker bond lines must have more junctions between the conducting elements.

conductivity considerations with respect to bond line thickness (see also [18]). Electrical conductivity results were compared to various literature values for carbon nanofiber filled adhesives [11-13, 19]. For all samples, the bond thickness is 0.127 mm. Values from the literature are for 5 volume percent of conductor. New values are also reported as part of this effort. For these samples, the volume loading of nickel nanostrands (NiNS) is 3.1 percent, and the volume loading of carbon nanofibers (CNF) is 3.5 percent. The samples from this study likely provide the most accurate contrast, as they are a direct comparison from within the same experiment. All resistance values are compared in Figure 2.8.

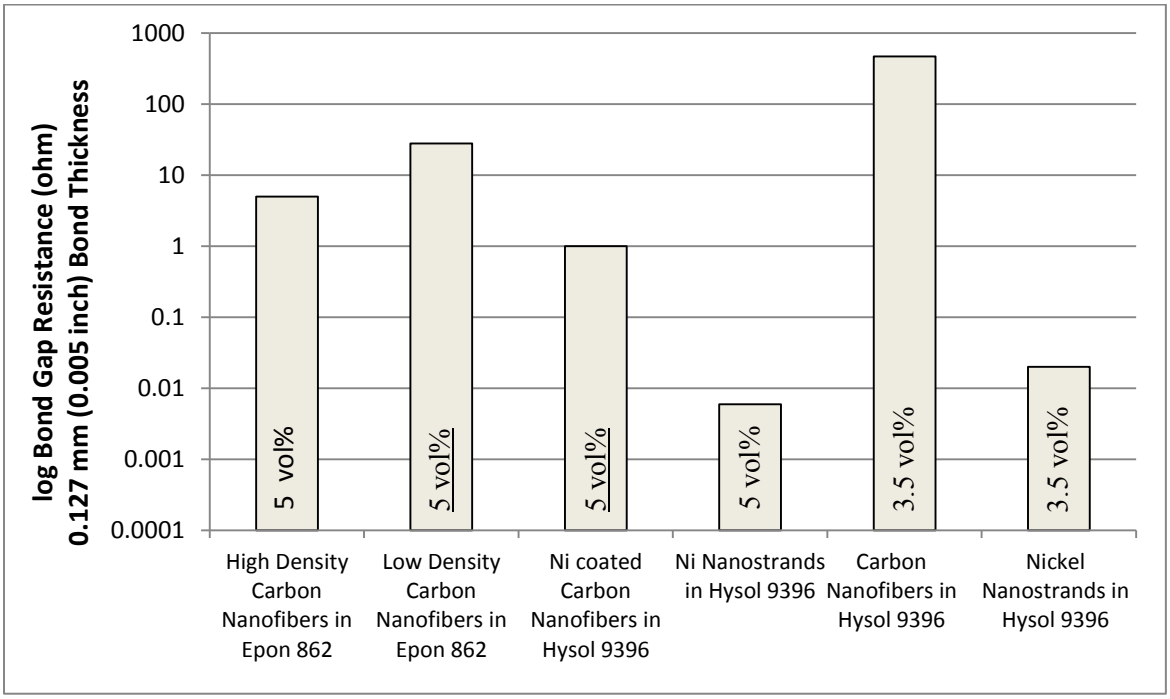

Figure 2.8: Bond gap resistance of carbon nanofibers and nickel nanostrands in adhesive. Nanostrand adhesives are orders of magnitude more conductive than carbon nanomaterial adhesives at equivalent loadings.

The general trend observed is that nanostrand adhesive formulations are several orders of magnitude more conductive than carbon based nanomaterials. This observation is likely due to several factors, including conductor geometry, intrinsic conductivity, dispersion state, and the number of interparticle contacts. The improvement seen by nickel coating of carbon nanofibers indicates a likely decrease in contact resistance, but that does not fully account for the decrease in resistance seen with nanostrands.

2.4.2 Structural Results

Lap shear properties were tested for several formulations of conductive adhesives using both carbon nanofibers and nickel nanostrands. These formulations include a proprietary dispersion method that produced an increase in the lap shear strength of the adhesive joint. These data points are denoted in Figure 2.9 with a star symbol (*). Several different formulations are capable of this increase in lap shear strength while providing electrical conductivity across the bond gap. All of the data in Figure 2.9 are for aluminum adherends prepared according to ASTM D3933 [20].

Matching the strength of unfilled adhesive while imparting excellent conductivity is an exciting and pertinent result of this research effort. Furthermore, this has been achieved with multiple conductive fillers, including nanostrand fillers capable of milliohm level gap resistance. These results indicate excellent adhesive strength relative to previously reported values [21].

Scanning Electron Microscope (SEM) images of joint failure surfaces were obtained following testing. In addition to investigating the failure modes observed, these images

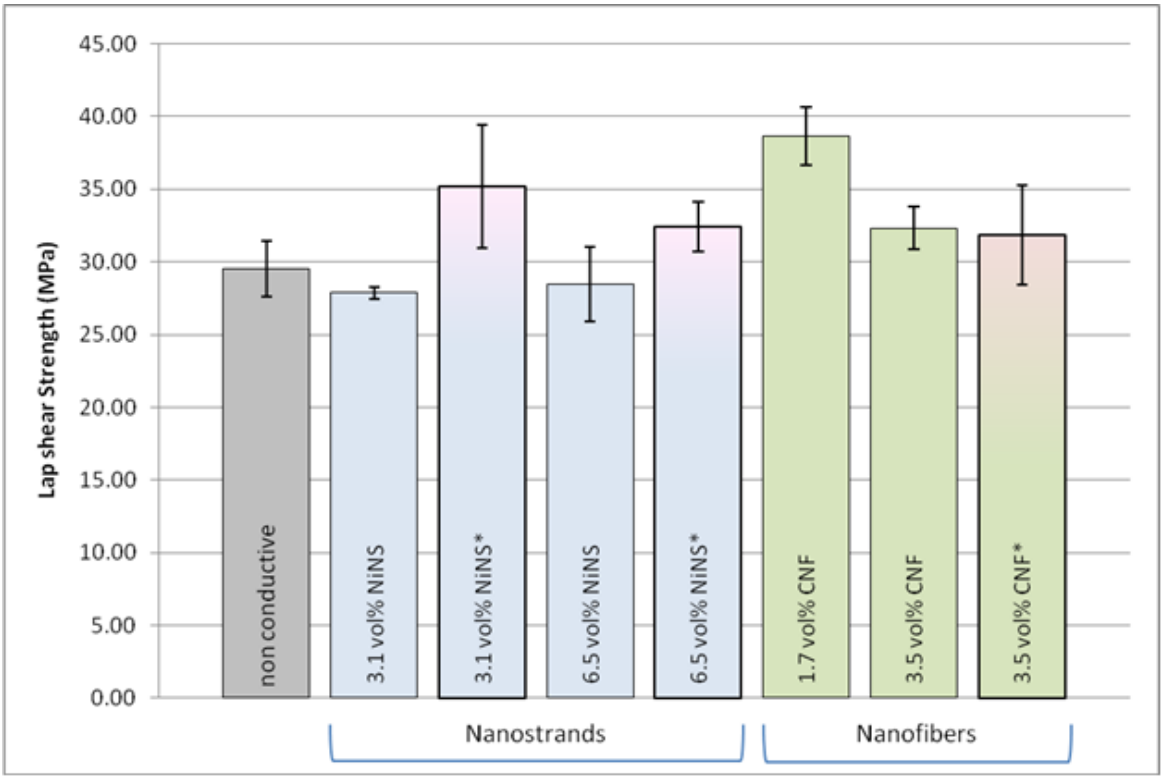

Figure 2.9: Lap shear strength of electrically conductive Hysol 9396 made with nickel nanostrands and carbon nanofibers.

were used to investigate the dispersion state of the conductive fillers. Example SEM images are shown in Figure 2.10 for nickel nanostrand and carbon nanofiber fillers. These SEM images indicate uniformity of dispersion for both conductive fillers.

The lap shear strength of nickel nanostrands in Hysol 9396 for carbon fiber composite adherends is shown in Figure 2.11. Bonded surfaces were prepared by abrading with 100 grit sandpaper, then cleaning with technical grade isopropyl alcohol immediately prior to bonding. These data have been normalized by dividing all values by the tested strength of the unmodified adhesive.

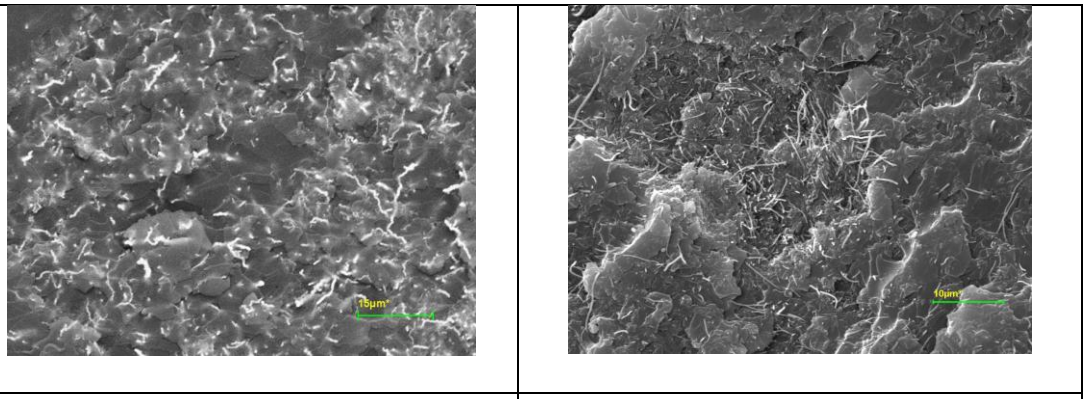

3.1 vol% Nickel Nanostrands	3.5 vol% Carbon Nanofibers

Figure 2.10: SEM micrographs of nickel nanostrand and carbon nanofiber ECA lap shear fracture surfaces. 10 µm scale bar.

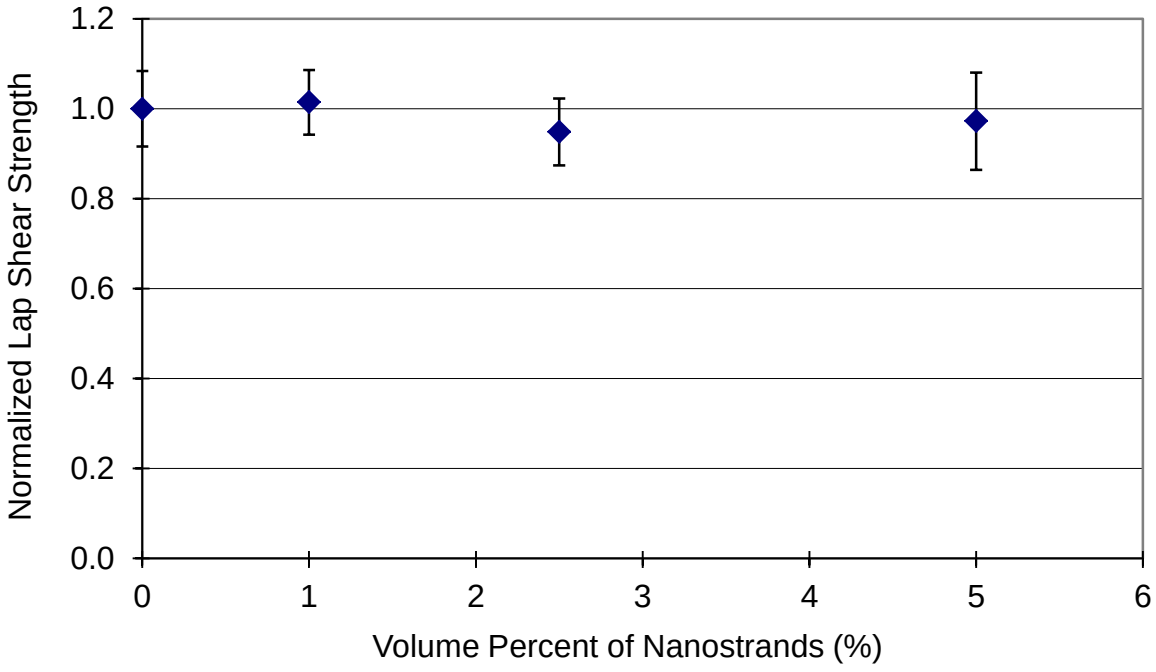

Figure 2.11: Lap shear strength of Hysol 9396 as a function of volume percent of nickel nanostrands. Carbon fiber composite lap plates tested as per ASTM D1002.

Thermal cycling testing was also conducted on lap shear samples with composite adherends. This test included only unfilled adhesive and 5 vol% nanostrand adhesive. Results from thermal cycling testing, shown in Figure 2.12, indicate that there is no statistically significant loss in lap shear strength after thermal cycling for nanostrand filled adhesive. These results have been normalized by dividing all values by the tested strength of the nonconductive and nonthermally cycled adhesive. Other authors have reported similar results for the lap shear strength of thermally cycled nanoconductor filled electrically conductive adhesive joints [11].

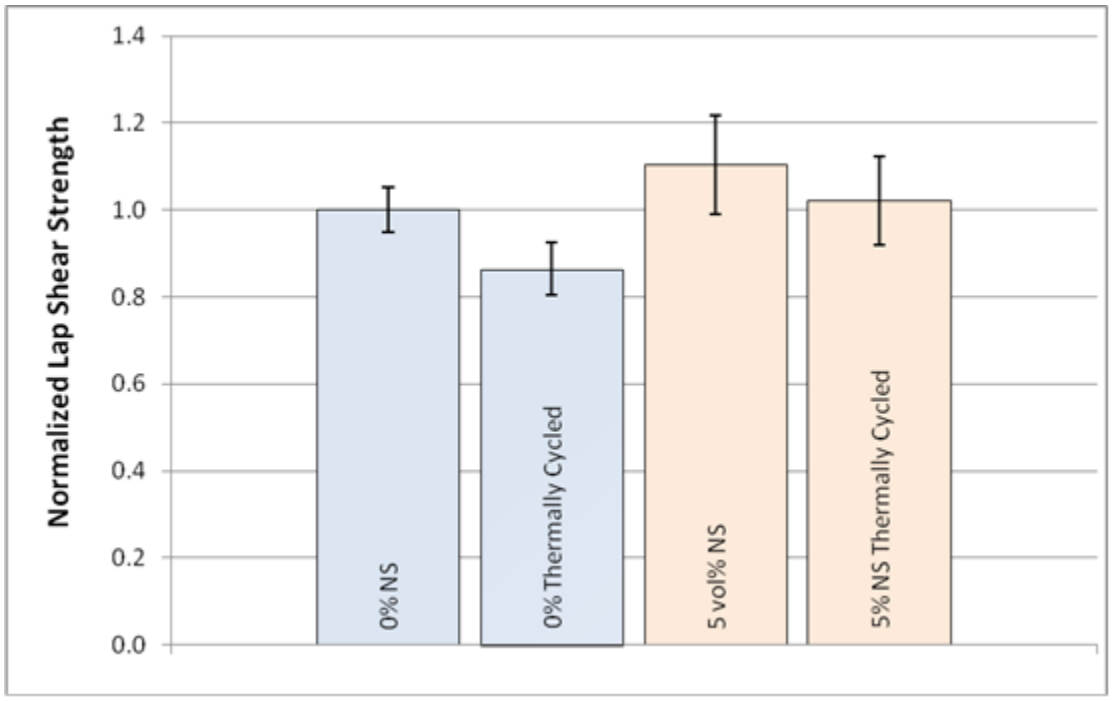

Figure 2.12: Lap shear strength of Hysol 9396 and nickel nanostrands in Hysol 9396 adhesive before and after thermal cycling. Samples were tested using carbon fiber composite adherends as per ASTM D1002.

2.5 Conclusion

The development of full strength structural conductive adhesives can enable a wide range of applications where the strength of currently available ECA systems is a limiting factor. Structural ECA systems have been investigated at low volume fractions of carbon nanofibers and nickel nanostrands, with superior conductivity results provided by the nickel nanomaterials. Milliohm gap resistance and resistivity on the order of 10^{-2} ohm-cm are possible at loadings of 5 volume percent. Initial results indicate that these systems present good survivability in thermal cycling conditions.

2.6 Acknowledgements

This work was funded, in part, by the United States Air Force under Contract No. FA8650-08-C-5009 under the direction of Mr. Max Alexander, Air Force Research Labs, Wright Patterson Air Force Base, Ohio.

2.7 References

1. R. Gomatam and K.L. Mittal (Eds), *Electrically Conductive Adhesives.* VSP/Brill, Leiden (2008).

2. D. D. Lu, Y. G. Li. and C. P. Wong, *J. Adhesion Sci. Technol.* **22,** 815-834 (2008).

3. G. Hansen, *SAMPE J.* **41,** 24-28 (2005).

4. J. Burghardt, N. Hansen, L. Hansen and G. Hansen, *The Mechanical and Electrical Properties of Nickel Nanostrands in Hysol 9396 Epoxy,* in: *Proc. International SAMPE Symposium Exhibition,* Long Beach, CA, USA, **51,** (2006).

5. J.-M. Park, S.-J. Kim, D.-J. Yoon, K. L. DeVries and G. Hansen, *Composites Sci. Technol.* **67,** 2121-2134 (2007).

6. O. K. Johnson , C. J. Gardner., D. T. Fullwood, B. L. Adams, N. Hansen and G. Hansen, *Computers, Materials & Continua* **15,** 87-112 (2010).

7. G. Hansen, J. A. E. Bell, G. Poe, M. Alexander, S. Juhl, B. Black, H. Dowty, *Multifunctional Thermoplastic Polyimide Composites,* in: *Proc. SAMPE Fall Technical Conference,* Dallas, TX, USA, **51,** (2006).

8. K. Li, X.-L. Gao. and J. C. Fielding, in: *Proc. 48th AIAA/ASME/ASCE/AHS/ASC Structures, Structural Dynamics, and Materials Conference,* Honolulu, HI, USA, **7,** 6822-6832 (2007).

9. L. Li, C. Lizzul, H. Kim, I. Sacolick and J.E. Morris, *IEEE Trans CMHT* **16,** 843-851 (1993).

10. M. Komagata, K. Yokoyama, Y. Tanaka and K. Suzuki, in: *Proc. 18th IEEE/CPMT International*, Omiya, Japan, pp. 429-432 (1995).

11. N. Gagliardi, B. Rice and K. Lindsay, *Formulation and Evaluation of Carbon Nanofiber-based Conductive Adhesives - II*, in: *Proc. SAMPE Fall Technical Conference,* Cincinnati, OH, USA, **52,** (2007).

12. L. Jing and J. K. Lumpp, in: *Proc. 2007 IEEE Aerospace Conference*, Big Sky, MT, USA, pp. 1-6 (2007).

13. G. G. Tibbits, M. L. Lake, K. L. Strong and B. P. Rice, *Composites Sci. Technol.* **67,** 1709-1718 (2007).

14. E. Sancaktar and N. Dilsiz, *J. Adhesion Sci. Technol.* **11,** 155-166 (1997).

15. G. Hansen, N. Hansen, D. O. Adams, J. Burghardt, D. Widauf and T. McNeill, *Electrically Conductive Putty Type Repair System for Composite Structures,* in: *Proc. International SAMPE Symposium Exhibition,* Baltimore, MD, USA, **52** (2007).

16. ASTM D2739 – 97(2004): Standard Test Method for Volume Resistivity of Conductive Adhesives.

17. ASTM D1002 – 05: Standard Test Method for Apparent Shear Strength of Single-Lap-Joint Adhesively Bonded Metal Specimens by Tension Loading (Metal to Metal).

18. Y. Wie and E. Sancaktar, *J. Adhesion Sci. Technol.* **10,** 1199-1219 (1996).

19. T. Gibson, B. Rice, W. Ragland, E. Silverman, H.-H. Peng, K. L. Strong and D. Moon, in: *Proc. International SAMPE Symposium Exhibition,* Long Beach, CA, USA, **50,** 1713-1726 (2005).

20. ASTM D3393 – 98(2004): Standard Guide for Preparation of Aluminum Surfaces for Structural Adhesive Bonding (Phosphoric Acid Anodizing).

21. J. Li, J. K. Lumpp, R. Andrews and D. Jacques, *J. Adhesion Sci. Technol.* **22,** 1659-1671 (2008).

3 QUANTITATIVE METHODS FOR CORRELATING DISPERSION AND ELECTRICAL CONDUCTIVITY IN CONDUCTOR POLYMER NANOSTRAND COMPOSITES

Nathan Hansen[1], Daniel O. Adams[1], David T. Fullwood[2]

[1] University of Utah
Department of Mechanical Engineering
50 S. Central Campus Dr. Room 2110 - MEB
Salt Lake City, UT 84112, USA

[2] Brigham Young University
Department of Mechanical Engineering
435 Crabtree Building,
Provo, UT 84602, USA

Submitted for Publication in Composites Part A: Applied Science and Technology.

3.1 Abstract

The development of electrically conductive polymer composite systems continues to be an area of wide interest. In this work, a method is presented for quantifying the macroscale dispersion characteristics of electrically conductive nickel nanostrands in polymer systems. A single polymer system is considered at multiple volume fractions of nanostrands, with variations in dispersion processing practices. Image analysis methods based on statistical homology parameters are developed to characterize samples of the dispersed nanostructure, including nearest neighbor distance, mean cluster size, area/perimeter ratios, and topological Betti number metrics. It is found that the Betti numbers are particularly well suited for monitoring nanostrands dispersed in polymer systems. Correlation of the dispersed structure to the electrical conductivity properties of the nanocomposite system is demonstrated. The method is well suited as a batch sampling technique for monitoring nanostructures during dispersion processes, and is also analogous for any dispersed system that involves highly structured materials.

3.2 Introduction

Polymer and fiber reinforced composites play an increasingly important role in commercial and defense sectors. While these systems are often well suited for replacing metallic structures with respect to mechanical and processing properties, the electrical properties of polymeric and fiber reinforced polymeric systems are significantly less conductive than metallic systems. This transition to polymeric structures and systems

occurs concurrently with growth in the utilization of and reliance on digital technologies, where electrical conductivity properties are increasingly critical.

Metals present a naturally conductive material, as metals generally have isotropic properties and free valence electrons to facilitate conduction. Composites are naturally not as well suited for electrical conductivity purposes, consisting of dielectric fibers or moderately conducting fibers in an insulating matrix. Thus, the challenge is to find methods of engineering electrical conductivity and electromagnetic shielding properties into polymers and composite systems while preserving the intrinsic advantages (mechanical, manufacturing, density, cost, etc.) of the polymer composite material. Electrically conductive polymer composites are desired in a large range of applications, including grounding, protection from electrostatic discharge (ESD), electromagnetic interference (EMI), and lightning strike effects (both direct and indirect). It should be noted that the above list considers only end use requirements of polymer composites, and there are other potential advantages to conductive polymer composites in processing, application, and extended multifunctional roles.

Traditional solutions for conductivity in polymers and composites have included metal filled polymers and intrinsically conductive polymers, along with meshes, foils, and wires for laminate structures. Metal filled polymer solutions have been incorporated directly into structures and also applied as a secondary surface coating. Conventional fillers materials, such as metal coated spheres or metal flakes, generally require a relatively high filler volume fraction for electrical percolation and conductivity.

The rapidly growing field of nanotechnology has presented many new and exciting materials that can be used more efficiently and with better performance than previously possible. The ability to design and create at the nanoscale has afforded new concepts and materials to help improve the electrical conductivity in composites [1,2]. Newly available conductive nanoparticles have shown great advances over previously available conductive particles for increasing the conductivity of polymer composites [3-5].

These new nanomaterials demonstrate some fundamental differences from previously available conductive particles, primarily in geometry. There are many important factors in adding conductive particles to nonconductive matrixes. Particle geometry is of primary importance. While previous conductive additives (such as milled powders, coated spheres, platelets, etc.) have aspect ratios on the order of 1 to 10, newer nanoparticles (such as carbon nanofibers) have aspect ratios in the thousands. This fact, in combination with the nanoscale diameter of these particles, means that less material is required, both in terms of volume percent and weight percent, to achieve the same conductivity levels [6-9].

The objective of the current study is to seek understanding of the structure property relationships that govern conduction in metal nanomaterial filled polymers; specifically, those using nickel nanostrands. Such polymer nanocomposites have shown great promise in a wide range of applications, and a need exists for an advanced understanding of the conduction mechanisms with composites samples. The main objective of this work is to develop a method for characterizing and quantifying the dispersed nanostrand structure. The *in situ* nanostructure parameters will then be correlated to nanocomposite electrical

resistivity properties. The methods developed will be analogous to other systems that involve dispersion of highly structured materials.

3.3 Metal Filled Polymers

Electrical properties of metal filled polymer systems can be modeled using percolation theory[10-13]. Classical percolation theory considers a network of conductive links in a nonconductive matrix, and models the connectivity across an infinite sample of a network structure. In a nanostrand composite, this network structure is created by nanostrands connecting throughout the sample. When a sufficient volume of nanostrands are present to create an electrically conductive path through a volume, an abrupt change is conductivity is observed, referred to as the percolation threshold. For loadings at and above this value, the resistivity of the composite follows a power law given by [14]:

$$\rho \sim (v - v_c)^{-t} \tag{3.1}$$

where v represents the volume fraction of conductive material, v_c represents the critical volume fraction of the percolation threshold, and t is a universal constant, which for a three-dimensional material approximately equals 2 (variations in the scaling exponent have been reported, for example, see reference [15]).

The resistivity of the composite continues to follow this power law until a percolation limit is reached. This loading presents a limiting value for the formation of well dispersed conductive networks. For loadings above this value, a decrease in electrical and mechanical properties is observed, indicating that the polymer host is no

longer capable of facilitating additional increase in metallic filler. A typical curve representing these behaviors is given in Figure 3.1.

Parameters such as aspect ratio, curvature and alignment of fillers often factor strongly in percolation models [16-19]. In a filled polymer composite, electrical resistivity is dominated by resistance between contacting or neighboring conductive elements (these contact areas are referred to as junctions), with the resistance across a connected component of conductive filler often adding a negligible amount to the total. For junctions with very small gaps (of the order of 1 nm) the junction resistance may be modeled by assuming a quantum tunneling effect [20]. A combined tunneling percolation model has been applied to carbon nanocomposites with reasonable results [21,23]. Recent studies have shown excellent correlation for the application of this combined tunneling percolation model to piezoresistive nanostrand polymer composites [24].

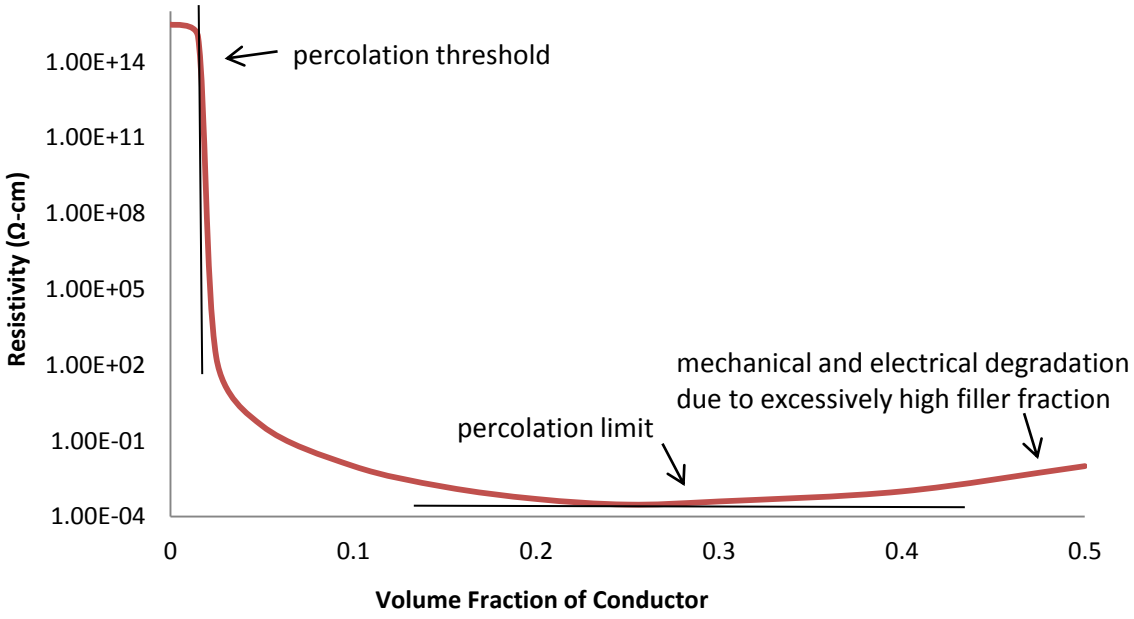

Figure 3.1: General electrical percolation behavior of conductor filled polymer systems.

3.4 Nanostrands: Metal Polymer Nanocomposites

Nickel nanostrands [24] are a relatively new material that offers significant advantages over alternative conductive fillers due to their metallic and geometrical properties. They are a submicron diameter, high aspect ratio nanostructure. Nanostrands feature an intrinsic three-dimensionally interconnected structure that creates completed loops and demonstrate a branched nature (see Figure 3.2).

Nanostrands are manufactured by a proprietary "bottom up" manufacturing method, using low temperature Chemical Vapor Deposition (CVD), as a continuously interconnected "cake" of highly structure nickel chains. This continuous form can be reduced to a nanostructured high porosity three-dimensional powder (see Figure 3.3).

Nanostrands can be used in composites via two methods. First, this "cake" can be used as a preform and infused with polymer. Second, the nanostructured aggregate powder form can be dispersed in a host matrix. The latter practice is most typical. Nanostrand powder clusters contain major nanostrands that interconnect and also contain branches, some of which interconnect again and some of which contain open ends. These nanostructured clusters are the key to the observed performance of nanostrand polymer composites, and to understanding their structure property relationships. Nanostrand structures at various volume fractions are visible in Figure 3.4.

The unique properties of nickel nanostrands are well suited to achieving excellent conductive properties in polymers relative to other metal fillers or nanoparticles. The high aspect ratio of individual strands requires fewer particles for effective volumetric percolative properties. The looped and branched nature of the nanostrand structure allows

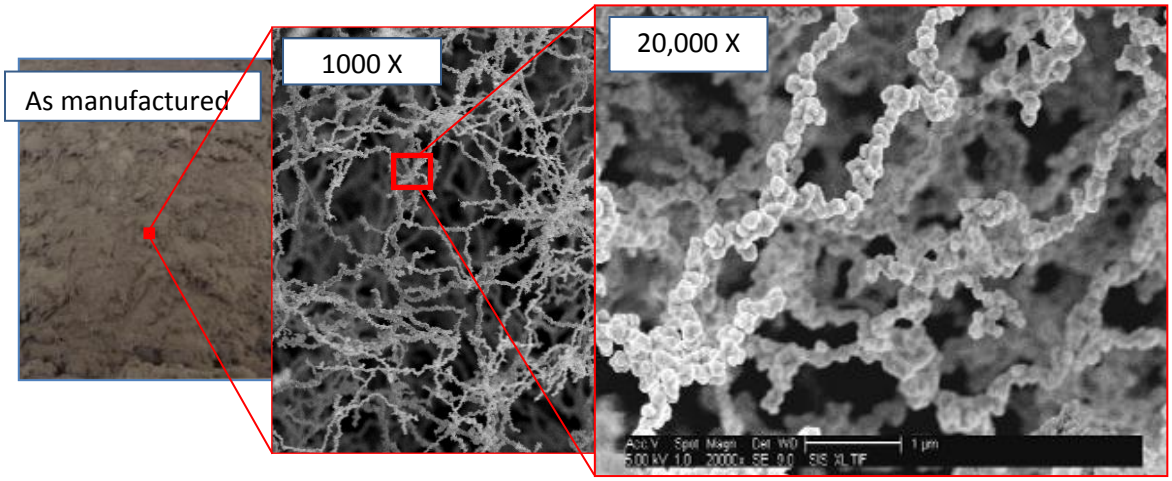

Figure 3.2: Nickel nanostrands, as manufactured, increasing magnification from 1x to 20,000x.

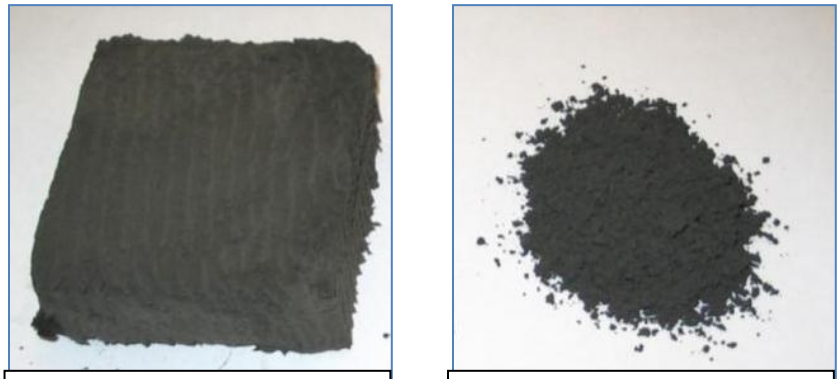

Figure 3.3: Nickel Nanostrand "cake" (left) and nanostrand "powder" (right).

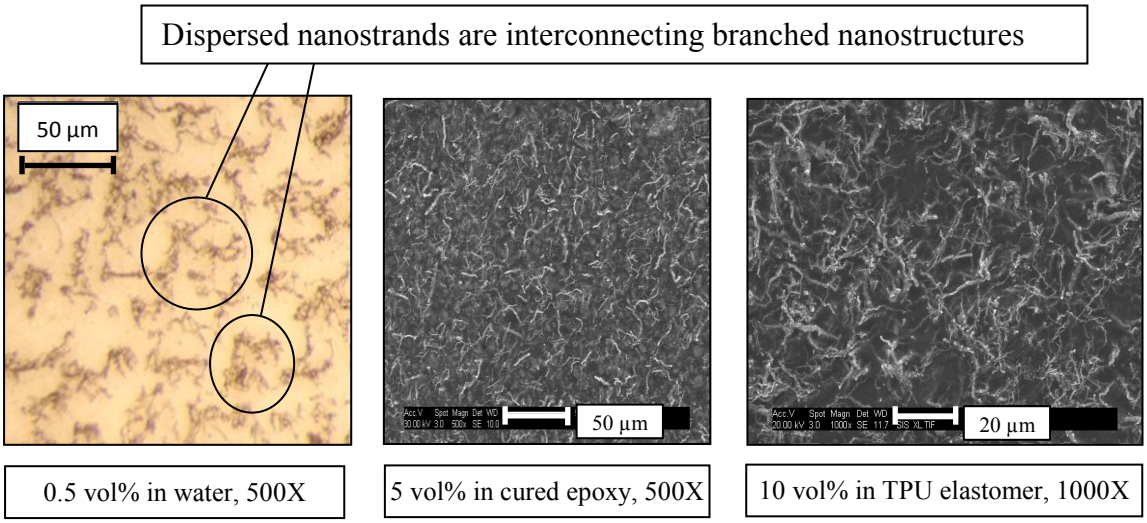

Figure 3.4: Left to Right: Nickel nanostrands dispersed in water at 0.5 volume percent, optical micrograph (50 µm scale bar), cured epoxy at 5 volume percent, SEM backscatter image (50 µm scale bar), and TPU elastomer at 10 volume percent, SEM backscatter image (20 µm scale bar).

for a high number of three-dimensional interconnects, and therefore higher conductivity. This looped nature also has some important implications in electromagnetic shielding performance. The branches on each strand help create further radial interconnects, and provide additional three-dimensional connection opportunities (for example, two parallel nanostrands do not need to intersect along their major axis, but can rather connect with branches extending transverse from the major axis). This branched nature can also offer benefits in mechanisms requiring wave properties, as the branches can serve as a multiplicity of antennas and transmitters.

A further feature found in nanostrand geometry is that the particle can be viewed as a "skeleton" rather than a full "body" (as with more solidly structured additive particles).

The void space of the nanostrand structure is thus filled with the host substrate, potentially facilitating better bonding and preservation of material properties while providing a conductive skeleton structure. Nanostrand mixtures will percolate to much higher conductivity levels than have been demonstrated with carbon nanomaterials [6,7,10,25].

As a metal, nickel benefits from a metallic bonding structure, high electrical conductivity, and ferromagnetic properties. The raw material cost of nickel is relatively low, and corrosion resistance is quite good. However, nanostrands are relatively weak compared to carbon nanofibers. Nanostrand materials are formed as a crystalline chain structure, and are therefore sensitive to processing methods which can break down the structure and reduce the aspect ratio and interconnects of the structure. Care must be taken when producing nanostrand mixtures to not over mix the system and break down the strands [24,27].

3.5 Understanding Conductivity in Nanostrand Polymer Composites

Nanostrand polymer composites have been shown to achieve conductivities in excess of 5000 Siemens/cm, and have been demonstrated in applications including electrostatic discharge [24], electromagnetic shielding [28-30], conductive adhesives [31,32], caulks and gaskets [33], paints [26,34], and lightning strike protection [28,34-38]. Previous studies have indicated that the resultant conduction of a nanostrand composite can depend on multiple factors. For example, an early study [39] indicates that the resistivity of nanostrand composites is a function of the type of polymer used. These studies serve as a foundation

for elucidating nanostrand behaviors and identify the variables which are most salient to electrical conduction. To date, the majority of studies on nanostrand systems have dealt with the empirical results of nanostrand polymer composites. Few authors have sought or developed an understanding of the structure and mechanisms of conductivity within nanostrand polymer composites. The goal of this study is to develop tools to correlate dispersion characteristics to nanocomposite bulk electrical resistivity.

3.6 Materials and Methods

3.6.1 Materials

The polymer chosen for this study is a widely available commercial water based coating system, Minwax® Polycrylic® acrylic/urethane. This system was chosen for its optical clarity, ease of use, commercial availability, relevant applications, and correlation to previous data [26,40]. The system was used in the as received state, which was found to be 31 weight percent polymer solids with a cured resin density of 1.2 g/cc. Nickel Nanostrands were provided by Conductive Composites and dispersed according to the manufacturer's recommendations, with a density value of 8.92 g/cc. Volume and mass fractions were calculated based on the densities of each constituent. All samples were mixed by mass fraction.

3.6.2 Dispersion: Conductivity Samples

A desired volume fraction of nickel nanostrands was added to a polymer sample, then "wet" by manual mixing methods. Dispersion was achieved by using a Thinky AR-250 centrifugal double planetary mixer. A mixing duration of 20 seconds at 2000 rpm

was used for baseline samples. This nanostrand polymer composite was then used as a conductive coating. Coating samples were screened through a -50 woven stainless steel mesh before spray application. Witness films were produced by spraying for different mixing durations, from 20 seconds (minimum mixing time) to 500 seconds (intentionally overmixed). Spray coatings were applied with a DeVilbiss FLG-3 High Volume Low Pressure (HVLP) gravity feed spray gun. A size 22 tip and Size 3 HVLP air cap were used, with nozzle pressure typically below 10 psi.

3.6.3 Dispersion: Imaging Samples

Nanostrand polymer systems typically are visibly percolated at volume fractions of nanostrands above 0.5%, and imaging of samples above this loading is challenging (due to the superposition of strands). However, the electrical conductivity of the nanocomposite at these levels is very close to the percolation threshold, and results can be highly sensitive with respect to differences in conductor volume fraction. Accordingly, samples for image analysis and dispersion characterization were taken at 0.1 volume percent of nanostrands. This low volume fraction allows for easier identification of discrete nanostrand structures. Images at this low volume fraction are then correlated to the conductivity of samples at 10 volume percent of nanostrands that are produced using identical dispersion procedures. These higher loading are closer to the percolation limit, where conductive behaviors are much less sensitive to slight changes in conductor volume fraction. Thus, the low volume fraction samples easily allow the feature of the nanostrands to be measured, while the higher volume fraction provides more reliable conductivity results for a given loading.

Multiple samples from each mixture were taken at various stages in processing. Three drops of nanostrands dispersed in fluid were taken from each sample and placed on a microscope slide, and each drop was then placed under a digital microscope at a fixed magnification. Three images were taken from each sample drop.

3.6.4 Resistivity and Thickness Measurements

Areal surface resistivity readings on coating samples were taken using an ohm-per-square jig and a four point Kelvin probe resistance method (per MIL-DTL-83528C [41]). The ohm-per-square jig uses two copper bars 2.54 cm in length and 6.35 mm wide, and 6.35 mm high. These bars are bonded to a jig that separates them by a distance of 2.54 cm, thus a unit square with a surface area of 6.45 cm^2 is measured between contact paths. Kelvin probe leads are attached to each bar, and resistance readings are taken across the surface of each sample. An Extech 380560 High Resolution Precision Milliohm meter was used for all resistance readings below 20 kΩ. In the rare case of resistances above 20kΩ, readings were taken with a handheld multimeter. Thickness readings were taken with a micrometer with 0.00254 mm (0.0001 inch) capability. Sample conductivities were calculated using a thin film approximation and surface resistivity according to:

$$\sigma^{-1} = \rho = R_s(A/l) \tag{3.2}$$

where σ is the electrical conductivity of the nanocomposite (Siemens/cm), ρ is the electrical resistivity (ohm-cm), R_s is the surface resistivity (ohm-per-square), l is the length of the separation path (cm), and A is the cross sectional area of the film between contact bars (given by l multiplied by the film thickness).

3.7 Results and Discussion

3.7.1 Spray Film Electrical Percolation

Test specimens of nanostrand polymer mixtures were spray applied (for uniformity) to an electrically insulating Kapton® polyimide film substrate, then tested for electrical resistivity. The data for these are given in Figure 3.5. The electrical resistivity trend follows the behavior shown in Figure 3.1; showing that the percolation threshold is passed at low volume fractions, and the percolation limit is approached in the 20 volume percent range.

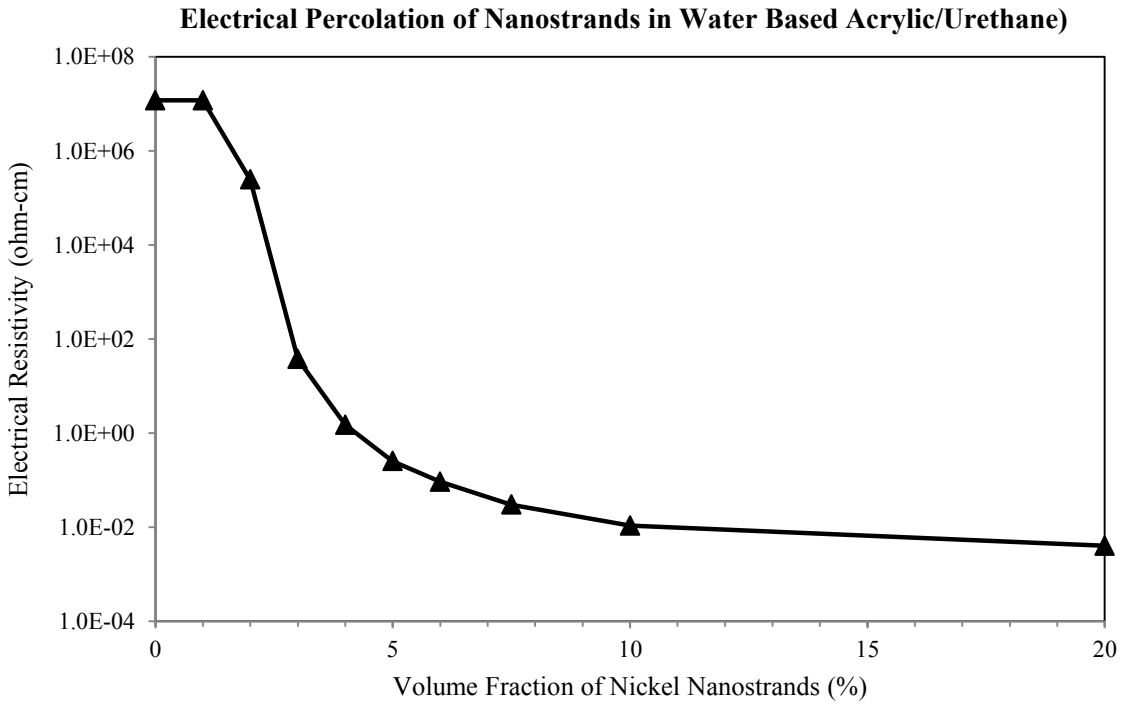

Figure 3.5: Electrical resistivity of nanostrands in water based acrylic/urethane polymer films.

3.7.2 Processing Conditions and Resistivity

The length of mixing time is a strong factor in the conductivity of a nanostrand composite, as excessive mixing will degrade the aspect ratio of the conductors. The data in Figure 3.6 show the relationship of mixing time to film conductivity for sprayed coating films at 15 volume percent nanostrands with a 0.10 mm film thickness. For this system and mixing method, 20 seconds is a general minimum mixing time. Mixing for 60 seconds by this method is representative of a sample that has settled and been remixed several times. Mixing for 500 seconds by this method is needlessly over processed. The data in Figure 3.6 have been normalized to the results at 60 seconds of mixing time. The conductivity of the coating specimen is seen to vary by an order of magnitude across the range of mixing times.

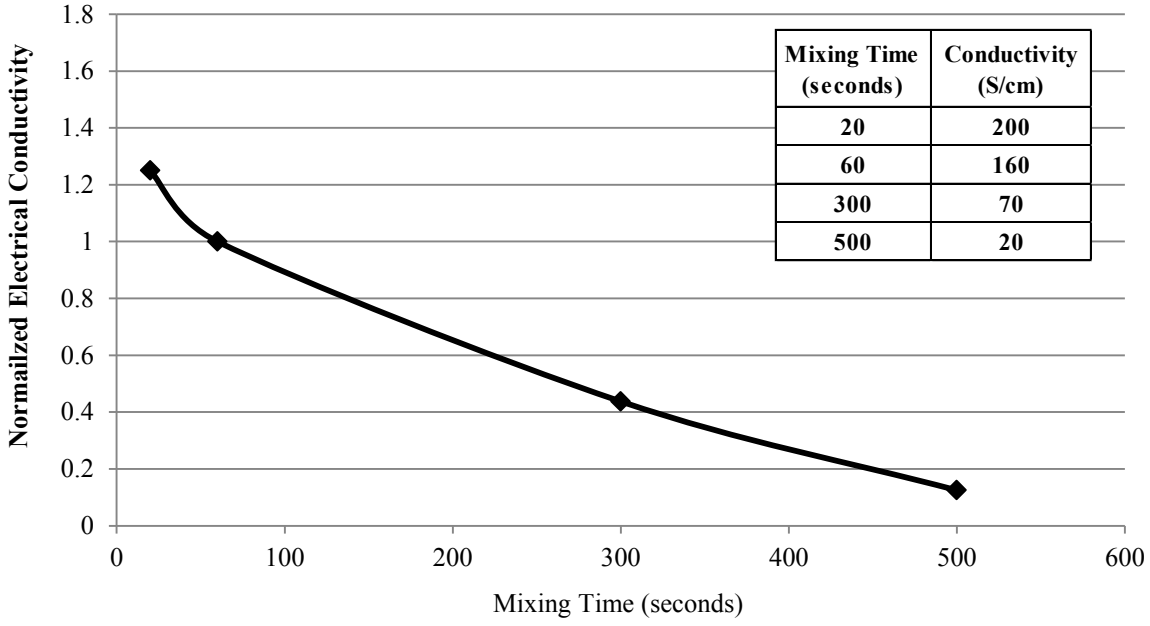

Figure 3.6: Electrical resistivity as a function of mixing time, 10 volume percent nanostrands in water based polymer at 0.10 mm dry film thickness.

3.7.3 Quantifying and Correlating Electrical Conductivity and Processing Conditions to *In Situ* Nanocomposite Structures

Despite the recent advances in the use of nanomaterials, few tools have been developed to quantify the *in situ* dispersion of nanomaterials within a polymer. Several authors have reported results for quantifying the dispersion of carbon nanomaterials in composite systems (for example,[42-44]), but no previous work has been undertaken on quantifying the unique nanostructure of nickel nanostrands in polymer composites, with correlation to resultant electrical conductivity. The ability to quantify the dispersed nanostructure will be an essential element to developing more universal models that predict the conductivity of nanostrand composites (or of any conductive filled system). This is the first study that quantifies the *in situ* structure of nanostrand polymer composites and correlates to electrical conductivity in a dispersed system.

An essential element of a useful technique is the ability to quantify the dispersed nanostructure when still in a wet polymer dispersion form, as well as in a dry format. Thus, the nature of the nanostructure can be monitored real time during dispersion practices. Additionally, a desirable feature is that the required equipment should consist of standard microscopes and commercial software.

Three main types of parameters are pertinent to nanostrand dispersions: clustering parameters (such as cluster size, perimeter ratio, etc), dispersion parameters (such as nearest neighbor functions), and the herein named "preservation parameters" (percolation, Betti numbers). The mean cluster size metric is analogous to measuring an aerodynamic diameter. The area/perimeter ratio gives a relative measure of the

smoothness or regularity of a structure (circles will have a very high area/perimeter ratio, whereas more irregular shapes, such as a star, will have a lower area/perimeter ratio). The nearest neighbor metric calculates the closest distance between adjacent discrete structures, giving an averaged measure of how close dispersed features (electrically conductive nanostructures in this case) will be to each other. The Betti "preservation parameters," as introduced in this work, are metrics that are used to monitor the structure and condition of dispersed conductors throughout processing and dispersion steps. Processing steps will alter or break down the conductive structures, and thus also affect the conductivity of the resulting composite. The approach to using preservation parameters is somewhat unique to the nanostrand structure, but can be extended to any system with a high aspect ratio or interconnected structure.

The calculation of the Betti numbers is particularly well suited to monitoring nanostrands in dispersion. The Betti numbers are invariants used to characterize topological features within a space. The Betti numbers increase in order as the unconnected surfaces of the features they represent increase in dimension. The first Betti number (dimension 0, β_0) counts the number of objects or connected components within a space (as applied herein, the number of independent nanostrand structures). The second Betti number (dimension 1, β_1) gives the number of completely enclosed holes or tunnels (preserved openness and connectedness of nanostructure). The third Betti number counts objects with two dimensional surface features, such as enclosed holes or voids. Two dimensional data sets (such as planar images) can provide only the first two Betti numbers.

An increase in the first Betti number (increasing the number of discrete nanostrand structures at a given volume fraction) accompanied by a decrease in the second Betti number (decrease in the open connected branching nature of the strands) should correlate to a breakdown of the nanostrand structure and a decrease in the conductivity of nanostrand polymer composites. Thus, the ratio of the second Betti number to the first Betti number provides a measure of the breakdown of a dispersed nanostrand structure.

A method was developed for obtaining optical images of nanostrands dispersed in polymer at intervals during processing steps. These images were enhanced using an automated series of Photoshop® commands, then imported into Matlab® as a binary array. This array can then be further thresholded and optimized for statistical analysis. Matlab subroutines were written for calculating the mean cluster size, nearest neighbor distance, and area/perimeter ratio. Betti numbers were calculated using a Matlab subroutine with code available as part of the Computational Homology Project (CHomP) [42] from Rutgers University. Typical images from this process are shown in Figure 3.7.

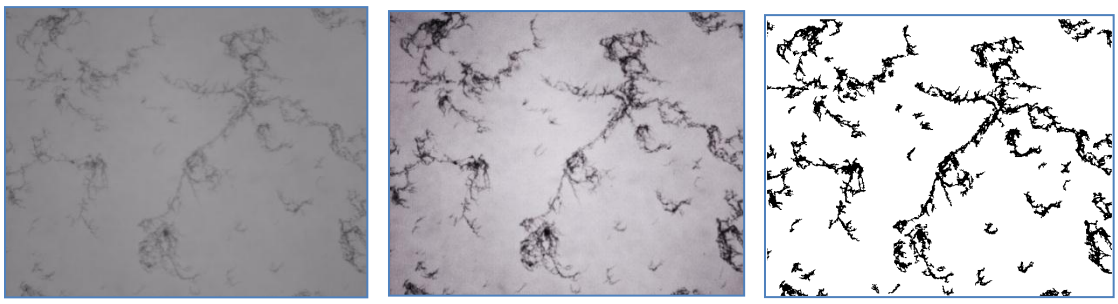

a) b) c)

Figure 3.7: Progression for preparing images for statistical homology analysis:. a) as obtained from microscope, b) enhanced using Photoshop® commands, c) following thresholding and conversion to binary array.

3.7.4 Quantified Image Correlation and Dispersion Methods

Figure 3.8 shows representative images for processing steps, one with standard processing, and the second with additional processing. The averaged statistical results of each set are reported in Table 3-1.

The mean cluster size metric shows correlation to reductions in conductivity in the sample, as electrical conductivity diminishes with cluster size. This is expected based on the visible changes in the overall diameter of the nanostrand structures, and the associated capability of the nanostructure to provide percolated conductivity through a space. The area/perimeter ratio and nearest neighbor metrics remain nearly constant across sample

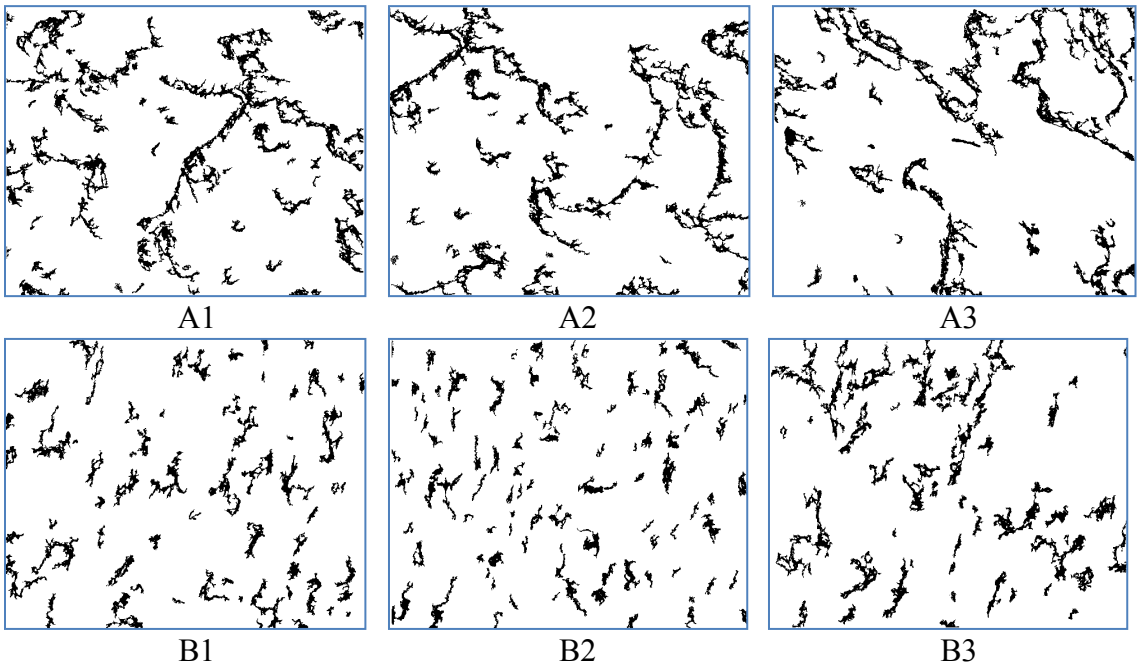

Figure 3.8: Black and white bitmap image replicate sets used for calculating statistical imaging parameters. A1 though A3: standard dispersion method (60 seconds of mixing time). B1 through B3: significant additional processing (500 seconds of mixing time). The nanostrand loading is 0.1 volume percent in all images.

Table 3-1: Average Statistical Parameter Results for Image Sets A and B in Figure 3.8.

Parameter	Parameter Type	Image Set A (less processing)	Image Set B (more processing)	Correlation to Conductivity
Mixing Time (seconds)		60	500	
Mean Cluster Size (pixels)	clustering	528	397	good
Area / Perimeter Ratio	dispersion	1.27	1.31	poor
Nearest Neighbor Distance	dispersion	20.3	20.3	poor
β_0 (first Betti number)	preservation	52	81	good
β_1 (second Betti number)	preservation	1645	1418	good
β_1/β_0	preservation	36.1	18.7	good
Conductivity (10 vol%, S/cm)		120	12	

sets, showing little sensitivity to structure changes and no correlation to changes in coating film conductivity. The Betti parameters are well correlated to coating film electrical conductivity values, showing expected changes in both the first and second Betti numbers that correlate to electrical conductivity readings.

A limitation of this two dimensional method is that imaging must be done at a volume fraction loading where the nanostructures are visible, which is near the percolation threshold. Electrical resistivities are highly sensitive in this region due to the nature of the onset of electrical conduction (see Figure 3.1). It is difficult to obtain reliable resistivity readings in this region, regardless of processing methods or nanomaterial structure. Accordingly, electrical conductivities for films are measured in a parallel set of samples that are subject to the same processing steps, but contain a higher volume fraction of nanostrands at a value closer to the more stable percolation limit. This same result can also be achieved by using a solvent to thin down a sample for imaging

(such as when sampling from a large master batch of higher volume fraction). The correlation of statistical imaging properties to film conductivities is shown in Figure 3.9. The Betti numbers are for samples at low volume fraction, and electrical conductivity values are from parallel samples at higher volume fraction. Both samples sets are subject to the same processing conditions, and the lower volume fraction set represents a thinned sample of the higher volume fraction set. The data are averaged based on five sample images from each mixing time.

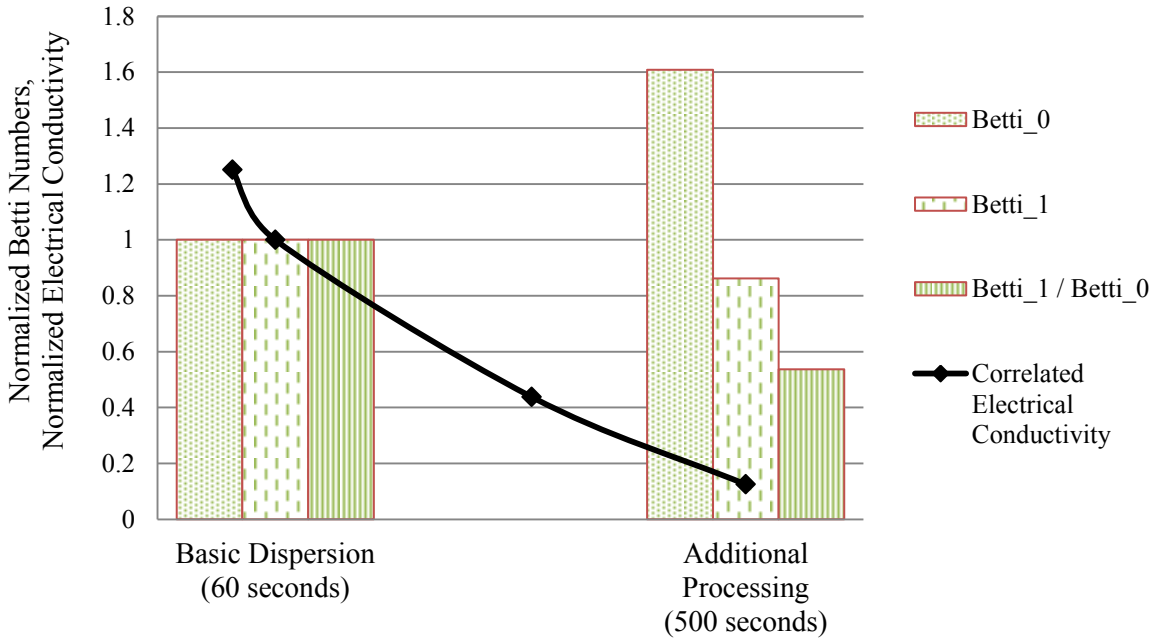

Figure 3.9: Correlation of imaging "preservation parameters" to nanostrand/polymer film electrical conductivity. Imaging statistics are taken at 0.1 volume percent, electrical conductivities (from Figure 3.6) are taken at 10 volume percent. Preservation parameters are normalized to results at 60 seconds of mixing time.

An increase in the first Betti number (individual objects), accompanied by a decrease in the second Betti number (enclosed voids within volume, representing nanostrand porosity and interconnectedness), correlates to a decrease in conductivity. A notable feature of this method is that the nanostructure can be monitored real time during dispersion, and then correlated to a final conductivity value.

Though particularly suited to nanostrands, the ability to use this new method to quantify and correlate actual nanostructure dispersions can be used to better understand any dispersed system. This method can also be used as a quality control tool, where batch samples can be thinned, imaged, and analyzed at any step during processing. This process provides a predictive tool that can relate wet phase dispersions to end use properties. It is also noted that this method as presented above uses only microscale imaging methods, though an extension to the nanoscale is a natural next step and has already been demonstrated by other authors [43].

Ongoing research is focusing on developing a better understanding of nanostrand conduction, including investigation into fundamental polymeric physical properties that drive differences in conduction. The polymer filled junction that exists between dispersed nanostrand structures is also an area of great relevance. Three-dimensional methods for characterizing and correlating the *in situ* structure of nanostrand composites are also being developed.

3.8 Conclusions

An enhanced understanding of the dispersed nanostrand structure has been gained through the development and assessment of image based characterization methods. These methods include the quantification of topological parameters in the dispersed structure that can affect electrical percolation properties. While not all of the topological parameters tested are effective at measuring differences in the dispersed nanostructure during processing steps, the Betti number based "preservation parameters" show good correlation to both observed structure characteristics and measured electrical conductivities in cured films. The correlation of dispersion characteristics to measured physical properties indicates promise for this tool to correlate nanostrand dispersions during mixing steps, thus developing a predictive quality control tool based on batch sampling. Though this method has been presently developed specifically for nickel nanostrands, it can be used as a quantified method for characterizing and measuring dispersions of other materials, with particular application for highly structured materials.

3.9 References

[1] Osman T, Rardon D, Friedman L, Vega L. The commercialization of nanomaterials: Today and tomorrow. JOM Journal of the Minerals, Metals and Materials Society. 2006;58(4):21-4.

[2] Pitkethly MJ. Nanomaterials - the driving force. Materials Today. 2004;7:20-29.

[3] Min C, Shen X, Shi Z, Chen L, Xu Z. The electrical properties and conducting mechanisms of carbon nanotube/polymer nanocomposites: A review. Polymer-Plastics Technology and Engineering. 2010;49(12):1172 - 81.

[4] Roldughin VI, Vysotskii VV. Percolation properties of metal-filled polymer films, structure and mechanisms of conductivity. Progress in Organic Coatings. 2000;39:81-100.

[5] Hansen N, Hansen G. From inception to insertion: successful products and applications using nickel nanostrands. SAMPE Journal. 2011;47(3):6-13.

[6] Grunlan JC, Mehrabi AR, Bannon MV, Bahr JL. Water based single wall nanotube polymer filled composite with an exceptionally low percolation threshold. Advanced Materials. 2004;16(2):150-3.

[7] Park J-M, Kim D-S, Kim S-J, Kim P-G, Yoon D-J, DeVries KL. Inherent sensing and interfacial evaluation of carbon nanofiber and nanotube/epoxy composites using electrical resistance measurement and micromechanical technique. Composites: Part B. 2007;38:847-61.

[8] Shui X, Chung DDL. Submicron diameter nickel filaments and their polymer-matrix composites. Journal of Material Science. 2000;35:1773-85.

[9] Chung DDL. Electromagnetic interference shielding effectiveness of carbon materials. Carbon. 2001;39:279-85.

[10] Grunlan JC, Gerberish WW, Francis LF. Lowering the percolation threshold of conductive composites using particulate polymer microstructure. Journal of Applied Polymer Science. 2001;80:692-705.

[11] Jing L, Lumpp JK. Carbon nanotube filled conductive adhesives for aerospace applications. IEEE Aerospace Conference 2007, p. 1-6.

[12] Kyrylyuk AV, Schoot P. Continuum percolation of carbon nanotubes in polymeric and colloidal media. Proceedings of the National Academy of Sciences of the United States of America. 2008;105(24):8221-6.

[13] Wang SF, Ogale AA. Continuum space simulation and experimental characterization of electrical percolation behavior of particulate composites. Composites Science and Technology. 1993;46(2):93-103.

[14] Grimmett GR. Percolation. 2nd ed: Springer; 1999.

[15] Hernandez YR, Gryson A, Blighe FM, Cadek M, Nicolosi V, Blau WJ, et al. Comparison of carbon nanotubes and nanodisks as percolative fillers in electrically conductive composites. Scripta Materialia. 2008;58(1):69-72.

[16] Liliane B. Multiwall carbon nanotube elastomeric composites: A review. Polymer. 2007;48(17):4907-20.

[17] Ma HM, Gao XL. A three-dimensional Monte Carlo model for electrically conductive polymer matrix composites filled with curved fibers. Polymer. 2008;49(19):4230-8.

[18] Hicks J, Behnam A, Ural A. Resistivity in percolation networks of one-dimensional elements with a length distribution. Physical Review E. 2009;79:012102.

[19] Zeng QH, Yu AB, Lu GQ. Multiscale modeling and simulation of polymer nanocomposites. Progress in Polymer Science. 2008;33(2):191-269.

[20] Simmons JG. Generalized formula for the electric tunnel effect between similar electrodes separated by a thin insulating film. Journal of Applied Physics. 1963;34(6):1793-803.

[21] Balberg I. Tunneling and nonuniversal conductivity in composite materials. Physical Review Letters. 1987;59(12):1305-8.

[22] Rubin Z, Sunshine SA, Heaney MB, Bloom I, Balberg I. Critical behavior of the electrical transport properties in a tunneling-percolation system. Physical Review B. 1999;59(19):12196-9.

[23] Johnson OK, Gardner CJ, Fullwood DT, Adams BL, Hansen N, Hansen G. The colossal piezoresistive effect in nickel nanostrand polymer composites and a quantum tunneling model. CMC: Computers, Materials, & Continua.15(2):87-112.

[24] Hansen G. The roles of nanostrands and nickel coated fibers in electrically conductive composite design. 37th ISTC. Seattle, WA. 2005.

[25] Hansen G, Hansen N, Burghardt J, Bell JAE, Poe G, Adams DO. Electrically conductive thermoplastic polyimide resins and composites, Part II - establishment of baseline mechanical and electrical properties. SAMPE International Conference. Baltimore, MD. 2006.

[26] Hansen N, Hansen G. Electromagnetically shielding spray paints using commercial-off-the-shelf polymer systems. SAMPE Fall Technical Conference. Wichita, KS. 2009.

[27] Park J-M, Kim S-J, Yoon D-J, Hansen G, DeVries KL. Self sensing and interfacial evaluation of Ni nanowire/polymer composites using electro-micromechanical technique. Composites Science and Technology. 2007;67:2121-34.

[28] Hansen G. A concurrent solution for both lightning strike and electromagnetic protection of aerospace composites. SAMPE International Conference. Long Beach, CA. 2008.

[29] Hansen G. Highly effective broadband shielding materials. National Space and Missile Materials Symposium. Henderson, NV. 2008.

[30] Hansen G. Advances in HPM and EMP hardening materials. HEART Conference. Colorado Springs, CO. 2008.

[31] Hansen G. Nano-microstructured lightning strike protection system using nanostrands and conductive fiber composites. SAMPE International Conference. Long Beach, CA. 2006.

[32] Hansen N, Hansen L, Hansen G. Electrically conductive structural adhesive with milliohm resistance. SAMPE International Conference. Long Beach, CA. 2008.

[33] Hansen N, Hansen G, Silverman E. Versatile gap fillers and sealants for high level conductivity and electromagnetic shielding. SAMPE Spring Symposium. Seattle, WA. 2010.

[34] J. Tomblin J, Kostogorova-Beller Y, Hansen G, Hansen N. Evaluation of lightning strike protection schemes which employ conductive primers. SAMPE Fall Technical Conference. Wichita, KS. 2009.

[35] Bell J.A.E., Hansen G. Nickel coated fibers for aerospace applications. SAMPE International Symposium Proceedings. Anaheim, CA. 1991.

[36] Hansen G. Multifunctional thermoplastic polyimide composites. SAMPE Fall Technical Conference. Dallas, TX. 2006.

[37] Hansen G, Hansen N, Adams DO, Burghardt J, Widauf D, McNeill T. Electrically conductive putty type repair system for composite structures. SAMPE International Conference. Baltimore, MD. 2007.

[38] Hansen G, Hansen N. The role of nanomaterials in lightning strike protection of aircraft. National Nano Engineering Conference. Boston, MA. 2007.

[39] Hansen G. High aspect ratio sub-micron and nano-scale metal filaments. SAMPE Journal. 2005:24-8.

[40] Hansen N, Adams DO, DeVries KL, Goff A, Hansen G. Investigation of electrically conductive structural adhesives using nickel nanostrands. Journal of Adhesion Science and Technology. 2010;25:2659-70.

[41] Gasketing Material, Conductive, Shielding Gasket, Electronic, Elastomer, EMI/RFI, General Specification For. Military Detail Specification 83528C. United States Department of Defense, 2011.

[42] http://chomp.rutgers.edu/software/, accessed March 15, 2012.

[43] Bakshi SR, Batista RG, Agarwal A. Quantification of carbon nanotube distribution and property correlation in nanocomposites. Composites: Part A. 2009;40:1311-8.

[44] Heitkamp II C, Klosterman D. Processing and analysis of thermoplastic polyimide films containing carbon nanofibers. SAMPE International Conference. Long Beach, CA. 2009.

[45] Leer C, Carneiro OS, Covas JA, Maia JM, Hattum FWJ, Bernardo CA, et al. Dispersion of carbon nanotubes in polycarbonate and its effect on the composites properties. Material Science Forum. 2006;5154(2):1125-30.

4 INVESTIGATION AND CORRELATION OF PERCOLATION BEHAVIORS AND PHYSICAL PROPERTIES IN ELECTRICALLY CONDUCTIVE NICKEL NANOSTRAND POLYMER COMPOSITES

Nathan Hansen[1], Michael Koecher[2], Daniel O. Adams[1], David T. Fullwood[2]

[1]University of Utah
Department of Mechanical Engineering
50 S. Central Campus Drive
Salt Lake City, UT 84112, USA

[2]Brigham Young University
Department of Mechanical Engineering
435 Crabtree Building
Provo, UT 84602, USA

4.1 Abstract

The electrical percolation behaviors of nickel nanostrands in polymer composites are considered and studied in a wide range of polymer systems. The critical percolation threshold and percolation limit are presented, along with maximum electrical conductivities. Electrical percolation is found to vary widely in different types of polymers. Polymer physical properties are investigated for electrical resistivity, dielectric breakdown strength, wetting characteristics, resistance during cure, and solids weight percentage. These properties are then correlated to nanostrand polymer film conductivities. A combination of standard test methods and novel test methods are used. The intention of these tests is to seek correlation to both the wet phase dispersion of nanostrand in fluid polymer systems and the final solid phase, both with and without nanostrands. Ultimately, a screening/predictive tool is desired that will help predict conductivity results of nanostrands in polymer systems. It is found that the both the wet phase and solid phase polymer properties investigated in this study show poor prediction to polymer composite electrical conductivities. It is expected that test methods that are able to determine the thickness of and predict quantum tunneling effects at the nanostrand polymer junction will provide better correlation.

4.2 Introduction

Polymer and fiber reinforced composites play an increasing role in commercial, defense, and private sectors. While polymeric systems are well suited for replacing metallic structures with respect to mechanical and processing properties, the electrical properties of polymeric systems are intrinsically orders of magnitude apart from metallic

systems. This transition to polymeric structures and systems occurs concurrently with an increase in utilization and reliance on digital technologies.

Traditional metal structures present a naturally effective conductive material, as isotropic metals have free valence electrons to facilitate conduction. Polymer matrix composites are naturally not as well suited, consisting of insulating or moderately conducting fibers in an insulating matrix. Thus, the challenge is to find methods of engineering electrical conductivity and shielding properties into polymers and polymer composite systems while preserving the fundamental advantages (mechanical, manufacturing, weight, cost, etc.) of polymer composites. Traditional solutions for conductivity in polymers and polymer matrix composites have included metal filled polymers and intrinsically conductive polymers, along with meshes, foils, and wires for laminate structures. The rapidly growing field of nanotechnology has presented new materials that can be used to increase polymer conductivity more efficiently and with better performance. While traditional conductive additives (such as milled powders, coated spheres, platelets, etc.) have aspect ratios on the order of 1 to 10, newer nanoparticles (such as carbon nanofibers) have aspect ratios in the thousands. This fact, in combination with the nanoscale diameter of these particles, means that less conductive material is required, both in terms of volume percent and weight percent, to achieve high conductivity levels [1-4].

The objective of this study is to seek understanding of the structure property relationships that govern conduction in metal nanomaterial filled polymers using nickel nanostrands. A further intent of this effort is to find screening and predictive variables for understanding the polymer dependent (but processing method and volume fraction

independent) electrical conduction of nanostrand composites. To date, the majority of studies on nanostrand systems have dealt with the empirical results of nanostrand polymer composites. Few authors have sought an understanding of the fundamental mechanisms of conductivity within nanostrand polymer composites. Thus a main goal of this study is to investigate the polymer dependent conduction properties of nanostrand composites, and to correlate host polymer physical characteristics to nanocomposite bulk electrical resistivity properties. This approach includes classical percolation characterization along with several tests on polymer constituents. This is believed to be the first publication that presents nanostrand polymer electrical percolation curves that extend to the percolation limit. The onset of conduction in samples during cure is also studied.

4.2.1 Metal Filled Polymers

Electrical properties of metal filled polymer systems can be modeled using percolation theory [5-8]. Classical percolation theory considers a network of conductive links in a nonconductive matrix, and models the connectivity across an infinite sample of a network structure. In a nanostrand composite, this network structure is created by nanostrands connecting throughout the sample. When a sufficient volume of nanostrands are present to create an electrically conductive path through a volume, an abrupt change is conductivity is observed, referred to as the critical percolation threshold. For loadings at and above this value, the resistivity of the composite generally follows a power law relation given by [9]:

$$\rho \sim (v - v_c)^{-t} \qquad [4.1]$$

where v represents the volume fraction of conductive material, v_c represents the critical value of the percolation threshold, and t is a universal constant, which for a three-dimensional material approximately equals 2. The resistivity of the composite generally follows this power law from the percolation threshold until a percolation limit is reached. This loading at the percolation limit presents a limiting value for well dispersed conductive networks. For loadings above this value, a decrease in electrical and mechanical properties is often observed, indicating that the polymer host is no longer capable of facilitating additional increases in filler. A typical curve representing these behaviors is shown in Figure 4.1. The correlation of nanostrand percolation to material models is not presented herein, and will be the focus of future works by the authors.

4.2.2 Nanostrands: Metal Polymer Nanocomposites

Nickel nanostrands [10] are a relatively new material (abbreviated as NiNS or just NS). They are a submicron diameter, high aspect ratio nanostructure. Nanostrands feature an intrinsic three-dimensionally interconnected structure that creates loops and demonstrate a branched nature as shown in Figure 4.2.

Nanostrands are manufactured as a continuously interconnected “cake” of nickel, which can be reduced to a nanostructured high porosity three-dimensional nickel powder. The cake is subjected to a process which tears apart the nanostrand volume into nanostructured powder. The cake can be used as a preform and infused with polymer, or the nanostructured powder form can be dispersed in a host matrix. The latter practice is most typical. These discretized nanostrand structures are the key to the observed

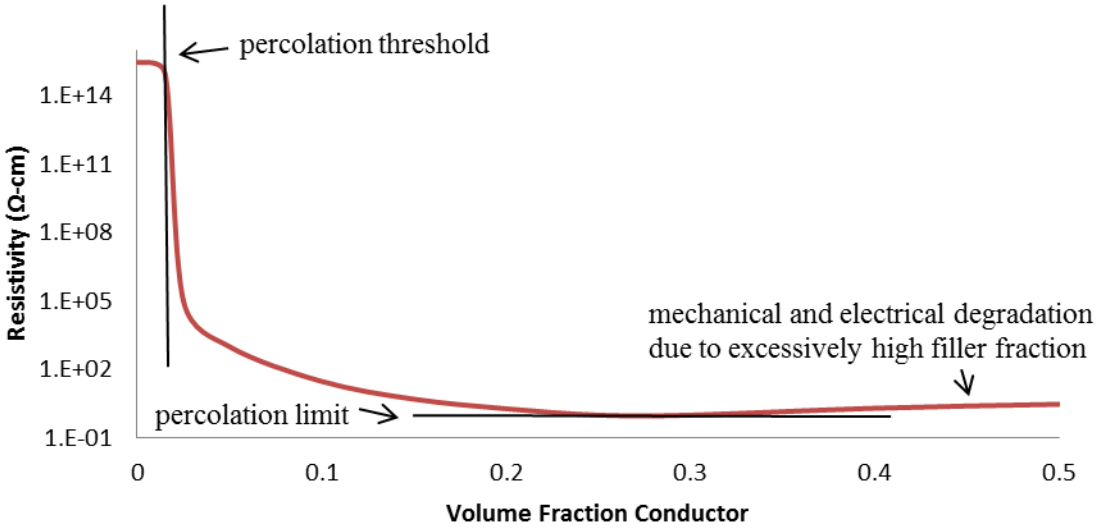

Figure 4.1: General electrical percolation behavior of conductive filled polymer systems.

performance of nanostrand polymer composites. Nanostrand structures at various volume fractions are visible in the micrographs in Figure 4.3.

The looped and branched nature of the nanostrand structure allows for three-dimensional interconnects, and therefore three-dimensional percolation at low volume fractions. The branches on each strand help create further radial interconnects, and provide additional three-dimensional connection opportunities (for example, two parallel nanostrands do not need to be oriented to intersect along their major axis, as they can connect with radial branches). This branched nature can also offer benefits in applications requiring wave properties, as the branches can serve as a multiplicity of antennas and transmitters.

The nanostrand structure can be viewed as a “skeleton” rather than a full “body” (as with more solidly structured additive particles). The void space of the nanostrand

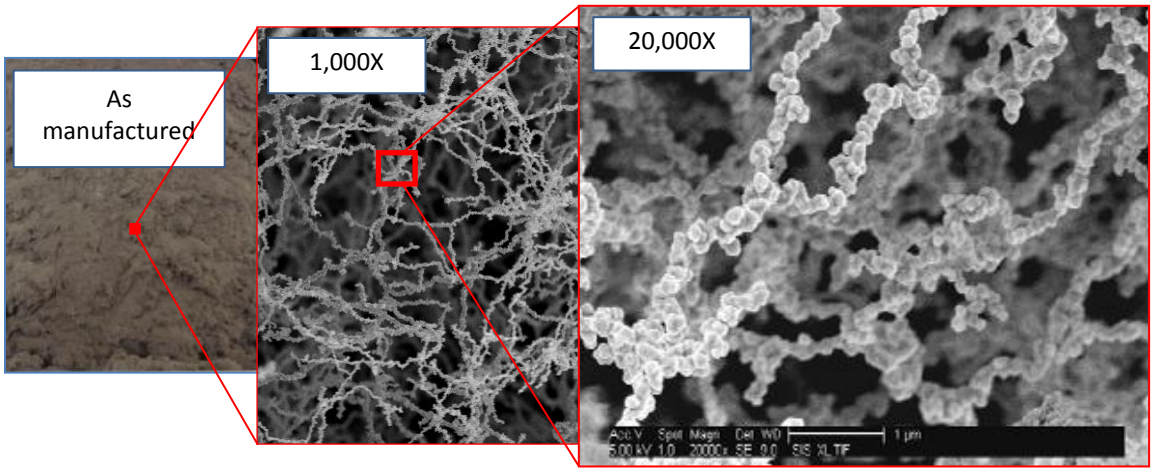

Figure 4.2: Nickel nanostrands, as manufactured, increasing magnification from 1X to 20,000X.

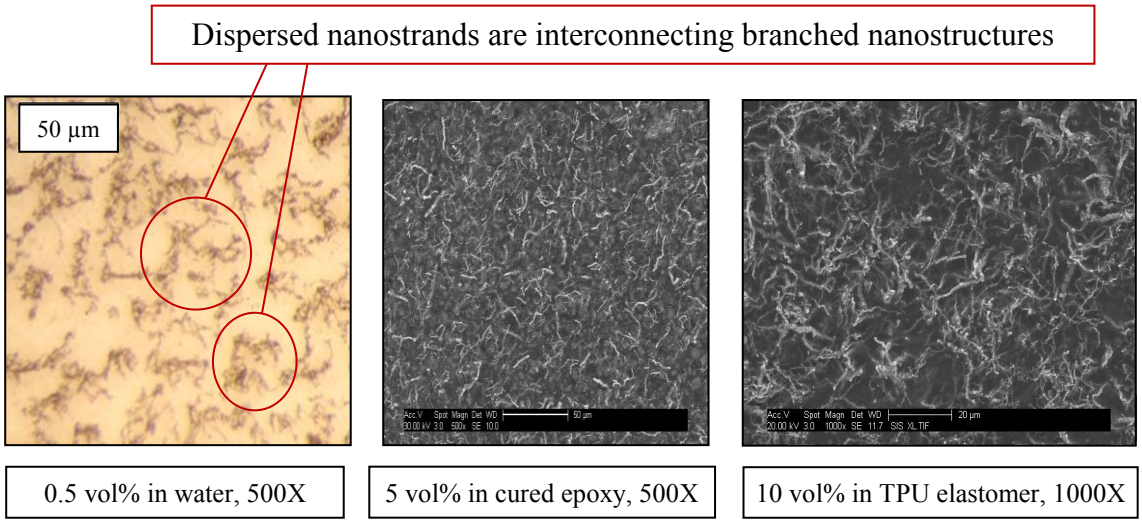

Figure 4.3: Nickel nanostrands dispersed in water at 0.5 volume percent (50 µm scale bar), cured epoxy at 5 volume percent (50 µm scale bar), and TPU elastomer at 10 volume percent (20 µm scale bar).

structure is filled with the host substrate, facilitating better bonding and preservation of material properties while still providing conductive interconnections. Nanostrand mixtures percolate to higher conductivity levels than have been demonstrated with carbon nanomaterials [3, 11-13]. This study will present nanostrand polymer film conductivities which regularly measure at or over 100 S/cm across multiple polymers, and as high as 1400 S/cm at the percolation limit. This is higher than the maximum conductivity of 100 S/cm reported for treated carbon nanotubes in a 2009 review by Bauhofer et al. [14]. The Bauhofer study considers carbon nanotube conductivity results that span 147 experimental results, and most authors in the Bauhofer study reported maximum conductivities between 10^{-6} and 10^{2} S/cm electrical conductivy. Typical results in this study span 10^{-3} to 10^{3} S/cm.

Nickel benefits from a metallic bonding structure, high electrical conductivity, and ferromagnetic properties. The raw material cost of nickel is relatively low, and corrosion resistance is quite high. However, nanostrands are relatively weak physically compared to carbon nanofibers. Nanostrand materials are formed as a crystalline chain structure, and are therefore sensitive to processing methods which can break down the structure and reduce the aspect ratio and interconnects of the structure. Care must be taken when producing nanostrand mixtures to not overmix the system and break down the strands [4, 10].

4.2.3 Understanding Conductivity in Nanostrand Polymer Composites

Nanostrand polymer composites have been able to achieve conductivities in excess of 5000 Siemens/cm, and have been demonstrated in applications including electrostatic

discharge [15], electromagnetic shielding [16-18], conductive adhesives [19, 20], caulks and gaskets [21], paints [22, 23], and lightning strike protection [16, 23-27]. Previous studies have indicated that the resultant conduction of a nanostrand composite can depend on multiple factors. For example, an early study [28] indicates that the resistivity of nanostrand composites is a function of the type of polymer used as the matrix material. A recent publication indicates the dependence of composites conductivities on processing condition [29].

4.3 Materials and Methods

The polymers chosen for this study are widely available commercial coating systems, as detailed in Table 4-1. These systems were chosen for ease of use, relevance to commercial applications, and correlation to previous data [22, 30]. All polymers were used in their as received state. Nickel nanostrands were provided by Conductive Composites Company and dispersed according to the manufacturer's recommendations. All calculations and plots use volume fraction, as this volumetric approach allows for a more relevant comparison to volumetrically driven percolation mechanisms.

4.3.1 Conductivity and Electrical Percolation Samples

A desired volume fraction of nickel nanostrands was added to a fluid polymer sample, then "wet" by manual mixing methods. Dispersion was achieved by using a Thinky AR-250 centrifugal double planetary mixer, with a mixing duration of 20 seconds at 2000 rpm for all samples. It was sometimes necessary to use additional solvents to wet the nanomaterials at higher volume fractions (10 percent and above) in systems with a high weight fraction of polymer solids in their as received state. The amount of solvent

Table 4-1: Host Polymers Used for Nanostrand Nanocomposites

Tradename	Manufacturer	Type	Weight % solids*	Processing Solvent	Notes
Polycrylic® Clear Gloss	Minwax®	Acrylic/Urethane	31	Water	Water based, low cost
LaRC-CP1™	NeXolve™	Polyimide	7	Diglyme	Space qualified, costly
Desothane® HS CA8201/F Clear	PRC-DeSoto	Urethane	64	Methyl Ethyl Ketone (MEK)	Commercial aviation coating
Armorseal® 1000 HS clear	Sherwin Williams®	Epoxy	72	PR54 (MEK/Xylene/Ethanol)	Commercial grade floor coating
Sylgard® 184	Dow Corning®	Silicone	100	Xylol	Silicone system, correlates to nano-indentation studies
CARC Clear MIL-DTL-64159 Ty II	Spectrum Coatings	Aliphatic Polyurethane	34	Water	Chemical & Abrasion Resistant
Irogran® PS455-302P	Hunstman	Thermoplastic Polyurethane (TPU)	100	Tetrahydrafuran (THF)	Thermoplastic elastomer, correlates to nano-indentation studies
PVP40	Sigma Aldrich®	Polyvinlypyrrolidone	100	Ethanol	Correlates to nano-indentation

***** Weight percentage of polymer solids in fluid solution, in as received state. This was often modified with solvents at higher volume fractions of nanostrands (e.g. above 10 volume percent). Polymers received at 100% solids were reduced with solvent to produce fluid mixtures, with an exception for Sylgard® 184, which is a fluid solution as received.

used was variable with the volume fraction of nanostrand, with the target of a viscosity appropriate for spray fabrication methods. Mixtures were screened through a -50 woven stainless steel mesh. Care was taken to control independent variables and process all nanostrand dispersions, at all volume fractions and in all polymers, in as equal of a method as was possible.

Dispersed nanostrand mixtures were used to produce thin coating samples on electrically insulating substrates (Kapton® polyimide film). Spray coatings were applied with a DeVilbiss FLG-3 High Volume Low Pressure (HVLP) gravity feed spray gun. A size 22 tip and Size 3 HVLP air cap were used, with nozzle pressure typically below 10 psi. Samples were sprayed in the appropriate number of coats to match the polymer manufacturer's specifications.

4.3.2 Electrical Resistivity of Highly Resistive Polymer Samples

The purpose of this test is to measure the electrical resistivity of polymer films without the presence of any nanostrands. These values are necessary to complete electrical percolation curves. These values were not available from the polymer manufacturers. Volume resistivity measurements were taken by ASTM D 257 – 07: Standard Test Methods for DC Resistance or Conductance of Insulating Materials [31]. Testing was performed by Intertek of Pittsfield, Massachusetts, using a guarded parallel plate fixture with concentric rings (as shown in Figure 4 of the test standard), with an electrification time of 60 seconds at 500 volts.

4.3.3 Electrical Resistivity of Conductive Samples

Areal surface resistivity readings of coating samples were taken using an ohm-per-square jig and a four point Kelvin probe resistance method, as specified in MIL-DTL-83528C: General Specification For Gasketing Material, Conductive, Shielding Gasket, Electronic, Elastomer, EMI/RFI [32]. The ohm-per-square jig for this study uses two copper bars 2.54 cm in length, 6.35 mm wide, and 6.35 mm high. These bars are bonded to an electrically insulating jig that separates them by a distance of 2.54 cm, thus a surface area of 6.45 cm^2 is measured between contact paths. Kelvin probe leads are attached to each bar and resistance readings are taken across the surface of each sample (see Figure 4.4). An Extech 380560 High Resolution Precision Milliohm meter was used for all resistance readings below 20 kΩ. In the rare case of resistances above 20kΩ, readings were taken with a handheld multimeter.

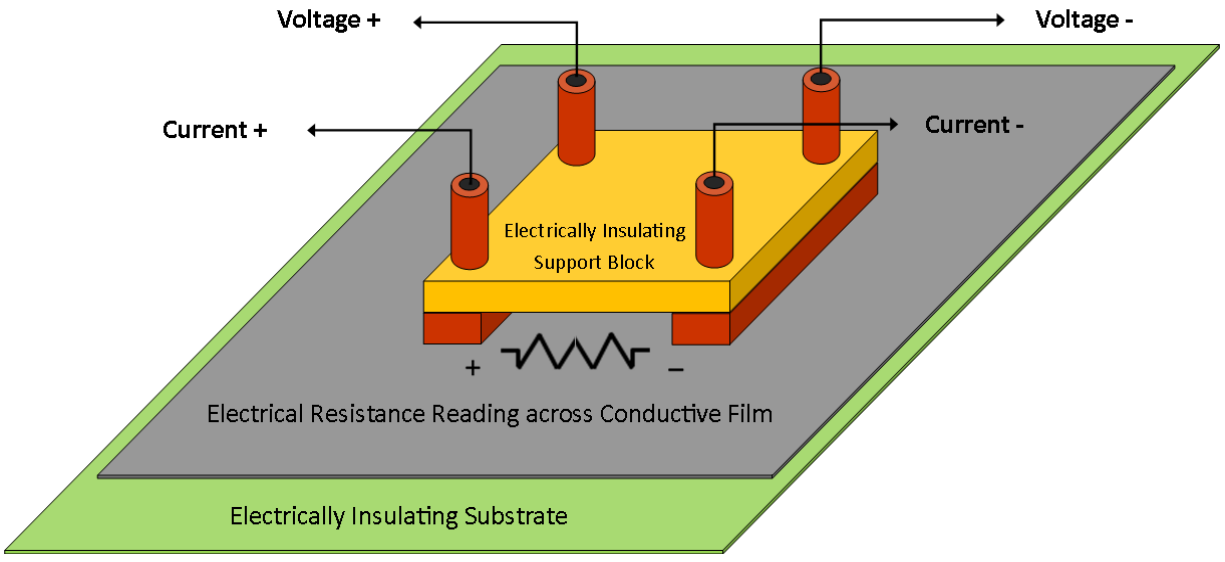

Figure 4.4: Kelvin Probe method for obtaining surface resistivity of conductive coating films.

Thickness readings were taken with a micrometer with 0.00254 mm (0.0001 inch) resolution. Sample conductivities were calculated using a thin film approximation and surface resistivity results according to:

$$\sigma^{-1} = \rho = R_s(A/l) \quad [4.2]$$

where σ is the electrical conductivity of the nanocomposite (Siemens/cm), ρ is the electrical resistivity (ohm-cm), R_s is the surface resistivity (ohm-per-square), l is the length of the separation path (cm), and A is the cross sectional area of the film between contact bars (given by l multiplied by the film thickness).

Critical percolation thresholds are calculated for samples with complete percolation curves. Linear regression methods for deducing the percolation threshold were used [33], but were found to be unreliable when including data points from higher conductivity samples. Percolation thresholds were then determined using a linear fit of the critical threshold region. For samples with incomplete percolation curves, the percolation threshold is estimated.

4.3.4 Dielectric Strength Testing of Polymer Film Samples

It is hypothesized that the high voltage insulating strength of the polymers will correlate to the behavior of the polymers at junctions between nanostrands [34]. The dielectric strength of unfilled polymer films was tested using ASTM D149 – 09: Standard Test Method for Dielectric Breakdown Voltage and Dielectric Strength of Solid Electrical Insulating Materials at Commercial Power Frequencies [35]. Testing was

performed by Intertek of Pittsfield, Massachusetts, using flat 2.54 cm diameter solid brass discs to contact the sample and Method A, Short Time Test of the standard.

4.3.5 Contact Angle Testing

This experiment tests the interfacial energies of uncured or unset wet phase polymer solutions and their associated solvents to a nickel surface. A second component of this test is to compare the surface energies of cured polymer films to gain insight into how the polymer structure may be expected to behave in a cured or set format. Both modes of this test are intended to learn more about how dispersed nanostrands interact with a host polymer matrix. A Rame-Hart Model 100-00 Goniometer was used to perform static sessile drop contact angle testing. To prevent contamination between different polymers and solvents, the syringe was thoroughly cleaned with MEK and then rinsed in deionized water after each test. New needles were used for each test. In order to simulate the pure nickel in nickel nanostrands, a 0.0254 cm x 2.54 cm x 2.54 cm sheet of high purity nickel was purchased from ESPI Metals Company and used as the base for fluid drops. A single fluid drop was placed on the nickel surface, and manually aligned in the goniometer to obtain the contact angle. The nickel surface was cleaned with MEK between each test. The second mode of contact angle tests were performed with deionized water as the fluid and a cured polymer surface as the base. Each polymer was mixed, spread, and cured according to the manufacturer's specifications. A smooth, flat surface was produced for each polymer film. A water droplet was placed on the surface, and the contact angle was measured. Figure 4.5 shows an example of the contact angle of water on a polyurethane film surface being measured at 80°.

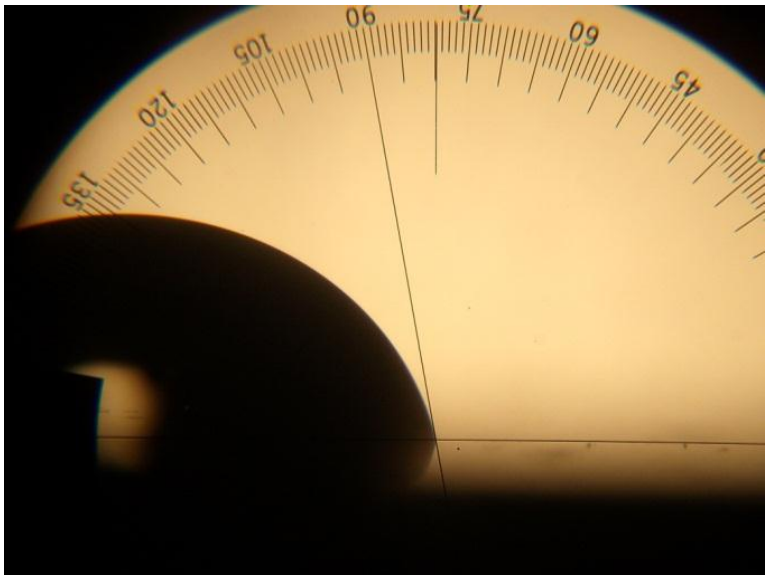

Figure 4.5: Measuring the static contact angle of deionized water on a polyurethane film surface.

4.3.6 Dynamic Testing: Resistance vs. Cure/Set Tests

This test measures the electrical resistance and mass of wet phase polymer films with dispersed nanostrands during cure (for thermosets) or set (for thermoplastics). Previous work [36] has indicated that multiple slopes of resistance vs. cure time are observed during electrical resistance monitoring of conductive films during cure/set, and the scope of this experiment is to additionally monitor the mass during this same process. This method requires samples to experience at least some change in mass to yield test data, thus it is expected that the primary mechanism that is correlated will be to the evacuation of solvents.

Samples are fabricated by cutting 0.0127 cm thick polyimide films to 13.97 cm by 7.62 cm. Sections of 12 gauge stranded copper wire are cut to 7.62 cm lengths, and stripped back to lengths of 2.54 cm and 1.27 cm on each end. The longer stripped end is

then fanned out and taped to the short edge of each sample with 2.54 cm wide copper tape. The copper tape is then masked with paper tape, and then the surface is cleaned with ethanol. A thin coating of primer is then applied to the surface. Following removal of the mask, the sample is cleaned again with ethanol, labeled, and weighed for a tare value. This sample is then taped to a 15.2 x 15.2 cm fiberglass phenolic card. All surfaces are then cleaned again with ethanol, and the tare weight of the assembly is recorded.

Conductive films were applied by spray coating methods (using the same equipment as for percolation samples). All films use a nanostrand concentration of 7.5 volume percent with a targeted dry film thickness of 0.01 cm. The coating area covered the width of the film substrate, including the copper tape leads. The sample was then immediately mounted on a balance and attached to a resistance measurement circuit as shown in Figure 4.6. All samples were left to cure/set at ambient conditions.

Mass readings were taken with a Highland HCB1002 balance using AdamDU data acquisition software. Resistance readings were obtained with a Mastech MAS-345

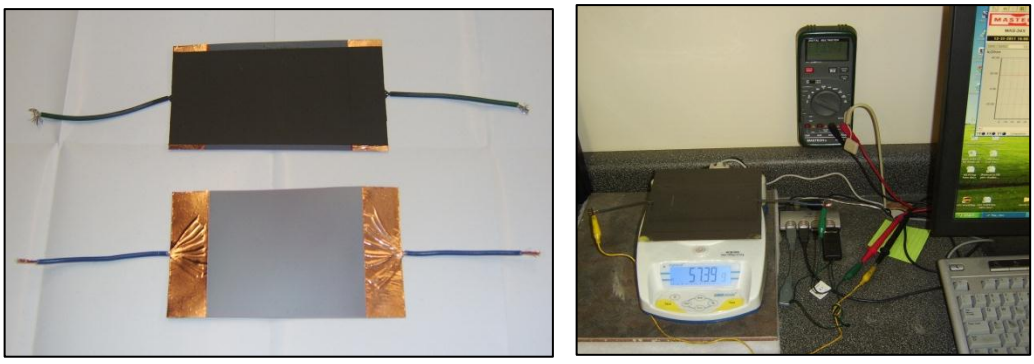

Figure 4.6: Substrates for measuring the mass and resistance of films during cure/set, before conductive film application (at left, lower), after conductive film application and post-cure characterization (at left, upper); during data acquisition (at right).

digital multimeter with DMM View software. Sampling was performed every 20 seconds until mass and resistance values stabilized for at least one hour. Samples were then removed from the supporting fiberglass card and inspected for spray coating thickness, surface resistivity, and electrical resistivity. Three replicates were made of each type of polymer.

4.3.7 Polymers Chosen for Each Test Method

The choice of polymers for a specific test was determined by electrical percolation characteristics (polymers should demonstrate a wide range of electrical resistivity results at an equal volume fraction of nanostrands), polymer physical properties, application constraints, relevance to previous works, and the ability to fabricate reasonable samples. Table 4-2 shows the polymer used for each type of test performed in this investigation.

Table 4-2: Host Polymers Used In Each Type of Test

Tradename	**Electrical Percolation**	**Electrical Resistivity**	**Dielectric Strength**	**Wetting Characteristics**	**Resistance During Cure/Set**
Polycrylic®	X	X	X	X	X
CP1™	X	X	X	X	
Desothane®	X	X	X	X	X
Armorseal®	X	X	X	X	
Sylgard®	X	X	X	X	X
CARC	X			X	
Irogran®	X	X	X		
PVP	X				

4.4 Results and Discussion

4.4.1 Electrical Resistivity and Percolation

The measured electrical percolation behavior for all polymers in this study are seen in Figure 4.7.

It is seen that there is a wide range of electrical conductivities for a given volume fraction of nanostrands, even at the percolation limit. Samples exhibit a critical percolation threshold between 1 and 5.5 volume percent, and a percolation limit generally at 10 to 20 volume percent. Electrical conductivities at the percolation limit are between 10 and 1400 S/cm. Values for the percolation limit, threshold, and electrical conductivities at the percolation limit are given in Table 4-3. It should be noted that previous studies [22] have presented data above 20 volume percent and give a higher percolation limit for CP1™.

4.4.2 Samples at Equal Volume, Equal Viscosity, and Variable Weight Percentage Solids

The viscosity of the nanostrand polymer mixture is somewhat controlled in this test by the manufacturing process, as a certain range of viscosity is required for successful film fabrication. Some polymer systems can be used in their as received solution form, and other are received as a 100% solid pellet or as a high solids solution format. As discussed above, these systems must be reduced with solvent in order to disperse nanostrands at equal viscosities and produce spray films. At higher loadings of nanostrands, most systems require an additional level of solvent correction.

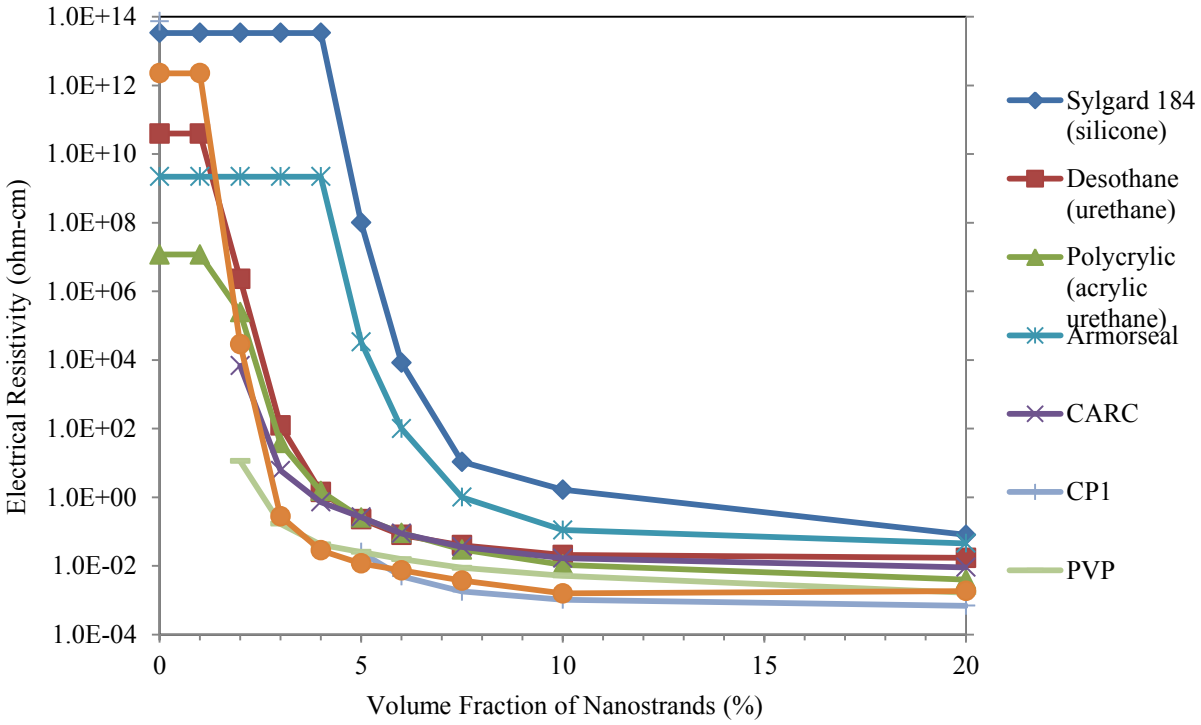

Figure 4.7: Electrical resistivity of nanostrand filled polymer films.

Table 4-3: Electrical Percolation Results for Nanostrand Filled Polymer Films

Tradename	Percolation Threshold	Percolation Limit	Conductivity at Percolation Limit (S/cm)
Polycrylic®	0.016	0.17	250
CP1™	~0.01	0.2	1400
Desothane®	0.014	0.2	58
Armorseal®	0.05	0.1	22
Sylgard®	0.055	0.2	12
CARC	~0.02	0.17	110
Irogran®	0.012	0.15	630
PVP	~0.02	0.2	598

The dispersed nanostrand polymer solution is affected by how well the polymer itself and any associated solvents “wet” as a mixture to produce a homogeneous solution. Polymer system wetting characteristics for nanostrands may be directly related to how well the system disperses a given amount of nanostrands at a fixed amount of solvents, or also related through identifying the amount of solvent needed to produce a mixture of matching viscosities across polymers. In this study, we choose to control viscosity to produce mixtures suitable for spray film application.

The weight percentage of nanostrands correlating to 10 volume percent in each polymer varies based on polymer density, and as conductive percolation is a volumetrically driven mechanism, we maintain presenting comparative conductivities by comparing equal volume percentages of conductor. Figure 4.8 shows the correlation of weight percentage of polymer solids in the polymer solution compared to the electrical resistivity of a cured film with 10 volume percent nanostrands.

An important factor when interpreting these results is that if the percentage of solids in the polymer is adjusted to be equal across samples, then the suspension of the nanostrands is often no longer possible, particularly in higher solids systems that require significant amounts of additional solvent. For example, if 100 wt% solids (as received) Sylgard® were mixed with solvent to obtain 7 wt% solids in order to match the as received CP1™ solution, then the Sylgard® mixture would not be able to achieve a reasonable suspension of nanostrands, and would have a low conductivity. This result could be due to the miscibility of polymers and solvents from the manufacturer. If the solvent ratio is too high, then the nanostrands fall out of suspension and spray films cannot be produced. The polymer systems used in this study require differing amount of

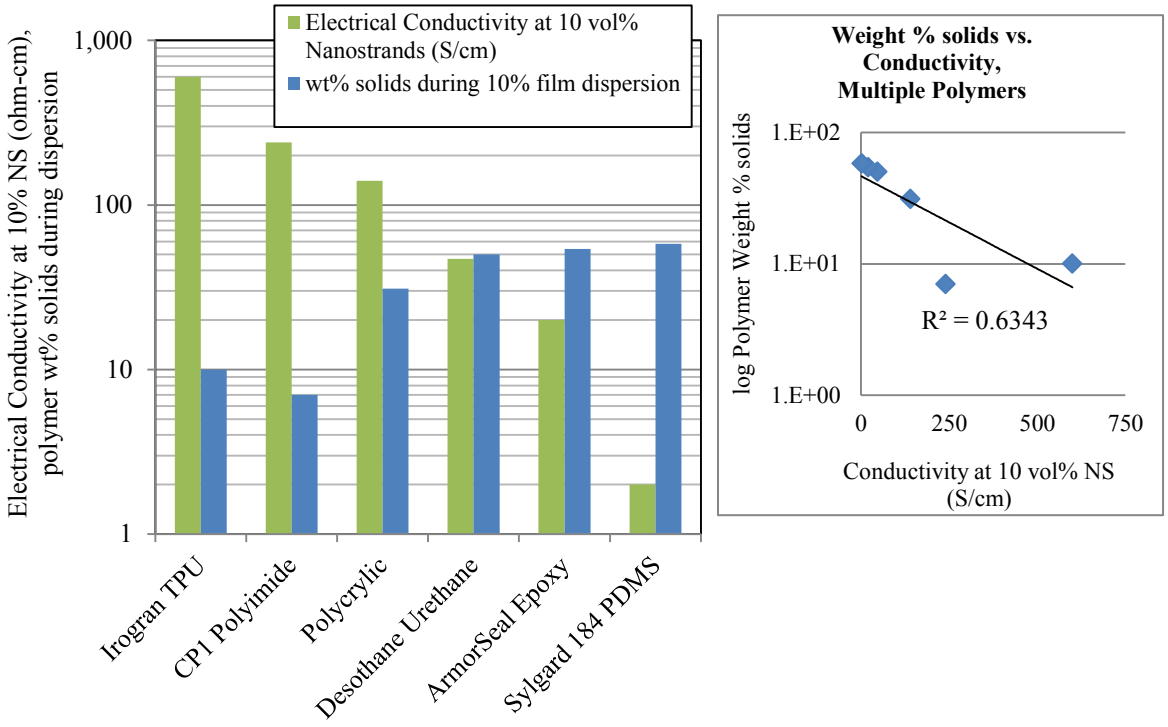

Figure 4.8: Film conductivites and weight percentage of polymer solids during dispersion for 10 volume percent of nanostrands, including correlation chart with R value.

solvents to achieve matching viscosities. The fact that the polymer to solvent ratios during fabrication correlate with the final film electrical conductivities may be purely coincidental.

Another consideration is that the volume percentage of nanostrands in the film is calculated relative to the final film (no solvents). All samples are mixed for matching final volume ratios and total sample volumes. However, samples with significant amounts of solvent will have a larger total volume during dispersion. Thus, the quantity of nanostrands in a sample remains fixed, while the polymer to solvent ratio, nanostrand volume ratio, and total sample volume during dispersion varies to achieve equal viscosities during fabrication. The measured electrical conductivity is at the final

cured/set state of 100% solids. For thermoset systems, this also includes the catalyzation and crosslinking of the polymer system. Thus, knowing the solids percentage of a fluid polymer system can give insight as to the effect on conductivity during processing conditions only. It is anticipated that altering the types of solvents used to reduce the polymer, and also the use of surfactants, could significantly impact the electrical conductivity results in the final film.

4.4.3 Dielectric Strength Testing

The dielectric strength and electrical resistivity of each polymer were tested using solid polymer discs, and thus are analogous to the dry phase films that are characterized with nanostrands. The results of this test are shown in Figure 4.9.

It is seen that the electrical resistivity (inverse of conductivity) of a polymer without nanostrands does not correlate with electrical conductivity with nanostrands. Likewise, the dielectric strength of the polymer film does not correlate to conductivity with nanostrands. The dielectric strength correlates to nanostrand sample conductivity with an R^2 value of 0.2965, and the unfilled polymer resistivity correlates to nanostrand sample conductivity with an R^2 value of 0.0668. This indicates that the film properties that drive conduction mechanisms in nanostrand composites must be related to some other physical property or phenomenon.

We hypothesize that the critical electrical interface in nanostrand polymer composites is at the junction between nanostrands, which will be a function of junction thickness, number of junctions, junction conductivity, and quantum tunneling mechanisms. The junction thickness will be determined not only by nanostrand

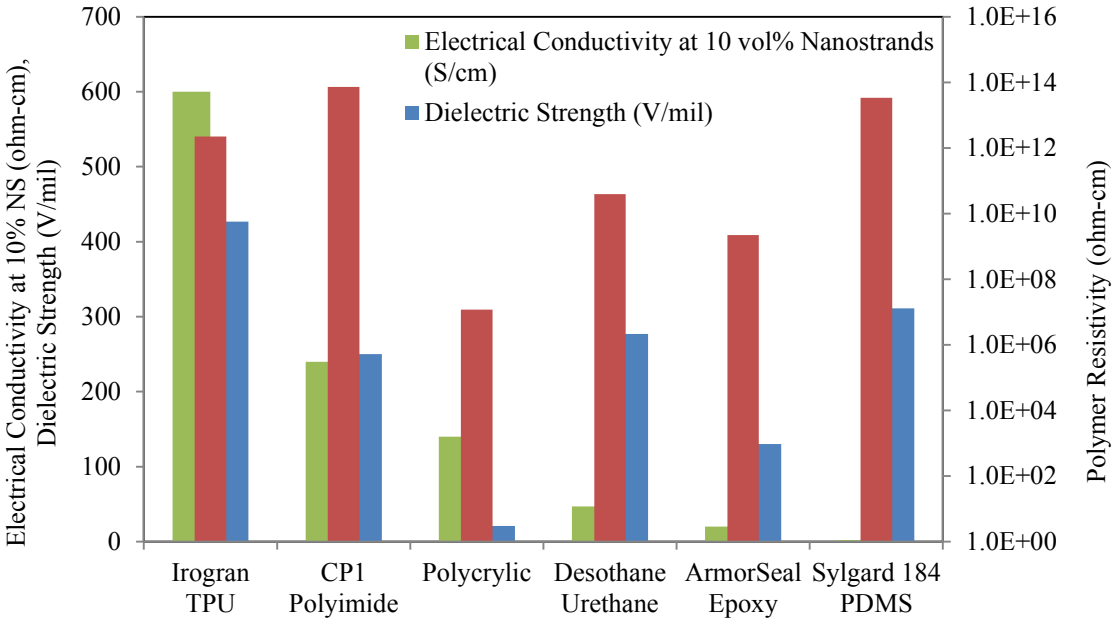

Figure 4.9: Correlation of base polymer resistivies and dielectric strength to electrical conductivity at 10 volume percent of nanostrands.

dispersion and volume fraction, but by the adsorbed layer [37, 38] of polymer on the nanostrand surface. These areas will be the subject of future studies.

4.4.4 Contact Angle Testing

The results of two modes of static contact angle testing are presented. The first mode tests the contact angle of polymer solutions on a pure nickel surface. This is intended to simulate how well nanostrands will wet to a host polymer during dispersion and fabrication processes. The next mode inspects the contact angle of a drop of deionized water on the cured or set polymer film surface. These polymer film surface samples do not contain any nanostrands or nickel. This tests the surface energy characteristics of the polymer to give insight to the surface energy and constituent interactions of the cured

film. The results of these tests are order ranked according to electrical resistivity results and correlated in Figure 4.10.

The contact angle of polymer solutions on a Ni surface correlates to nanostrand sample conductivity with an R^2 value of 0.0428, and the contact angle of water on the solid polymer surfaces correlates to sample conductivities with an R^2 value of 0.0071. These R values indicate that there is no correlation. The failure of either method to correlate to percolated sample conductivities indicates that wet film surface energy characteristics are a poor predictor of conductivity with nickel nanostrands. We conclude that within the scope of this experiment, the wet phase polymer solution contact angles on a nickel surface, as well as the surface energy wetting angles of polymer films, are poor predictors of percolated conductivity results.

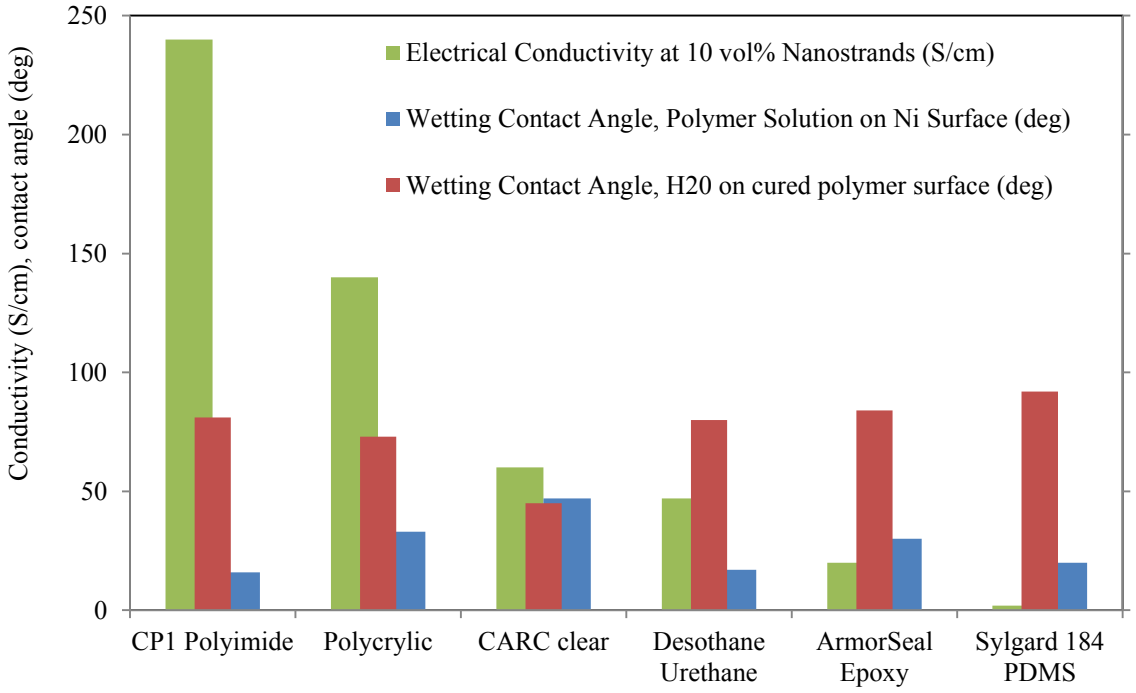

Figure 4.10: Electrical resistivity and contact angle results of polymer solutions on a Ni surface and deinoized water on a polymer surface.

4.4.5 Electrical Properties during Cure/Set (Dynamic Resistance vs. Cure)

A plot of the electrical resistance of nanostrand/polymer films during cure is shown in Figure 4.11. Sylgard® and Desothane® are two part catalyzed systems, whereas Polycrylic® is a single stage acrylic urethane. All of these systems are considered thermosets for the purposes of this test. It is seen that the onset of conduction follows the evacuation of solvents from the sample. It is noted that the percentage of mass loss in the sample follows the discussion and data from Section 4.2, with higher percentage mass loss for samples with a lower percentage of polymer solids during nanostrand dispersion. Polycrylic® samples exhibit some irregularity at the onset of conduction, which was previously hypothesized to indicate multiple factors at the onset of conduction. We deduce that the stabilization of resistivity at approximately one hour is directly related to the final evacuation of solvents from the sample. The first change in slope at approximately 30 minutes may be due to another factor, such as the settling and interconnection of the nanostrand lattice. Much smoother conduction onset curves are seen for urethane (Desothane®) and silicone (Sylgard®) samples. The silicone samples exhibit a conduction curve that stabilizes more rapidly than the corresponding mass reduction curve, indicating that crosslinking of the polymer film may be a factor in developing and stabilizing conduction properties. The urethane conduction curves show that the solvent evaporates more slowly than for the other samples, and also that conduction loosely follows the mass reduction curve but then continues to develop over much longer time periods, indicating a longer cure process.

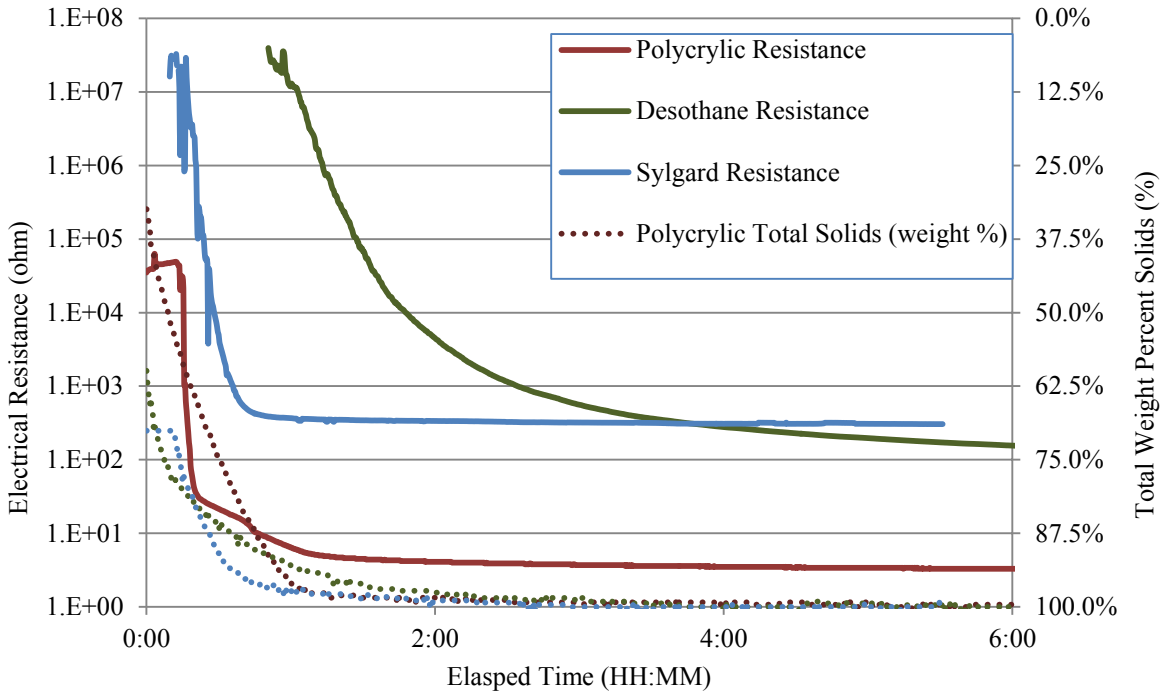

Figure 4.11: Time dependent resistance and mass data for spray film samples with 7.5 volume percent nanostrands. Solids are considered as polymer plus nanostrands.

Figure 4.12 shows the resistance of the films during cure as a function of volume percent nanostrands in the curing film. It is noted that this is a plot of resistance as opposed to resistivity. As the sample volume changes during solvent evacuation, the sample volume required to calculate a resistivity also changes. The effect of this offset is small and does not prohibit conclusions from the resistance plots. All films end at 7.5 vol% nanostrands after solvent evacuation. It is noted that the onset of conduction follows behavior similar to a percolation curve, with steep changes in conductivity over a narrow range, preceded and followed by much more stable behaviors. The critical percolation thresholds and general behaviors for Polycrylic® and Sylgard® are remarkably similar to those given in Figure 4.7. For Desothane®, the percolation

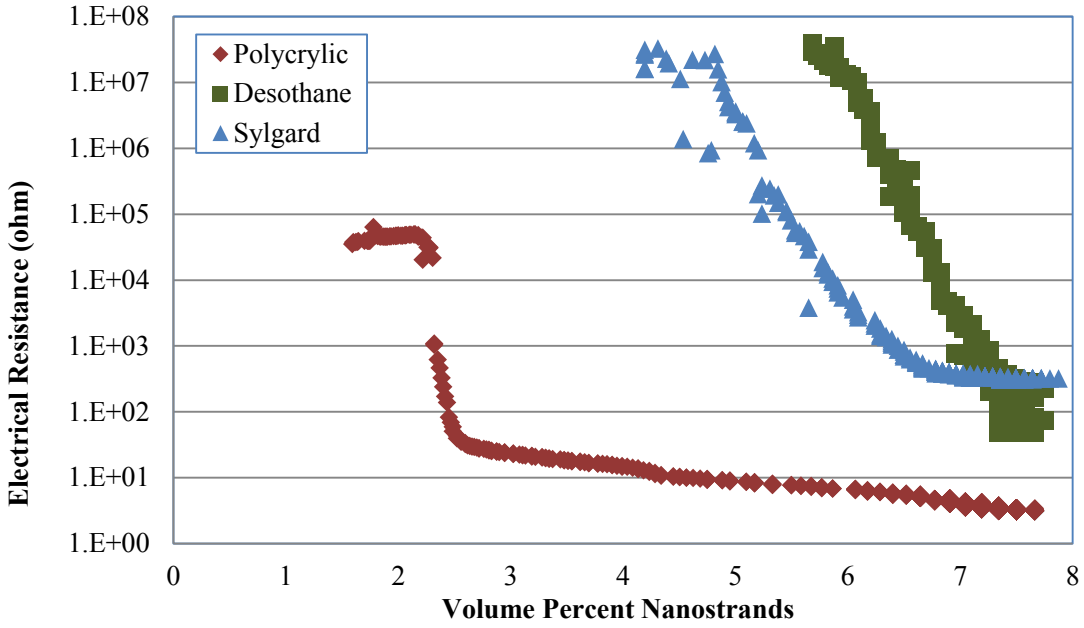

Figure 4.12: Electrical resistance during cure/set versus volume percent of nanostrands (polymer plus nanostrands are solids relative to evacuating solvent). All samples have a final ratio of 92.5 vol% polymer to 7.5 vol% nanostrands.

behavior is not seen until an apparent nanostrand volume percentage of over 5%, significantly higher than the dry film percolation threshold of less than 2%. This is also seen in the time required for the onset of conduction. We consider that this indicates that conduction in Polycrylic® and Sylgard® is strongly related to solvent evacuation, where conduction in Desothane® is not related to solvent evacuation but is strongly related to polymer cure.

4.5 Conclusions

Through this study, a better understanding of the interactions and salient variables that affect polymer nanostrand film conductivity at equal volume fractions of filler has been contributed. Specific investigation into percolation behaviors and polymer physical

properties has been made. While most of the polymer physical property tests have not correlated to conductivity results, they have been necessary tests that give insight to the true mechanisms of conductivity and variables of impact.

This improved understanding of the parameters through which polymer physical properties relate to dispersed nanostrand film electrical conductivities is an important step in developing predictive capabilities for assessing candidate polymers prior to nanostrand dispersion. This information is also an important for understanding improved material models for nanostrand polymer conductivity.

The next steps from this effort will be to seek understanding of the critical interfaces in nanostrand polymer composites at the conductive junctions between adjacent strands. The polymers must next be tested for adsorption on a nanostrand surface, molecular weight, and quantum tunneling characteristics. Investigations into the electromagnetic field effects within a nanostrand sample as well as modeling efforts and predictive capability development will follow.

4.6 Acknowledgements

This work was funded, in part, under Technology Investment Agreement FA8650-11-2-5504 between Conductive Composites Company and The United States of America, under the direction of Mr. John A. Crabill of USAF/AFMC, Wright Patterson Air Force Base, Ohio. The authors gratefully acknowledge the support of the US Government program management team.

4.7 References

[1] X. Shui and D. D. L. Chung, "Submicron diameter nickel filaments and their polymer-matrix composites," *Journal of Material Science,* vol. 35, pp. 1773-1785, 2000.

[2] D. D. L. Chung, "Electromagnetic interference shielding effectiveness of carbon materials," *Carbon,* vol. 39, pp. 279-285, 2001.

[3] J. C. Grunlan, A. R. Mehrabi, M. V. Bannon, and J. L. Bahr, "Water Based Single Wall Nanotube Polymer Filled Composite with an Exceptionally Low Percolation Threshold," *Advanced Materials,* vol. 16, pp. 150-153, 2004.

[4] J.-M. Park, S.-J. Kim, D.-J. Yoon, G. Hansen, and K. L. DeVries, "Self Sensing and interfacial evaluation of Ni nanowire/polymer composites using electro-micromechanical technique," *Composites Science and Technology,* vol. 67, pp. 2121-2134, 2007.

[5] J. C. Grunlan, W. W. Gerberich, and L. F. Francis, "Lowering the Percolation Threshold of Conductive Composites Using Particulate Polymer Microstructure," *J Appl Polym Sci,* vol. 80, 2001.

[6] X. Jing, W. Zhao, and L. Lan, "The Effect of Particle Size on Electric Conducting Percolation Threshold in Polymer/Conducting Particle Composites," *J Mater Sci Lett,* vol. 19, 2000.

[7] A. V. Kyrylyuk, "Continuum percolation of carbon nanotubes in polymeric and colloidal media," *Proceedings of the National Academy of Sciences of the United States of America,* vol. 105, pp. 8221-226, 2008.

[8] S. F. Wang and A. A. Ogale, "Simulation of Percolation Behavior of Anisotropic Short-Fiber Composites with a Continuum Model and Non-Cubic Control Geometry," *Comp Sci and Tech,* vol. 46, 1993.

[9] G. Grimmett, *Percolation. 2nd ed.* vol. 321: Springer, 1999.

[10] G. Hansen, "The Roles of Nanostrands and Nickel Coated Fibers in Electrically Conductive Composite Design," in *37th ISTC*, Seattle, WA, 2005.

[11] J. C. Grunlan, W. W. Gerberish, and L. F. Francis, "Lowering the Percolation Threshold of Conductive Composites Using Particulate Polymer Microstructure," *Journal of Applied Polymer Science,* vol. 80, pp. 692-705, 2001.

[12] X. Sun and M. Song, "Highly Conductive Carbon Nanotube/Polymer Nanocomposites Achievable?," *Macromolecular Theory and Simulations,* vol. 18, pp. 155-161, 2009.

[13] C. Min, X. Shen, Z. Shi, L. Chen, and Z. Xu, "The Electrical Properties and Conducting Mechanisms of Carbon Nanotube/Polymer Nanocomposites: A Review," *Polymer-Plastics Technology and Engineering,* vol. 49, pp. 1172 - 1181, 2010.

[14] W. Bauhofer and J. Z. Kovacs, "A review and analysis of electrical percolation in carbon nanotube polymer composites," *Composites Science and Technology,* vol. 69, pp. 1486-1498, 2009.

[15] G. Hansen, N. Hansen, and L. Hansen, "The Roles of Nanostrands and Nickel Coated Fibers in Electrically Conductive Composite Design " presented at the SAMPE Fall Technical Conference, Seattle, WA, 2005.

[16] G. Hansen, "A Concurrent Solution for both Lightning Strike and Electromagnetic Protection of Aerospace Composites " presented at the SAMPE International Conference, Long Beach, CA, 2008.

[17] G. Hansen, "Highly Effective Broadband Shielding Materials," presented at the National Space and Missile Materials Symposium, Henderson, NV, 2008.

[18] G. Hansen, "Advances in HPM and EMP Hardening Materials," presented at the HEART Conference, Colorado Springs, CO, 2008.

[19] J. Burghardt, N. Hansen, L. Hansen, and G. Hansen, "The Mechanical and Electrical Properties of Nickel Nanostrands in Hysol 9396 Epoxy," in *SAMPE International Conference*, Long Beach, CA, 2006.

[20] N. Hansen, L. Hansen, and G. Hansen, "Electrically Conductive Structural Adhesive with Milliohm Resistance," presented at the SAMPE International Conference, Long Beach, CA, 2008.

[21] N. Hansen, G. Hansen, and E. Silverman, "Versatile Gap Fillers and Sealants for High Level Conductivity and Electromagnetic Shielding," presented at the SAMPE Spring Symposium, Seattle, WA, 2010.

[22] N. Hansen and G. Hansen, "Electromagnetically Shielding Spray Paints Using Commercial-Off-The-Shelf Polymer Systems," presented at the SAMPE Fall Technical Conference, Wichita, 2009.

[23] J. Tomblin, J. Kostogorova-Beller, G. Hansen, and N. Hansen, "Evaluation of Lightning Strike Protection Schemes which Employ Conductive Primers," presented at the SAMPE Fall Technical Conference, Wichita, KS, 2009.

[24] J. A. E. Bell and G. Hansen, "Nickel Coated Fibers for Aerospace Applications," presented at the SAMPE International Symposium Proceedings, Anaheim, CA, 1991.

[25] G. Hansen, "Nano-Microstructured Lightning Strike Protection System Using Nanostrands and Conductive Fiber Composites " presented at the SAMPE International Conference, Long Beach, CA, 2006.

[26] G. Hansen, N. Hansen, D. O. Adams, J. Burghardt, D. Widauf, and T. McNeill, "Electrically Conductive Putty Type Repair System For Composite Structures " presented at the SAMPE International Conference, Baltimore, MD, 2007.

[27] G. Hansen and N. Hansen, "The Role of Nanomaterials in Lightning Strike Protection of Aircraft," presented at the National Nano Engineering Conference, Boston, MA, 2007.

[28] G. Hansen, "High Aspect Ratio Sub-Micron and Nano-scale Metal Filaments," *SAMPE Journal,* pp. 24-28, April 2005.

[29] N. Hansen, D. O. Adams, K. DeVries, A. Goff, and G. Hansen, "Investigation of Electrically Conductive Structural Adhesives using Nickel Nanostrands," *Journal of Adhesion Science and Technology,* vol. 25, pp. 2659-2670, 2010.

[30] N. Hansen, D. O. Adams, K. L. DeVries, A. Goff, and G. Hansen, "Investigation of Electrically Conductive Structural Adhesives using Nickel Nanostrands," *Journal of Adhesion Science and Technology,* vol. 25, pp. 2659-2670, 2011.

[31] ASTM Standard D257-07, 2007, “Standard Test Methods for DC Resistance or Conductance of Insulating Materials" ASTM International, West Conshocken, PA, 2007, DOI: 10.1520/D0257-07, www.astm.org

[32] Detail Specification MIL-DTL-83528C, 2001, "Gasketing Material, Conductive, Shielding Gasket, Electronic, Elastomer, EMI/RFI, General Specification For," United States Department of Defense.

[33] B. E. Kilbride, J. N. Coleman, J. Fraysse, P. Fournet, M. Cadek, A. Drury, S. Hutzler, S. Roth, and W. J. Blau, "Experimental observation of scaling laws for alternating current and direct current conductivity in polymer-carbon nanotube composite thin films," *Journal of Applied Physics,* vol. 92, p. 4024, 2002.

[34] O. K. Johnson, C. J. Gardner, D. T. Fullwood, B. L. Adams, N. Hansen, and G. Hansen, "The Colossal Piezoresistive Effect in Nickel Nanostrand Polymer Composites and a Quantum Tunneling Model," *CMC: Computers, Materials, & Continua,* vol. 15, pp. 87-112, 2010.

[35] ASTM Standard D149-09, 2009, "Standard Test Method for Dielectric Breakdown Voltage and Dielectric Strength of Solid Electrical Insulating Materials at Commercial Power Frequencies" ASTM International, West Conshocken, PA, 2009, DOI: 10.1520/D0149-09, www.astm.org

[36] N. Hansen, "Structure-Property Relationships of Highly Conductive Nickel Nanostrand Polymer Composites," presented at SAMPE International 2010, Seattle, WA, 2010.

[37] E. Tadd, A. Zeno, M. Zubris, D. Nily, and R. Tannenbaum, "Adsorption and Polymer Film Formation on Metal Nanoclusters," *Macromolecules,* vol. 36, pp. 6497-6502, 2003.

[38] H. Inoue, H. Fuuke, and M. Katsumoto, "The effect of adsorbed polymer molecular weight on magnetic particle dispersibility," *Journal of Colloid and Interface Science,* vol. 148, pp. 533-540, 1992.

5 EVALUATION AND DEVELOPMENT OF PERCOLATION MODELS FOR ELECTRICAL CONDUCTIVITY IN NICKEL NANOSTRAND POLYMER COMPOSITES

Nathan Hansen[1], Daniel O. Adams[1], David T. Fullwood[2]

[1]University of Utah, Department of Mechanical Engineering, 50 S. Central Campus Dr., Salt Lake City, UT 84112 USA

[2]Brigham Young University, Department of Mechanical Engineering, 435 Crabtree Building, Provo, UT 84602 USA

Submitted for Publication in the Journal of Applied Polymer Science.

5.1 Abstract

The electrical conductivity of composites and polymeric based systems is frequently improved by the addition of conductive additives to form a conductor-insulator binary system. This study considers nickel nanostrands as a conductive element in polymer systems. Materials characteristics are considered in order to form a basis for understanding and predicting the electrical percolation behaviors of nanostrand composites, specifically seeking models that can distinguish between different polymer systems. Empirical percolation data for nickel nanostrands in four different polymeric systems is presented and used to evaluate candidate electrical conductivity models. Classical percolation approaches are found to not show good fit, but more advanced models are able to provide good correlation to tested results. Specifically, Tunneling Percolation (TPM) models and the Two Exponent Phenomenological Percolation Equation (TEPPE) model based on the Generalized Effective Media (GEM) theory show good fit. A combined TEPPE-TPM approach is developed that applies tunneling percolation to the GEM theory. This combined model includes tunneling considerations in equations that accurately represent behaviors in all regions of percolation behavior.

5.2 Introduction

The development of highly conductive polymeric systems has led to broad interest in both commercial and defense applications. Required electrical specifications often span many orders of magnitude in resistivity performance, and the development of highly conductive systems remains an intense area of interest. A common approach to imparting

electrical conductivity into otherwise insulating polymer systems is to use conductive fillers to form a binary composite system which percolates electrically[1,2]. Newly available nanomaterials show promise for improved properties in these conductor-polymer composites[3,4].

Nickel nanostrands[5] are a new material that show advantageous geometric and percolation properties. They are sub-micron diameter (typically 50-300 nm), high aspect ratio nanostructures. Nanostrands feature an intrinsic three-dimensionally interconnected structure that creates completed loops and demonstrate a branched nature (See Figure 5.1). This interconnecting structure is observed *in situ* when dispersed in polymeric or fluid systems.

The looped and branched nature of the nanostrand structure facilitates three-dimensional interconnection at low volume fractions. The nanostrand structure can be

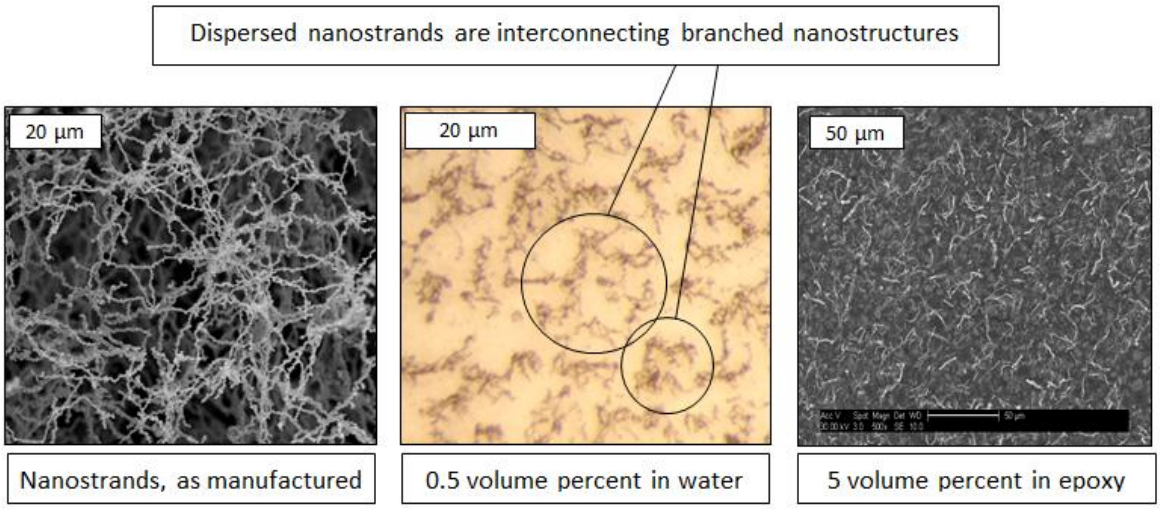

Figure 5.1: Nickel nanostrands, as-manufactured (left) and dispersed in fluid and polymer systems (center and right).

viewed as a "skeleton" rather than a full "body" (such as solidly structured conductive particles, e.g. spheres and flakes). The void space of the nanostrand structure is filled with the host matrix, facilitating better preservation of material properties while providing a conductive percolating skeleton structure. Nickel also provides from high intrinsic electrical conductivity, ferromagnetic properties, and corrosion resistance. Test results have indicated electrical performance that is significantly more conductive, at equal volume fractions than other conductive fillers. For example, nanostrand mixtures percolate to higher electrical conductivity levels than carbon nanomaterials[3,4,6-8].

In this work, the percolation characteristics of nickel nanostrands as the conductive phase in metal-polymer composites are investigated. Nanostrand polymer composites are used in applications including electrostatic discharge, electromagnetic shielding, caulks, gaskets, adhesives, paints, and lighting strike protection. However, previous work has been primarily empirical, and there has been little investigation in developing models to explain and predict nanostrand-polymer system electrical properties. Thus, a primary purpose of this study is to identify suitable models for understanding and predicting the electrical percolation properties of nanostrand polymer composites across multiple polymer systems.

5.3 Modeling Background

Previous work[9] on the static state modeling of nanostrands systems have followed the effective medium method of Maxwell[10] and shown poor correlation across relatively few data points. Recent work by Johnson has provided a piezoresistive model with good fit[11]. A central purpose of this effort is to include a broad consideration of modeling

approaches that investigate the polymer dependent percolation behaviors of nanostrand systems. Several common classes of models are considered and examined for relevance to nanostrand composites. As the intention of this work is to serve as an overview and evaluation of the models deemed most suitable for nanostrands, only brief reviews of each model are given. The reader is encouraged to consult the included references of each approach for further details on each approach. Many excellent works are available on modeling electrically conductive materials in insulating systems (for example, see [1-3,12-16] and the references therein).

Most efforts towards understanding mixtures of conductive materials dispersed in insulating polymers are based on percolation theory. Percolation theory deals with the behaviors of interconnected random clusters, and is regularly applied to randomized and/or distributed cases dealing with transport mechanisms through a volume. This effort is focused on percolation as applied to mixtures of dispersed electrical conductors (nanostrands) in electrically insulating matrices (polymer films). Percolation models for this case are generally divided into two categories: physical percolation and tunneling percolation. Based on the results of previous publications[17] and the observed percolation behaviors in sample sets, it is expected that nanostrands will be accurately modeled by percolation models and tunneling models. In physical percolation approaches, the conductors are assumed to touch physically as a dispersed system. In tunneling models, the conductors remain isolated from adjacent conductors by the insulating host, and electron transport mechanisms are governed by non-contact mechanisms such as quantum mechanical tunneling of electrons across an energy barrier. It is typical for authors to

consider both cases (for example, see[1,12]). Physical percolation is classically approached using the Excluded Volume Approach[18], which led to the Random Void and Inverse Random Void models[19] to explain nonuniversal behaviors. Classical percolation as presented by Stauffer and Aaharoni[2] explains conduction in a mixture of insulating and conductive particles based on the probability of electrical contact, which generally follows a power law form (as presented in the following section). Mclachlan[20,21] developed a generalized media approach to conductor insulator mixtures based on Bruggemans symmetric theory, which is detailed in the following section.

Percolation based thermodynamic models account for the surface energies of the constituent materials, thus including conductor-insulator interactions between different types of polymer hosts. Previous work[22] has shown that this is a critical variable for nanostrand-polymer composites, and the intention of previous efforts[23] has been to identify which polymer characteristics are most relevant to the conductivity of nanostrand composites at equal volume fractions in different polymers. Thermodynamic models such as those proposed by Mamunya[24] and Clingerman[25] have shown good correlation to carbon based systems in thermoplastic polymers[16,25]. These models involve several fitting factors and constants that must be obtained empirically through regression analysis. While these models have worked well for carbon based thermoplastic systems, previous work[23] has not shown good correlation of polymer surface energy characteristics to nanostrand composite electrical conductivities in wet phase dispersed thin films. An additional difficulty in correlation is that the dispersion of the nanostructure occurs during the uncured (for thermosets) or solvent reduced (for thermoplastics) phase, but the

conductivity of the sample is measured in the cured/set solid phase. The surface energy characteristics of the constituents must be determined for both the un-catalyzed or solvent based fluid phase and solid phase of the polymer system. In the previous study, no correlation was seen in the polymer fluid solution phase or solid phase surface energies to electrical conductivities in nanostrand composite. As the available surface energy data does not show correlation to percolation samples conductivities, thermodynamic models are not pursued in this present work. It is anticipated that manufacturing methods that do not involve solvent based alterations to the polymer phase will provide better correlation, as this has been the basis of success in previous studies[25]. Further characterization efforts in nanostrand polymer systems will include improved methods for studying constituent surface energy properties, particularly for fluid phase polymer systems.

Recent works have provided valuable insight to the tunneling-percolation relationships in conductor-insulator percolation systems[19,26-28]. Tunneling approaches consider that the conductors in an insulator conductor composite remain physically separated (such as by a thin polymer layer adsorbed on the conductor surface[29,30]), and must thus rely on quantum tunneling effects to achieve conduction between adjacent elements. Tunneling in conductor insulator mixtures was suggested by Sichel[31] and further developed by Carmona[32], Balberg[19], Rubin[33], and more recently by Grimaldi and Balberg[28]. There have been several recent works regarding Monte Carlo simulations for tunneling percolation conductivity in graphene nanocomposites[34,35] and carbon nanotube composites[36]. Nickel nanostrands were specifically considered in a piezoresistive tunneling model developed by Johnson[11]. In this study, the tunneling percolation

approach of Rubin is followed, which explains nonuniversal behaviors and transport mechanisms in conductor insulator composite systems.

5.4 Models Used in This Study

5.4.1 Classical Statistical Percolation

Classical percolation models are statistical in nature, and are based on the probability of contact between adjacent constituents in a representative area (two dimensions) or volume (three dimensions). Classical models consider a network of conductive links in a nonconductive matrix, and model the connectivity across an infinite sample of a network structure. When a sufficient volume of conductors are present to create an electrically conductive path through a volume, an abrupt change is conductivity is observed, referred to as the critical percolation threshold. For loadings at and above this value, the conductivity of the composite follows a power law given by[2,15,37]:

$$\sigma \sim (p - p_c)^{t_{un}}, p > p_c \tag{5.1}$$

where σ is the electrical conductivity of the sample, p is the probability of contact between conductors, p_c is the critical contact probability associated with a drastic change in electrical conductivity in the sample, and t_{un} is the scaling exponent, which is generally reported as 2 for three-dimensional percolation. Variations in the scaling exponent are regularly reported[3,12,19,28,38,39].

If the probability of contact is determined by the volume fraction of the percolating filler and scaled by the conductivity of the filler, the percolation relationship takes the following form as expressed by Kirkpatrick[40] and Zallen[41]:

$$\sigma \sim \sigma_f(\varphi - \varphi_c)^{t_{un}}, \varphi > \varphi_c \tag{5.2}$$

where σ_f is the electrical conductivity of the filler, φ is the volume fraction of conductor, and φ_c is the critical volume fraction of conductor at the percolation limit. The resistivity of the composite continues to follow this power law until a percolation limit is reached. This loading presents a limiting value for well dispersed conductive networks. For loadings above this value, a decrease in electrical and mechanical properties is often observed, indicating that the polymer host is no longer capable of facilitating additional increase in metallic filler. For nanostrands, the conductivity of the filler is assumed to be that of nickel, with a value of 1.44E6 S/cm. As demonstrated in the results, this classical model does not generally show sensitivity or good fit. The approach has been included here as a reference basis for more advanced models.

5.4.2 Modified Statistical Percolation (MSP) Models

A natural extension of the classical percolation approach is to remove the assumption of universality in the scaling exponent and to seek appropriate scaling factors. The use of scaling factors is not considered to invalidate universality, as even the linear fitting of naturally occurring processes typically requires a constant correction factor to match theoretical analysis. The classical percolation approach then takes the form:

$$\sigma \sim K\sigma_f(\varphi - \varphi_c)^t, \varphi > \varphi_c \quad (5.3)$$

where t is a nonuniversal scaling exponent that can be obtained by various methods, and K is a scaling factor based on differences in percolation behaviors. In this study, t is obtained through linear regression of experimental data. The value of K is determined through curve-fitting techniques.

5.4.3 Tunneling Percolation Models (TPM)

In a conductor-polymer composite, electrical resistivity is dominated by resistance between neighboring conductive elements. The contact points where electron transport occurs can be referred to as "junctions". Resistance through the conductors is considered to be much smaller that resistance of the junction. For junctions with very small gaps (on the order of several nanometers), the junction resistance may be modeled by assuming a quantum tunneling effect[42].

An approach to classical percolation that includes electron tunneling at insulator filled junction is given by Rubin[33]. This model is referred to as a tunneling-percolation model (TPM). The TPM approach also includes consideration for if a dispersed conductor features a "high structure," and this metric is judged relative to spherical structures. Spheres are considered as a "low" structure; more randomized or elongated structure are considered to be more "high." This consideration is significant for the random and interconnected structure of nanostrands.

Using a simplified Hertz distribution for particle distribution, the probability of electron tunneling in the percolated composite, and the nodes-link-blobs (NLB) approach common in percolation theory[2,19,43], the TPM percolation model takes the form of:

$$\sigma \sim \sigma_f \left(\frac{\varphi}{1-\varphi_c} - \frac{\varphi_c}{1-\varphi_c} \right)^{t_{un}+\left(\frac{a}{d}-1\right)}, \varphi > \varphi_c \tag{5.4}$$

where t_{un} is the universal critical exponent, a is the separation distance between conductors, and d is the characteristic tunneling distance of the polymer system. Typically it is assumed that the separation distance between conductors is dependent on dispersion characteristics[44,45], the thickness of the polymer layer that is adsorbed on the conductor surface[12,29,30], and the volume fraction (and packing arrangement) of conductor.

For this TPM approach, the packing fraction and corresponding distance between conductors is estimated to be inversely proportional to the volume fraction of nanostrands. The critical percolation threshold of a particular polymer system is also estimated to be directly proportional to the characteristic tunneling distance. The separation distance is then given by:

$$a \sim \frac{10\varphi_c}{\varphi} \tag{5.5}$$

The characteristic tunneling distance d for nanostrand polymer composites has been the subject of previous studies[11]. The tunneling voltage and tunneling current of thin polymer films on a nickel surface was tested by nano-indentation. The displacement at

which the tunneling voltage and current curves cross over is taken as the characteristic tunneling distance. The cross over is fully transitioned within a 1 nm range. Four polymers were tested, of which two (TPU and silicone) are included in the present study. Accordingly, the TPM model is tested only for these two polymer systems.

A scaling correction factor K is required to shift the curve to the proper region of the nanostrand percolation curve. This correction factor is assumed to be dependent on the polymer tunneling characteristics, with a larger correction factor needed for systems with larger characteristic tunneling distances and percolation thresholds. The TPM model then takes the following form:

$$\sigma \sim K\sigma_f \left(\frac{\varphi}{1-\varphi_c} - \frac{\varphi_c}{1-\varphi_c}\right)^{t_{un}+\left(\frac{10\varphi_c}{d\varphi}-1\right)}, \varphi > \varphi_c \tag{5.6}$$

5.4.4 Generalized Effective Medium (GEM or TEPPE model)

A Generalized Effective Medium (GEM) approach has been developed by McLachlan, with works published in 1985[20] and 1986[21,46]. This approach is based on interpolation between Bruggemans symmetric and asymmetric theories. The symmetric theory is based on random mixture of contacting spheres, and the asymmetric theory is based on a two component dispersion of spheres in a host, where the spheres are coated with the host component. McLachlan considered this model to describe the conductivity of isotropic binary mixtures in terms of the conductivities, volume fraction, and morphology of each parameter. This work was later extended to consider complex electrical behaviors through the effective media approach[13]. This is expressed in recent

works[17,44] as the Two-Exponent Phenomenological Percolation Equation (TEPPE), given by:

$$(1-\varphi)\frac{\sigma_p^{\frac{1}{s}}-\sigma^{\frac{1}{s}}}{\sigma_p^{\frac{1}{s}}+\left(\frac{1-\varphi_c}{\varphi_c}\right)\sigma^{\frac{1}{s}}}+\varphi\frac{\sigma_f^{\frac{1}{t}}-\sigma^{\frac{1}{t}}}{\sigma_f^{\frac{1}{t}}+\left(\frac{1-\varphi_c}{\varphi_c}\right)\sigma^{\frac{1}{t}}}=0 \tag{5.7}$$

Solving at limits of zero and infinity yields the following expressions:

$$|\sigma_f| \to \infty:\ \sigma=\sigma_p\left(\frac{\varphi_c}{\varphi_c-\varphi}\right)^s, \varphi<\varphi_c \tag{5.8}$$

$$|\sigma_p| \to 0:\ \sigma=\sigma_f\left(\frac{\varphi-\varphi_c}{1-\varphi_c}\right)^t, \varphi>\varphi_c \tag{5.9}$$

$$\sigma \cong \sigma_p^{\frac{t}{s+t}}\sigma_f^{\frac{s}{s+t}}, \varphi\sim\varphi_c \tag{5.10}$$

These equations function as the normalized standard percolation equations characterized by the exponents s and t. Mclachlan gives a universal value for s of 0.87, with reported values ranging between 0.37 and 1.28. The exponent t is reported to have a universal value of 2 with values between 1 and 6.27. In this work, a value of 0.2 is used for s, and a value that varies across polymer types between 3.2 and 4.7 is used for t.

A main advantage to this approach is the ability to account for conductivity behaviors that are different below and above the percolation threshold, thus providing a model across any level of conductor volume fraction. McLachlan ([17] and the references therein) also explains that percolation curves for DC conductivities will indicate whether

measured electrical behaviors indicate continuum behavior for conductor-host or insulator-host models, or percolation driven TEPPE-like behaviors. Observed nanostrand percolation curves indicate that nanostrand composites behave as percolation systems.

5.4.5 Combined TEPPE-TPM Model

Based on the approaches of Rubin (TPM) and McLachlan (TEPPE), a combined model is developed based on the effective media approach with explicit consideration of electron tunneling above the critical percolation threshold. Where Rubin applies tunneling behavior in the exponent of the generalized classical percolation case, it is applied herein to the TEPPE solutions at the lower limit (above the percolation threshold) to yield the following:

$$\sigma = \sigma_p \left(\frac{\varphi_c}{\varphi_c - \varphi}\right)^s, \varphi < \varphi_c \tag{5.11}$$

$$\sigma = K\sigma_f \left(\frac{\varphi - \varphi_c}{1 - \varphi_c}\right)^{t_{un}+\left(\frac{10\varphi_c}{d\varphi}-1\right)}, \varphi > \varphi_c \tag{5.12}$$

$$\sigma \cong \sigma_p{}^{\frac{t}{s+t}}\, \sigma_f{}^{\frac{s}{s+t}}, \varphi \sim \varphi_c \tag{5.13}$$

This approach includes the implied hypothesis that conduction mechanisms up to and within the percolation threshold can be understood by generalized media theories, and that conduction mechanisms above the percolation threshold must also include consideration of tunneling mechanisms. As sufficient data for the TPM model are only

available for two of the polymers in this study, this combined model is also tested against only those polymers.

5.5 Experimental

The polymers chosen for this study are widely available commercial systems, as detailed in Table 5-1. These systems were chosen for ease of use, relevance to commercial applications, and correlation to previous data[22,47]. All polymers were used in their as-received state and prepared according to the manufacturer recommendations. Nickel nanostrands were provided by Conductive Composites Company and were dispersed according to the manufacturer recommendations[48]. All calculations and plotted data use volume fraction, as this gives more relevant comparison to volumetrically driven percolation mechanisms.

Table 5-1 Host Polymers for Nanostrand Nanocomposites (this study)

Tradename	**Manufacturer**	**Type**	**Notes**
Polycrylic®	Minwax®	Acrylic Urethane	Water based, low cost
Desothane®	PRC-DeSoto	Urethane	Commercial aviation coating
Sylgard®	Dow Corning®	Silicone	Multifunctional silicone system, tested in previous nano-indentation study[11]
Irogran®	Huntsman Chemical	Thermoplastic Polyurethane (TPU)	Thermoplastic elastomer, tested in previous nano-indentation study[11]

5.5.1 Conductivity and Electrical Percolation Samples

Polycrylic®, Desothane®, and Sylgard® samples were received as fluid mixtures suitable for nanostrand dispersion, with solvent correction for viscosity as needed. Irogran® samples were received as a solid pellet, and were dissolved in tetrahydrafuran and methyl ethyl ketone prior to nanostrand dispersion. A desired volume fraction of nickel nanostrands was added to a polymer system and wet by manual mixing. Dispersion was achieved by using a Thinky AR-250 centrifugal double planetary mixer. A mixing duration of 20 seconds at 2000 rpm was used for all samples. It was sometimes necessary to use additional solvents at higher volume fractions (10 percent nanostrands and above), particularly in systems with a higher volume fraction of polymer solids. Mixtures were screened through a -50 woven stainless steel mesh. Care was taken to control independent variables and to process all samples in as equal of a method as was possible, across all volume fractions and for all polymer types.

Dispersed nanostrand mixtures were applied as thin coatings on electrically insulating substrates (Kapton® polyimide film). Spray coatings were applied with a DeVilbiss FLG-3 High Volume Low Pressure (HVLP) gravity feed spray gun. A size 22 tip and Size 3 HVLP air cap were used, with nozzle pressure typically below 10 psi. Samples were sprayed in the appropriate number of coats to match the polymer manufacturer's wet mil and build specifications. Target final sample film thickness was 100 μm, which was achieved with ± 10 μm accuracy.

5.5.2 Electrical Resistivity of Highly Resistive Polymer Samples

The purpose of this test is to measure the electrical resistivity of polymer films without the presence of any nanostrands. These values were not available from polymer system manufacturers. Volume resistivity measurements were made by ASTM D257 – 07: Standard Test Methods for DC Resistance or Conductance of Insulating Materials. Testing was performed by Intertek of Pittsfield, Massachusetts, using a guarded parallel plate fixture with concentric rings, with an electrification time of 60 seconds at 500 volts.

5.5.3 Electrical Resistivity of Conductive Samples (Beyond Percolation Threshold)

Areal surface resistivity readings of coating samples were taken using an ohm-per-square jig and a four point Kelvin probe method, as specified in MIL-DTL-83528C: General Specification for Gasketing Material, Conductive, Shielding Gasket, Electronic, Elastomer, EMI/RFI. The ohm-per-square jig for this study uses two copper bars 2.54 cm in length, 6.35 mm wide, and 6.35 mm high. These bars are bonded to an electrically insulating jig that separates them by a distance of 2.54 cm, thus a surface area of 6.45 cm^2 is measured between contact paths. Kelvin probe leads are attached to each bar and resistance readings are taken across the surface of the sample (see Figure 5.2). An Extech 380560 High Resolution Precision Milliohm meter was used for all resistance readings below 20 kΩ. In the rare case of resistances above 20kΩ, readings were taken with a handheld multimeter.

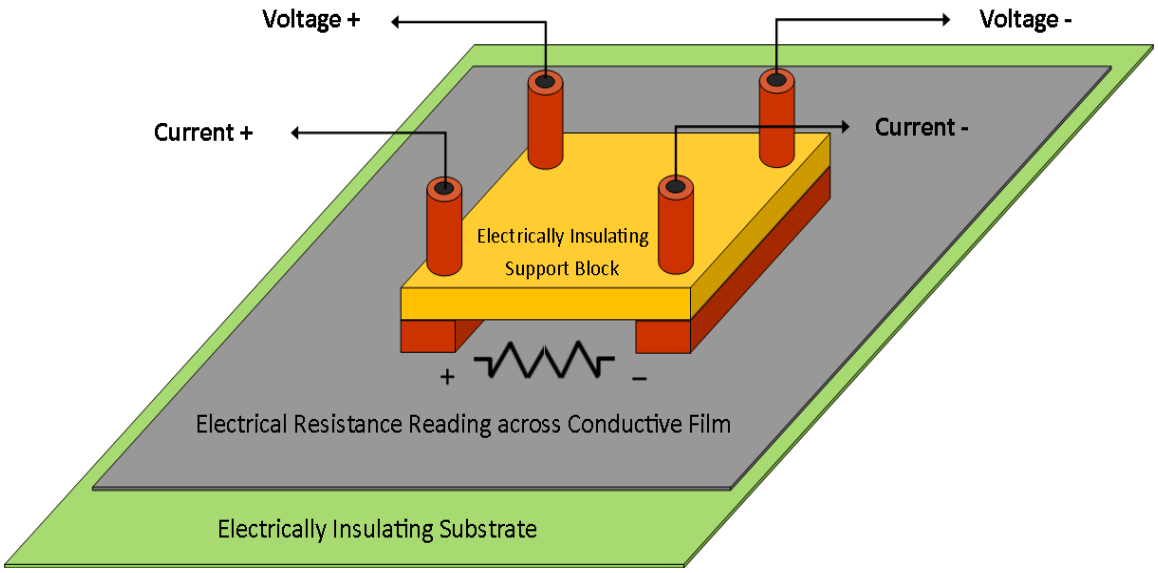

Figure 5.2: Kelvin Probe method for surface resistivity of conductive coating films.

Thickness readings were taken with a Mutitoyo IP65 micrometer having 0.002 mm resolution. Sample conductivities were calculated using a thin-film approximation and surface resistivity according to:

$$\sigma^{-1} = \rho = R_s \frac{A}{l} \tag{5.14}$$

where σ is the electrical conductivity of the nanocomposite (Siemens/cm), ρ is the electrical resistivity (ohm-cm), R_s is the surface resistivity (ohm-per-square), l is the length of the separation path (cm), and A is the cross sectional area of the film between contact bars (given by the bar separation distance l multiplied by the film thickness t).

5.6 Results and Discussion

5.6.1 Electrical Resistivity and Percolation

The measured electrical percolation behavior for the polymers from Table 5-1 is presented in Figure 5.3. There is a wide range of electrical conductivities for a given volume fraction of nanostrands, even at the percolation limit. Samples exhibit a critical percolation threshold between 1 and 5.5 volume percent, and a percolation limit generally at 10 to 20 volume percent. Electrical conductivities at the percolation limit are between 12 and 630 S/cm.

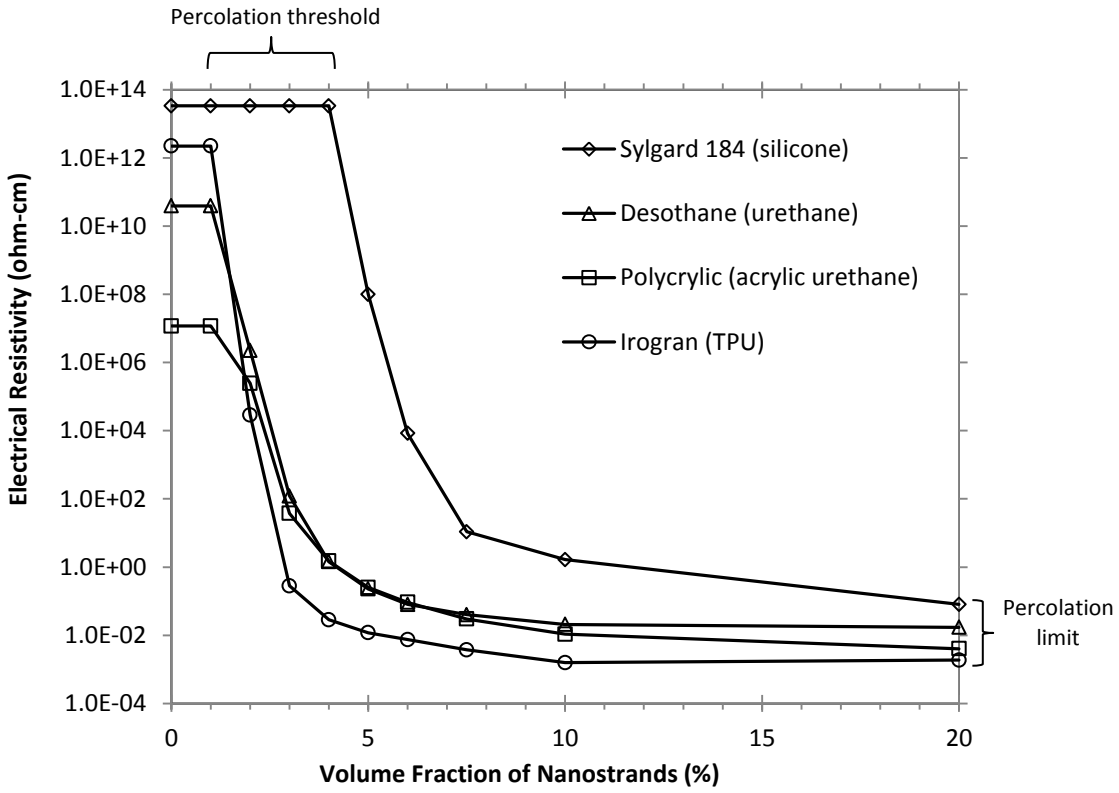

Figure 5.3: Electrical resistivity percolation of nickel nanostrands in polymer films.

Percolation thresholds were determined using fitting methods at just the critical threshold region. Linear regression methods were also tested for fitting the percolation threshold[49], but were found to be unreliable when including data points from higher conductivity samples. Values for the percolation threshold, limit, and electrical conductivities at the percolation limit are given in Table 5-2.

5.6.2 Models Fit to Experimental Data

The fit of the classical statistical power law is shown in Figure 5.4. While the basic power law does capture differences in the percolation threshold, it cannot distinguish between differences in the percolation limit across polymers, nor does it lie within the proper region of actual conductivity behaviors.

The use of the modified statistical percolation (MSP) model, as shown in Figure 5.5, yields an improved fit to experimental data. Scaling exponent values remain close to the universal case, which indicates a conductive filler with a highly irregular structure [19,33]. A relatively constant value of K is used to shift the modified statistical percolation model to the proper conduction regime. It was theorized in previous efforts [23] that the electrical resistivity of the polymer would be an appropriate correction factor for scaling the percolation power law. However, measured resistivities for the unfilled polymers reveal that the electrical resistivity of the polymer does not regularly correlate to either the percolation threshold or percolation limit for available data.

The TPM model shows a significantly improved fit over standard power law approaches. Figure 5.6 shows that the TPM has a good fit to both of the polymers with tunneling data available for this study.

Table 5-2 Electrical Percolation of Nanostrands across Polymer Types

Tradename/type	Critical Percolation Threshold	Percolation Limit	Conductivity at Percolation Limit (S/cm)
Polycrylic® acrylic urethane	0.016	0.20	250
Desothane® urethane	0.017	0.15	58
Sylgard® silicone	0.055	0.20	12
Irogran® TPU	0.015	0.15	630

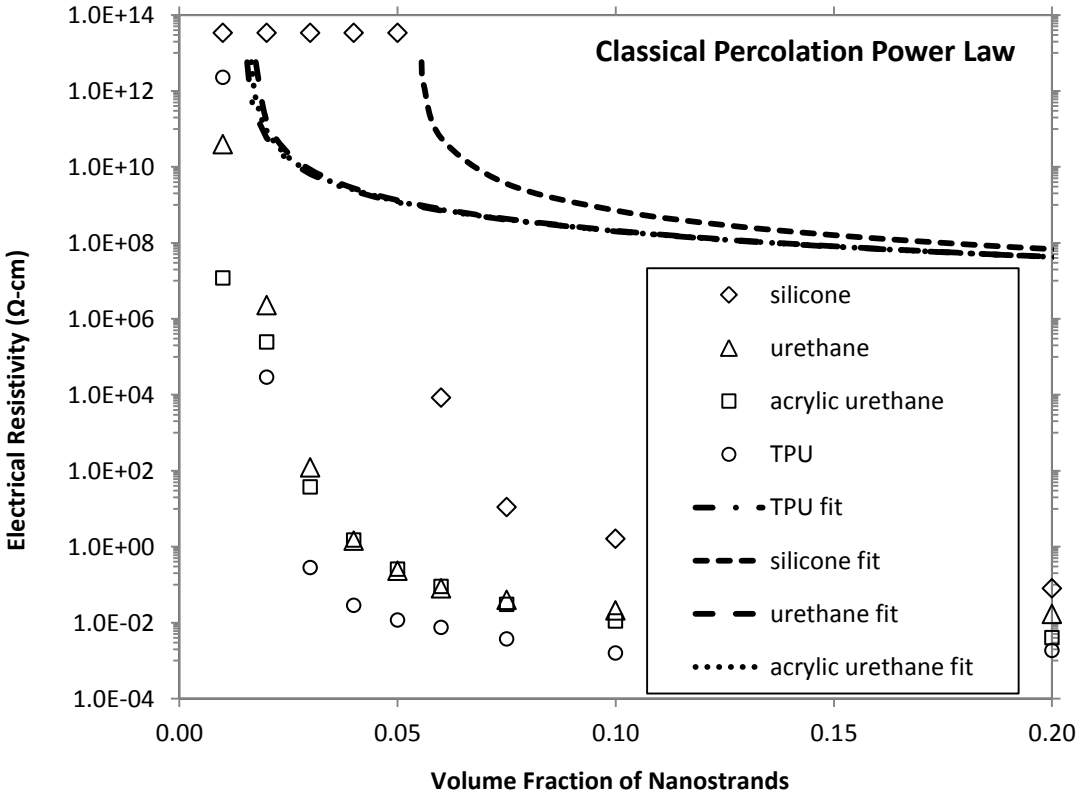

Figure 5.4: Experimental results compared to the classical percolation power law model.

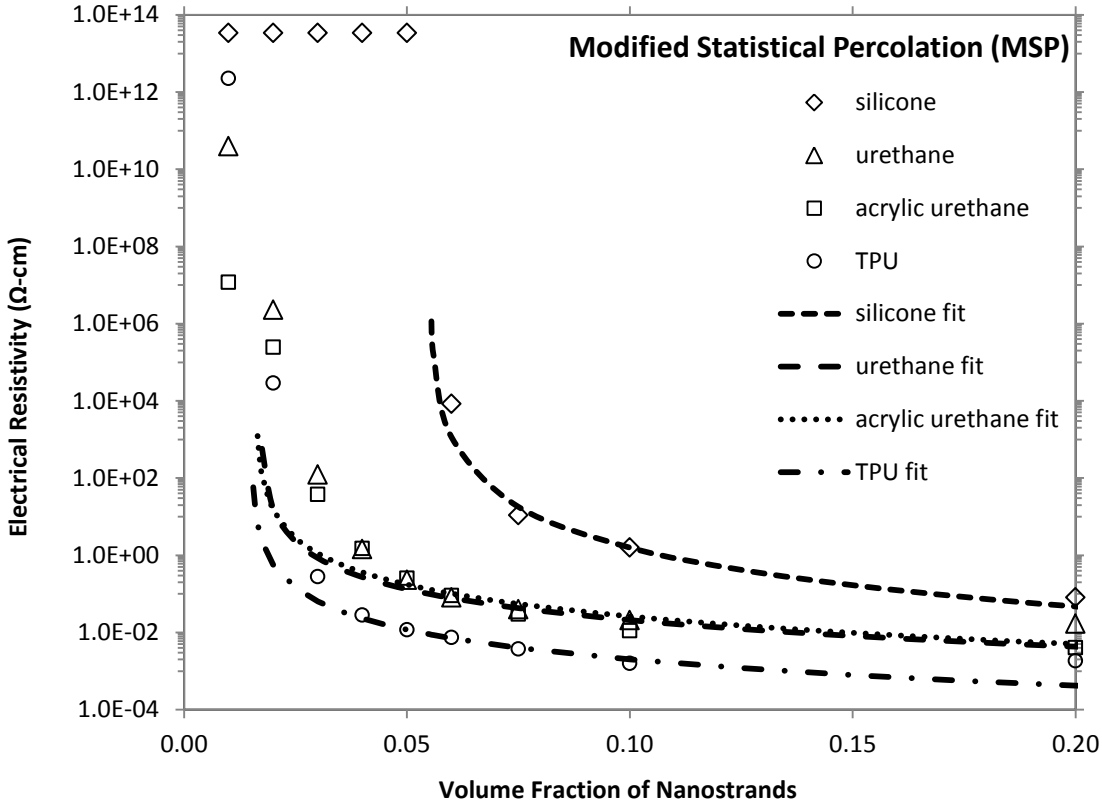

Figure 5.5: Experimental results compared to the Modified Statistical Percolation (MSP) model.

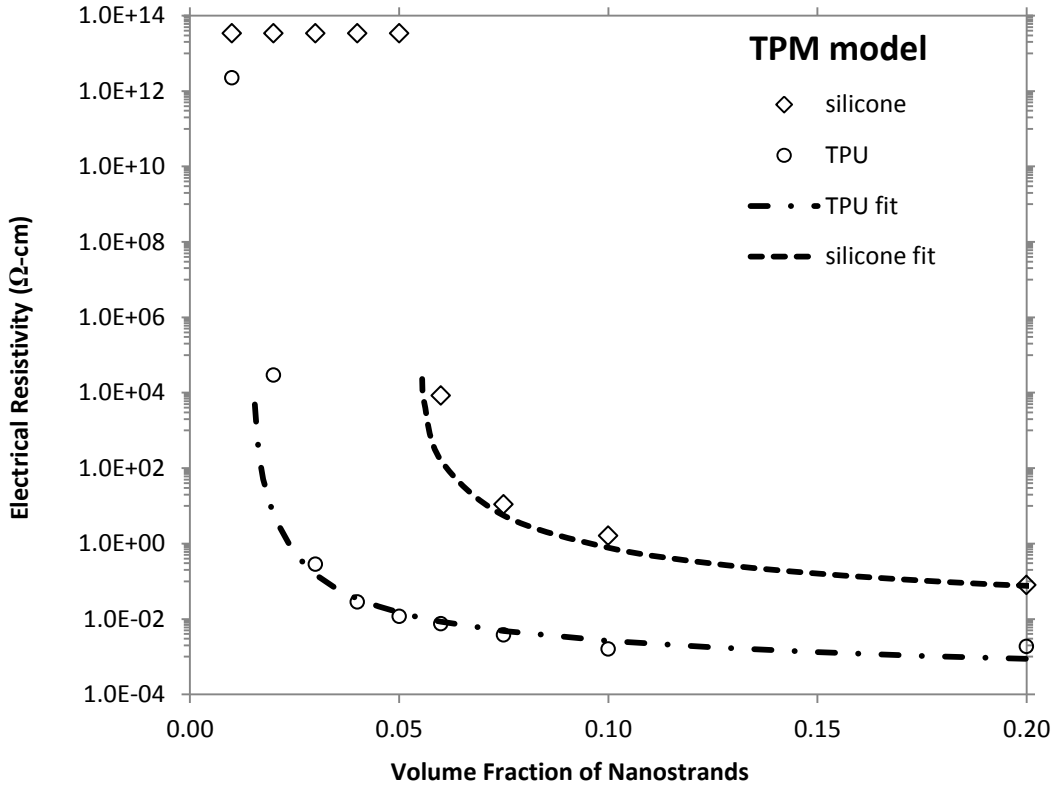

Figure 5.6: Experimental results compared to the TPM approach.

The TEPPE approach allows fitted exponents for each conduction region (thus accounting for different behaviors above and below the percolation threshold) along with polymer and filler conductivities. In order to avoid plotting asymptotic behaviors at transition regions, the divergence of the equations near the limits of each bound must be considered when selecting resolution levels for plotting results. Fits to the TEPPE are given in Figure 5.7.

It is seen that the TEPPE models fits very well in the regions of the percolation limit, but not as well at the percolation limit. The scaling exponent is seen to be relative to the

critical percolation threshold of each polymer system. The combined TEPPE-TPM model includes tunneling considerations above the critical threshold to yield the fits given in Figure 5.8.

The combined TEPPE-TPM model shows superior fit at all volume fractions. The strength of this model lies in the combined ability to distinguish between the different regions of the percolation curve with separate equations, strengthened by the inclusion of quantum tunneling behaviors above the percolation threshold.

Values used for modeling fits are summarized in Table 5-3.

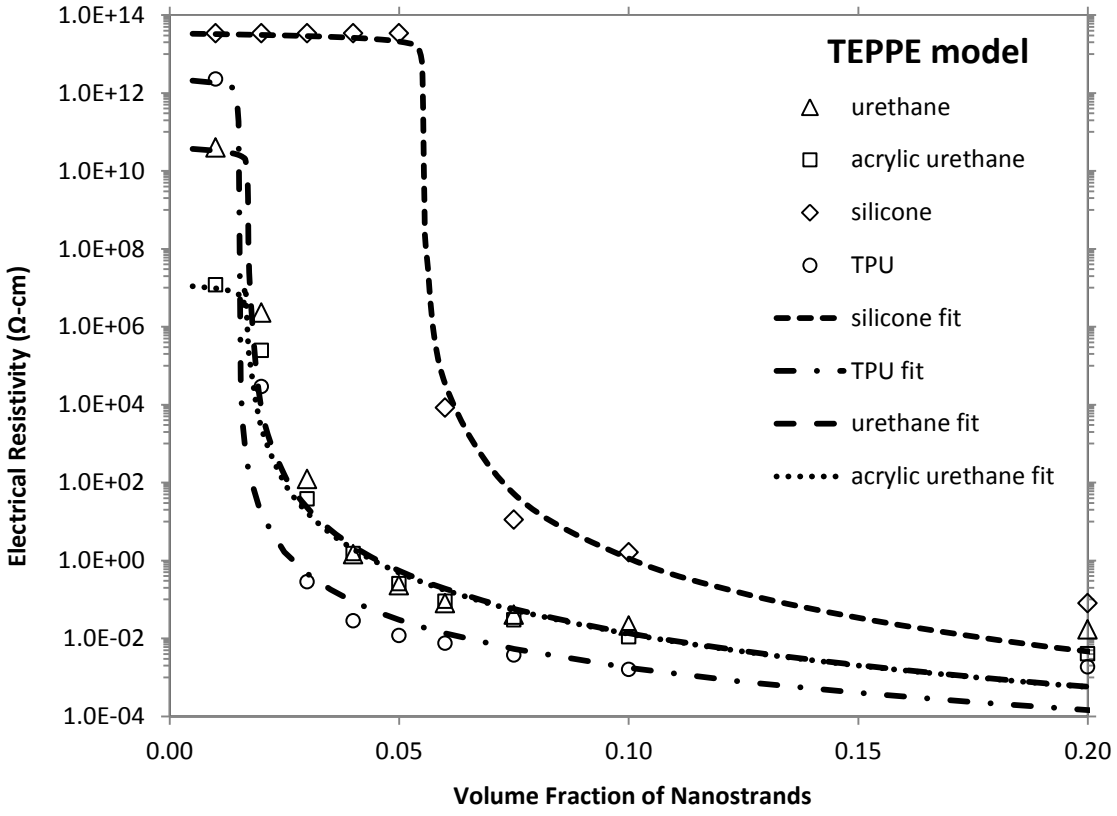

Figure 5.7: Experimental results compared to the TEPPE approach.

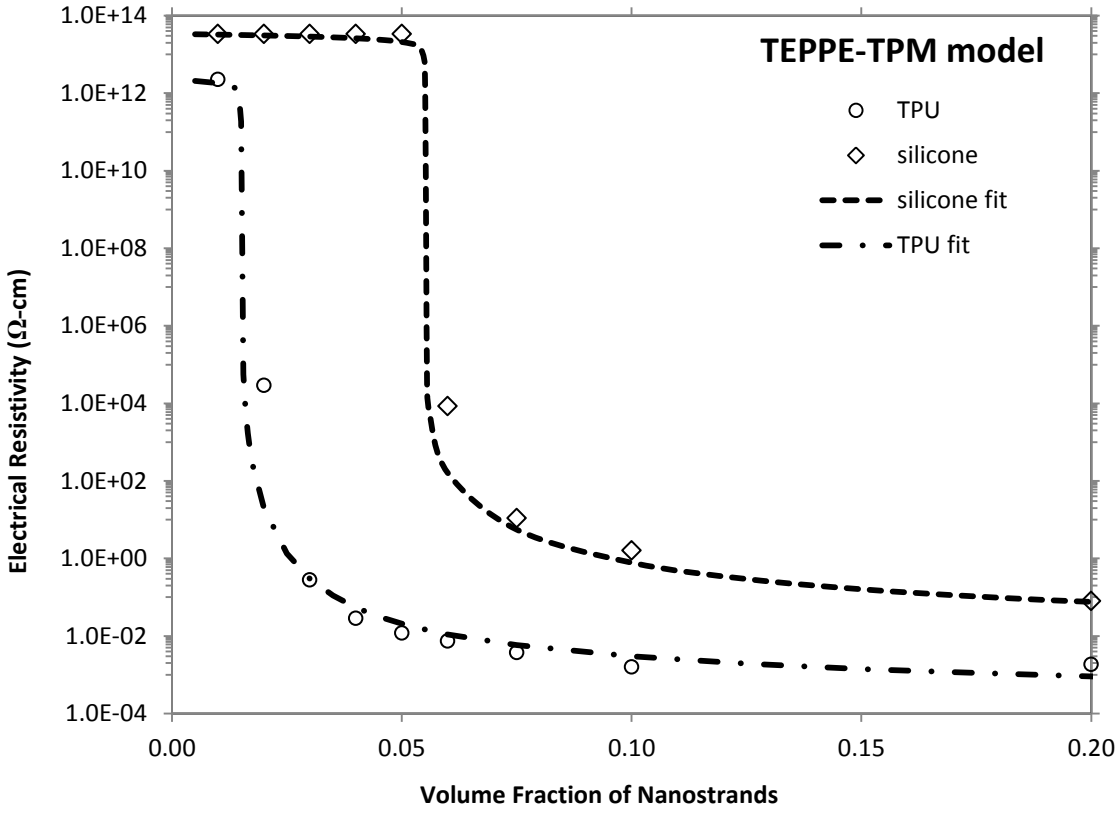

Figure 5.8: Experimental results compared to the combined TEPPE-TPM approach.

Table 5-3 Values for Modeling Fits

Polymer	φ_c	σ_f (S/cm)	σ_p (S/cm)	t (MSP)	K (MSP)	d (nm)	K (TPM)	t (TEPPE & TEPPE-TPM)	s (TEPPE & TEPPE-TPM)
Polycrylic®	0.016	1.44E6	8.47E-8	2.1	1.0E-10			4	0.2
Desothane®	0.017	1.44E6	2.54E-11	2	1.0E-10			4	0.2
Sylgard®	0.055	1.44E6	2.96E-14	3	1.0E-10	10	1.0E-4	4.7	0.2
Irogran®	0.015	1.44E6	4.42E-13	2	1.0E-11	6	0.5E-3	3.2	0.2

5.7 Conclusions

Nickel nanostrands show promise as a conductive element in conductor-insulator polymer composites. This work specifically seeks nanostrand polymer composite electrical resistivity models that can distinguish between polymer systems. Classical approaches in the simplest forms do not show good fit, but more advanced theories based on tunneling percolation and GEM theory show improved accuracy. Specifically, the TPM model and TEPPE models show good fit. The combined TEPPE-TPM approach developed herein considers both generalized effective media approaches and tunneling percolation, and this model shows the best fit to electrical resistivity in nanostrand composites. This model is able to combine the physical considerations of both approaches in separate equations that represent behaviors both below and above the percolation threshold.

Future efforts that focus on the conductor-insulator-conductor (”junction”) will yield models with even further improvements, as is evidenced by the promise shown by the TPM model. Future studies will also seek to include polymer system properties in terms of molecular weight and adsorbed layer thickness, along with additional studies of surface energy characteristics.

5.8 Acknowledgements

The authors gratefully acknowledge the support and insight of Mr. George Hansen of Conductive Composites Company in regard to the physical basis for a combined TEPPE-TPM approach.

5.9 References

1. *Metal Filled Polymers*, CRC Press, New York, 1986.

2. D. Stauffer and A. Aharony, *Introduction to Percolation Theory*, CRC Press, 1994.

3. W. Bauhofer and J. Z. Kovacs, *Composites Science and Technology*, **69**, 1486-1498 (2009).

4. C. Min, X. Shen, Z. Shi, L. Chen and Z. Xu, *Polymer-Plastics Technology and Engineering*, **49**, 1172 - 1181 (2010).

5. G. Hansen, *SAMPE Journal*, 24-28 (2005).

6. J. C. Grunlan, A. R. Mehrabi, M. V. Bannon and J. L. Bahr, *Advanced Materials*, **16**, 150-153 (2004).

7. J. C. Grunlan, W. W. Gerberish and L. F. Francis, *Journal of Applied Polymer Science*, **80**, 692-705 (2001).

8. X. Sun and M. Song, *Macromolecular Theory and Simulations*, **18**, 155-161 (2009).

9. X.-L. G. K. Li, J. C. Fielding. in *48th AIAA/ASME/ASCE/AHS/ASC Structures, Structural Dynamics, and Materials Conference*, Honolulu, HI, 2007.

10. J. C. Maxwell, *A Treatise on Electricity and Magnetism I*, Dover, New York, 1954.

11. O. K. Johnson, C. J. Gardner, D. T. Fullwood, B. L. Adams, N. Hansen and G. Hansen, *CMC: Computers, Materials, & Continua*, **15**, 87-112.

12. V. I. Roldughin and V. V. Vysotskii, *Progress in Organic Coatings*, **39**, 81-100 (2000).

13. D. S. McLachlan, M. Blaszkiewicz and R. E. Newnham, *Journal of the American Ceramic Society*, **73**, 2187-2203 (1990).

14. F. Lux, *Journal of Materials Science*, **28**, 285-301 (1993).

15. G. R. Grimmett, *Percolation*, Springer, 1999.

16. M. L. Clingerman, J. A. King, K. H. Schulz and J. D. Meyers, *Journal of Applied Polymer Science*, **83**, 1341-1356 (2002).

17. D. S. McLachlan and G. Sauti, *J. Nanomaterials*, **2007**, 1-9 (2007).

18. I. Balberg, C. H. Anderson, S. Alexander and N. Wagner, *Physical Review B*, **30**, 3933-3943 (1984).

19. I. Balberg, *Physical Review Letters*, **59**, 1305-1308 (1987).

20. D. S. McLachlan, *Journal of Physics C: Solid State Physics*, **18**, 1891 (1985).

21. D. S. McLachlan, *Solid State Communications*, **60**, 821-825 (1986).

22. N. Hansen and G. Hansen. in *SAMPE Fall Technical Conference*, Wichita, 2009.

23. N. Hansen, D. O. Adams, D. T. Fullwood, M. T. Koecher and J. Weese. SAMPE International Conference, Baltimore, MD May 21-24 2012.

24. Y. P. Mamunya, Y. V. Muzychenko, P. Pissis, E. V. Lebedev and M. I. Shut, *Journal of Macromolecular Science, Part B: Physics*, **40**, 591 - 602 (2001).

25. M. L. Clingerman, E. H. Weber, J. A. King and K. H. Schulz, *Journal of Applied Polymer Science*, **88**, 2280-2299 (2003).

26. J. G. Simmons, *Journal of Applied Physics*, **34**, 1793-1803 (1963).

27. R. D. Sherman, *Polymer engineering and science*, **23**, 36-46 (1983).

28. C. Grimaldi and I. Balberg, *Physical Review Letters*, **96**, 066602 (2006).

29. E. Tadd, A. Zeno, M. Zubris, D. Nily and R. Tannenbaum, *Macromolecules*, **36**, 6497-6502 (2003).

30. H. Inoue, H. Fukke and M. Katsumoto, *Journal of Colloid and Interface Science*, **148**, 533-540 (1992).

31. E. Sichel, J. Gittleman and P. Sheng, *Journal of Electronic Materials*, **11**, 699-747 (1982).

32. F. Carmona, P. Prudhon and F. Barreau, *Solid State Communications*, **51**, 255-257 (1984).

33. Z. Rubin, S. A. Sunshine, M. B. Heaney, I. Bloom and I. Balberg, *Physical Review B*, **59**, 12196-12199 (1999).

34. J. Hicks, A. Behnam and A. Ural, *Physica Review E*, **79**, 012102 (2009).

35. M. Baniassadi, M. Safdari, A. Ghazavizadeh, H. Garmestani, S. Ahzi, J. Grácio and D. Ruch, *Journal of Physics D: Applied Physics*, **44**, 455306 (2011).

36. X. Zeng, X. Xu, P. M. Shenai, E. Kovalev, C. Baudot, N. Mathews and Y. Zhao, *The Journal of Physical Chemistry C*, **115**, 21685-21690 (2011).

37. M. Sahimi, B. D. Hughes, L. E. Scriven and H. T. Davis, *Journal of Physics C: Solid State Physics*, **16**, L521-L527 (1983).

38. Y. R. Hernandez, A. Gryson, F. M. Blighe, M. Cadek, V. Nicolosi, W. J. Blau, Y. K. Gun'ko and J. N. Coleman, *Scripta Materialia*, **58**, 69-72 (2008).

39. S. Vionnet-Menot, C. Grimaldi, T. Maeder, S. Strässler and P. Ryser, *Physical Review B*, **71**, 064201 (2005).

40. S. Kirkpatrick, *Reviews of Modern Physics*, **45**, 574-588 (1973).

41. R. Zallen. in *The Physics of Amorphous Solids*; Wiley-VCH Verlag GmbH & Co. KGaA, 2005, p 135-204.

42. J. G. Simmons, *J Appl Phys*, **34**(1963).

43. S. Feng, B. I. Halperin and P. N. Sen, *Physical Review B*, **35**, 197-214 (1987).

44. D. S. McLachlan, C. Chiteme, C. Park, K. E. Wise, S. E. Lowther, P. T. Lillehei, E. J. Siochi and J. S. Harrison, *Journal of Polymer Science Part B: Polymer Physics*, **43**, 3273-3287 (2005).

45. N. Hansen, D. O. Adams and D. T. Fullwood, *Composites Part A: Applied Science and Manufacturing* (2012).

46. D. S. McLachlan, *Journal of Physics C: Solid State Physics*, **20**, 865 (1987).

47. N. Hansen, D. O. Adams, K. L. DeVries, A. Goff and G. Hansen, *Journal of Adhesion Science and Technology*, **25**, 2659-2670 (2011).

48. Nickel Nanostrands Users Guide - Best Practices, Conductive Composites Company (www.conductivecomposites.com), 2010.

49. B. E. Kilbride, J. N. Coleman, J. Fraysse, P. Fournet, M. Cadek, A. Drury, S. Hutzler, S. Roth and W. J. Blau, *Journal of Applied Physics*, **92**, 4024 (2002).

6 CONCLUSIONS AND RECOMMENDATIONS

The characteristics of nickel nanostrands as the conductive phase in polymer composites have been investigated. Results indicate electrical performance that is significantly more conductive, at equal volume fraction, than alternative conductive fillers. This work has shown the research progression for conductive behaviors and structure property relationships, with an overall goal to seek understanding of polymer dependent percolation behaviors.

The conductivity performance of nanostrands is first investigated in an epoxy adhesive. This first effort also includes baseline electrical and mechanical properties. Variations in electrical resistivity properties based on sample volumes are observed, indicating the criticality of the nature and number of conductor insulator interfaces. This effort also clearly indicates the dependence of conductivity to processing conditions. Nanostrands are not a significant factor in altering the mechanical behaviors of the polymer system.

Statistical topology tools can identify and quantify the *in situ* nanostrand structure. These topology tools enable a predictive capability for quantifying fluid phase nanostrand dispersions, and correlating to cured film properties. This is an important predictive and sampling capability for dispersions in polymer systems. The quantification of the *in situ* structure is an important step toward providing more universal methods in characterizing dispersed conductors.

Testing across multiple polymers indicates a strong dependence on polymer type in electrical conductivity performance. The critical percolation threshold and percolation limit are identified across multiple polymer systems. The characterization of the onset of conduction during cure or set indicate the onset of conduction as a function of mass and cure time, and shows the correlation of electrical conduction percolation behaviors to the volumetric concentration of nanostrands. In some cases, conduction is clearly related to total volume fraction. In other cases, conduction depends more strongly on polymer cure state. Physical and interfacial property tests of constituent materials indicate that bulk polymer properties and polymer fluid phase interfacial properties are not good predictors of conduction properties. It is expected that the key predictors for conduction of nanostrand polymer composites must be identified at the interfacial junction between adjacent nanostrands.

Several materials models are identified as suitable candidates for representing nanostrand percolation behaviors. Scaling exponents and factors are developed, and the accuracy of each approach is evaluated. More advanced models based on tunneling percolation model (TPM) and generalized effective media (TEPPE) approaches show improved accuracy. These advanced models are combined in a TEPPE–TPM model that shows good correlation to percolation behaviors. This combined model applies a general field solution and a tunneling percolation solution, indicating that both factors are significant in understanding conduction behaviors. It is expected that this combined approach will show improved correlation to modeling efforts for similarly structured conductive materials (such as carbon nanotubes) in an insulating matrix. It is also

expected that further investigation into mechanisms and characteristics at the conductive junction will lead to more universal models that can rely more heavily on polymer properties.

Enhanced understanding of conduction in nanostrand polymer systems contributes in several areas, particularly regarding percolation points and conduction models. Empirical solutions are no longer the only method for characterizing nanostrand polymer conductivities. Conduction can be understood in terms of dispersion practices, polymer types, constituent properties, quantified characteristics of the dispersed structure, and an expectation of the onset of conduction. These predictive capabilities provide valuable insight for the integration of nanostrands into polymeric systems. Results are analogous to other conductor insulator composites; thus the field of conductor insulator composite applications is advanced.

Recommendations for work include focusing more closely on the insulating polymer regions between dispersed nanostrands (the polymer-nanostrand-polymer "junction"). Investigation topics should include the adsorbed polymer layer between nanostrands, the molecular weight of the polymer system, and the energy barrier heights related to quantum tunneling behaviors.

6.1 References

[1] X. Shui and D. D. L. Chung, "Submicron diameter nickel filaments and their polymer-matrix composites," *Journal of Material Science,* vol. 35, pp. 1773-1785, 2000.

[2] D. D. L. Chung, "Electromagnetic interference shielding effectiveness of carbon materials," *Carbon,* vol. 39, pp. 279-285, 2001.

[3] J. C. Grunlan, A. R. Mehrabi, M. V. Bannon, and J. L. Bahr, "Water Based Single Wall Nanotube Polymer Filled Composite with an Exceptionally Low Percolation Threshold," *Advanced Materials,* vol. 16, pp. 150-153, 2004.

[4] J.-M. Park, S.-J. Kim, D.-J. Yoon, G. Hansen, and K. L. DeVries, "Self Sensing and interfacial evaluation of Ni nanowire/polymer composites using electro-micromechanical technique," *Composites Science and Technology,* vol. 67, pp. 2121-2134, 2007.

[5] J. C. Grunlan, W. W. Gerberich, and L. F. Francis, "Lowering the Percolation Threshold of Conductive Composites Using Particulate Polymer Microstructure," *J Appl Polym Sci,* vol. 80, 2001.

[6] X. Jing, W. Zhao, and L. Lan, "The Effect of Particle Size on Electric Conducting Percolation Threshold in Polymer/Conducting Particle Composites," *J Mater Sci Lett,* vol. 19, 2000.

[7] A. V. Kyrylyuk, "Continuum percolation of carbon nanotubes in polymeric and colloidal media," *Proceedings of the National Academy of Sciences of the United States of America,* vol. 105, pp. 8221-226, 2008.

[8] S. F. Wang and A. A. Ogale, "Simulation of Percolation Behavior of Anisotropic Short-Fiber Composites with a Continuum Model and Non-Cubic Control Geometry," *Comp Sci and Tech,* vol. 46, 1993.

[9] G. Hansen, "The Roles of Nanostrands and Nickel Coated Fibers in Electrically Conductive Composite Design," in *37th ISTC*, Seattle, WA, 2005.

[10] J. C. Grunlan, W. W. Gerberish, and L. F. Francis, "Lowering the Percolation Threshold of Conductive Composites Using Particulate Polymer Microstructure," *Journal of Applied Polymer Science,* vol. 80, pp. 692-705, 2001.

[11] X. Sun and M. Song, "Highly Conductive Carbon Nanotube/Polymer Nanocomposites Achievable?," *Macromolecular Theory and Simulations,* vol. 18, pp. 155-161, 2009.

[12] C. Min, X. Shen, Z. Shi, L. Chen, and Z. Xu, "The Electrical Properties and Conducting Mechanisms of Carbon Nanotube/Polymer Nanocomposites: A Review," *Polymer-Plastics Technology and Engineering,* vol. 49, pp. 1172 - 1181, 2010.

[13] W. Bauhofer and J. Z. Kovacs, "A review and analysis of electrical percolation in carbon nanotube polymer composites," *Composites Science and Technology,* vol. 69, pp. 1486-1498, 2009.

[14] G. Hansen, N. Hansen, and L. Hansen, "The Roles of Nanostrands and Nickel Coated Fibers in Electrically Conductive Composite Design " presented at the SAMPE Fall Technical Conference, Seattle, WA, 2005.

[15] G. Hansen, "A Concurrent Solution for both Lightning Strike and Electromagnetic Protection of Aerospace Composites " presented at the SAMPE International Conference, Long Beach, CA, 2008.

[16] G. Hansen, "Highly Effective Broadband Shielding Materials," presented at the National Space and Missile Materials Symposium, Henderson, NV, 2008.

[17] G. Hansen, "Advances in HPM and EMP Hardening Materials," presented at the HEART Conference, Colorado Springs, CO, 2008.

[18] J. Burghardt, N. Hansen, L. Hansen, and G. Hansen, "The Mechanical and Electrical Properties of Nickel Nanostrands in Hysol 9396 Epoxy," in *SAMPE International Conference*, Long Beach, CA, 2006.

[19] N. Hansen, L. Hansen, and G. Hansen, "Electrically Conductive Structural Adhesive with Milliohm Resistance," presented at the SAMPE International Conference, Long Beach, CA, 2008.

[20] N. Hansen, G. Hansen, and E. Silverman, "Versatile Gap Fillers and Sealants for High Level Conductivity and Electromagnetic Shielding," presented at the SAMPE Spring Symposium, Seattle, WA, 2010.

[21] N. Hansen and G. Hansen, "Electromagnetically Shielding Spray Paints Using Commercial-Off-The-Shelf Polymer Systems," presented at the SAMPE Fall Technical Conference, Wichita, 2009.

[22] J. Tomblin, J. Kostogorova-Beller, G. Hansen, and N. Hansen, "Evaluation of Lightning Strike Protection Schemes which Employ Conductive Primers," presented at the SAMPE Fall Technical Conference, Wichita, KS, 2009.

[23] J. A. E. Bell and G. Hansen, "Nickel Coated Fibers for Aerospace Applications," presented at the SAMPE International Symposium Proceedings, Anaheim, CA, 1991.

[24] G. Hansen, "Nano-Microstructured Lightning Strike Protection System Using Nanostrands and Conductive Fiber Composites " presented at the SAMPE International Conference, Long Beach, CA, 2006.

[25] G. Hansen, N. Hansen, D. O. Adams, J. Burghardt, D. Widauf, and T. McNeill, "Electrically Conductive Putty Type Repair System For Composite Structures " presented at the SAMPE International Conference, Baltimore, MD, 2007.

[26] G. Hansen and N. Hansen, "The Role of Nanomaterials in Lightning Strike Protection of Aircraft," presented at the National Nano Engineering Conference, Boston, MA, 2007.

[27] G. Hansen, "High Aspect Ratio Sub-Micron and Nano-scale Metal Filaments," *SAMPE Journal,* pp. 24-28, April 2005.

[28] N. Hansen, D. O. Adams, K. DeVries, A. Goff, and G. Hansen, "Investigation of Electrically Conductive Structural Adhesives using Nickel Nanostrands," *Journal of Adhesion Science and Technology,* vol. 25, pp. 2659-2670, 2010.

[29] S. R. Bakshi, R. G. Batista, and A. Agarwal, "Quantification of carbon nanotube distribution and property correlation in nanocomposites," *Composites: Part A,* vol. 40, pp. 1311-1318, 2009.

[30] C. H. II and D. Klosterman, "Processing and analysis of thermoplastic polyimide films containing carbon nanofibers," in *SAMPE International Conference*, Long Beach, CA, 2009.

[31] C. Leer, O. S. Carneiro, J. A. Covas, J. M. Maia, F. W. J. v. Hattum, C. A. Bernardo, L. P. Biro, Z. E. Horvath, and I. Kiricsi, "Dispersion of Carbon Nanotubes in Polycarbonate and its Effect on the Composites Properties," *Material Science Forum,* vol. 5154, pp. 1125-1130, 2006.

[32] X.-L. G. K. Li, J. C. Fielding, "Electrical Conductivity of Nickel Nanostrand-Polymer Composites," presented at the 48th AIAA/ASME/ASCE/AHS/ASC Structures, Structural Dynamics, and Materials Conference, Honolulu, HI, 2007.

[33] O. K. Johnson, C. J. Gardner, D. T. Fullwood, B. L. Adams, N. Hansen, and G. Hansen, "The Colossal Piezoresistive Effect in Nickel Nanostrand Polymer Composites and a Quantum Tunneling Model," *CMC: Computers, Materials, & Continua,* vol. 15, pp. 87-112, 2010.

[34] O. K. Johnson, C. J. Gardner, D. T. Fullwood, B. L. Adams, and G. Hansen, "Deciphering the Structure of Nano-Nickel Composites," presented at the SAMPE Spring Technical Conference, Baltimore, MD, 2009.

[35] N. Hansen, D. O. Adams, K. L. DeVries, A. Goff, and G. Hansen, "Investigation of Electrically Conductive Structural Adhesives using Nickel Nanostrands," *Journal of Adhesion Science and Technology,* vol. 25, pp. 2659-2670, 2011.